Proliferative and survival pathways in oesophageal cancer

Luke Emmanuel Esau

Thesis Presented for the Degree of

DOCTOR OF PHILOSOPHY

in the Department of

Medical Biochemistry

UNIVERSITY OF CAPE TOWN

September 2011

ACKNOWLEDGEMENTS

I would like to thank:

My supervisor Prof. Denver Hendricks for his supervision and inspiration, shaping me into a better scientist.

Dr Virna Leaner for the advice, guidance and support

Cancer lab members:

Catherine Whibley and Widaad Zemanay for warmly welcoming me into the lab and assisting me with experimental procedures.

Bo Wang and Wei Wei for helping with experimental techniques, especially the lentiviral knockdown experiments.

Pauline van der Watt and Nina Holderness for advice and support

Kate Hadley for guidance, support and assistance with experiments

Nelusha Shunmoogen-Gounden for always being a true friend and an outstanding lab colleague

Hajira Guzgay for general laboratory assistance and management

Robert Samuels for laboratory maintenance

National Research Foundation, DAAD and UCT for financial assistance

My family for their love and support especially during trying times

"Every great dream begins with a dreamer. Always remember, you have within you the strength, the patience, and the passion to reach for the stars to change the world."

Harriet Tubman

CONTENTS

CHAPTER 5: MATERIALS AND METHODS

ABBREVIATIONS

AC	Adenocarcinoma
Amp	Ampicillin
AP-1	Activator protein 1
APS	Ammonium Persulphate
BCA	Bicinchoninic acid
BSA	Bovine Serum Albumin
bp	Base pairs
cDNA	Complementary DNA
CO_2	Carbon Dioxide
Conc	Concentration
CM	Conditioned medium
°C	Degrees Celcius
C_T	Threshold cycle
Ctrl	Control
CXCR2	CXC chemokine receptor 2
DAPI	4',6'-diamidino-2'-phenylindole dihydrochloride
DEPC	Diethylpyrocarbonate
DMEM	Dulbecco's Modified Eagle's Medium
DMSO	Dimethyl sulphoxide
DNA	Deoxyribonucleic acid

dNTP	Deoxynucleoside triphosphate
E2F	Gene encoding transcription factors
ECL	Enhanced Chemiluminescence
EGF	Epidermal Growth Factor
EGFR	Epidermal Growth Factor Receptor
ERK1/2	Extracellular signal-regulated kinases 1/2
FACS	Fluorescent activated cell sorting
FCS	Foetal Calf Serum
GusB	β-glucuronidase
GFP	Green Fluorescent Protein
GPCR	G-protein coupled receptor
GROα	Growth related oncogene alpha
GROβ	Growth related oncogene beta
Hr	Hour
HRP	Horse Radish Peroxidase
IGF-1	Insulin Growth Factor 1
IGF-1R	Insulin-like Growth Factor 1 Receptor
Ippt	Immunoprecipitation
Kb	Kilobase
kDa	Kilodaltons
M	Molar
Mab	Monoclonal antibody

MAPK	Mitogen-Activated Protein Kinase
mg	Milligram
min	Minutes
ml	Millilitre
mRNA	message Ribonucleic acid
mTORC	Mammalian target of rapamycin
MTT	3'-(4',5'-Dimethylthiazol-2'-yl)-2',5'-diphenyltetrazolium bromide
Neut	Neutralising
NF-κB	Nuclear Factor-KappaB
ng	Nanogram
nM	Nanomolar
nt	Nucleotides
NSCLC	Non-small cell lung cancer
OD	Optical Density
OSCC	Oesophageal squamous cell carcinoma
p-EGFR	phosphorylated EGFR
p-IGF-1R	phosphorylated IGF-1R
p-Tyr	phosphorylated Tyrosine
PAGE	Polyacrylamide Gel Electrophoresis
PBS	Phosphate Buffered Saline
PCR	Polymerase Chain Reaction
pH2AX	phospho-histone H2AX

PKC	Protein kinase C
PMSF	Phenylmethylesulfonyl fluoride
p/s	Penicillin and Streptomycin
qRT-PCR	quantitative real time PCR
RCC	Renal cell carcinoma
RIPA buffer	Radioimmunoprecipitation assay buffer
RNA	Ribonucleic Acid
RNAi	RNA interference
RNAsin	Ribonuclease inhibitor
rpm	Revolutions per minute
RT-PCR	Reverse Transcription Polymerase Chain Reaction
STDEV	Standard Deviation
SDS	Sodium dodecyl sulfate
siRNA	Small interfering RNA
shRNA	Small hairpin RNA
Ta	Annealing Temperature
Tm	Melting Temperature
TBST	Tris-Buffered Saline Tween-20
Tx	Treated
µl	Microlitre
WB	Western Blot

Abstract:

Oesophageal squamous cell carcinoma (OSCC) is the 8th most common cancer worldwide with high incidence in areas that include China, Iran and South Africa. The current treatment available for OSCC does not significantly enhance patient survival. A better understanding of proliferative and survival pathways activated in OSCC could allow identification of more specific therapeutic targets, potentially improving management of OSCC. Cell surface receptors are known to play important roles in relaying signals from the extracellular environment. They are often overexpressed in cancer cells, thus making them interesting drug targets for cancer therapy. The epidermal growth factor receptor (EGFR), the type 1 insulin-like growth factor receptor (IGF-1R) and the chemokine CXC receptor 2 (CXCR2) are examples of receptors commonly overexpressed in OSCC. The aim of this study was to determine the role of EGFR, IGF-1R and CXCR2 in proliferation and survival of OSCC cells.

Here we show that in OSCC cell lines, stimulation with EGF resulted in rapid phosphorylation of IGF-1R which was dependent on EGFR kinase activity. IGF-1R/Akt activity suppressed EGFR and ERK1/2 activity when cells were treated with IGF-1. This repression was relieved when IGF-1R was knocked down, as cells displayed elevated pEGFR and pERK1/2 levels. Ablation of EGFR activity by antagonist or siRNA reduced proliferation of WHCO1 and WHCO6 cells by 30-40% suggesting a role for EGFR in proliferation. Furthermore, co-targeting of EGFR and IGF-1R, but not IGF-1R combined with Cisplatin or doxorubicin, resulted in increased apoptosis in WHCO1 and WHCO6 OSCC cells.

In a previous study we have shown that the chemokine CXC receptor 2 (CXCR2) and its ligands Groα and Groβ are upregulated in OSCC patient tissue compared to normal adjacent tissue. Inhibition of CXCR2 with neutralising antibody or shRNA specific to CXCR2 had no effect on cell proliferation or survival. However, treatment of OSCC cells WHCO1 and WHCO6 with CXCR2 antagonist SB225002 blocked proliferation with an IC_{50} of 2.5 μM, while normal fibroblast cell DMB and WI38 were unaffected. Cell proliferation was significantly inhibited in the presence of 2 μM SB225002 and a G2/M arrest was observed after 8 hrs of incubation with drug. SB225002 induced DNA damage and apoptosis in WHCO1 and WHCO6 OSCC cells at the 24 and 48 hr time points. WHCO1 and WHCO6 CXCR2 knockdown cells were less sensitive to SB225002 as no effect on cell cycle and proliferation was observed in the presence SB225002 compared to control cells. Taken together these data suggests that CXCR2 is important in mediating SB225002-induced apoptosis of OSCC cells which over-express this receptor while CXCR2 negative cells are not affected by SB225002.

Our data suggest that EGFR, IGF-1R and CXCR2 are novel potential therapeutic targets for OSCC as either co-targeting of EGFR and IGF-1R or targeting of CXCR2 results in apoptosis of OSCC cells.

Chapter 1

Literature Review

1.1 Cancer

Despite references to cancer in texts dating as far back as 3000 BC, our knowledge of this disease has not yet lead to its eradication – in fact, it is still one of the leading causes of morbidity and death worldwide (Hajdu 2011). It is estimated that one quarter of people living in the developed world will die as a result of cancer (Hamilton, 2010). Better diagnostic markers and more specific treatment targets need to be identified for improving patient survival. This explains the huge amount of funding and resources poured into research to better understand cancer as a disease process. As a direct result of this relentless effort, researchers were able to identify distinct differences between normal and cancer cells that could potentially be exploited to identify and target cancer cells. These multiple and complex differences were succinctly summarized by Hanahan and Weinberg (2000) as the six hallmarks of cancer, including the evasion of apoptosis, uncontrolled proliferation and angiogenesis with the 7th proposed hallmark linking inflammation with cancer (Cavallo *et al.* 2011). Major differences separating cancer cells from normal cells include tumour specific antigens, tumour specific oncogenes e.g. BCR-ABL and loss of tumour suppressor-gene function (Basilion *et al.* 1999). Selective targeting of tumour specific oncogenes like BCR-ABL in chronic myologenous leukemic patients and HER2 in breast cancer patients results in improved survival (Cao *et al.* 2008). Sadly, not all cancers share the same 'Achilles' heel' and rigorous research searching for tumour specific oncogenes is still on-going. Esophageal cancer (OC), which will be discussed further, is a cancer plaguing many developing countries.

1.2 Oesophageal Cancer

Oesophageal cancer (OC) is the 8th most common cancer worldwide, the sixth leading cause of cancer related deaths with an overall 5 year survival around 10% (Enzinger & Mayer 2003; Pickens & Orringer 2003; Ekman *et al.* 2007; Stoner *et al.* 2007; Mitry *et al.* 2008). Oesophageal cancer presents predominantly as two histological subtypes namely: squamous cell carcinoma (SCC) occurring in the middle and lower third of the oesophagus and adenocarcinoma (AC) which is found in the distal part of the oesophagus. In developed regions like Western Europe and North America incidence rates for oesophageal squamous cell carcinoma (OSCC) are as low as 3-5/100 000 while in certain regions including Iraq, parts of Europe, Southern Africa and Iran the incidence is between 8-13/100 000 (Layke & Lopez, 2006; Pickens & Orringer, 2003; Zhou *et al.* 2006). Incidence rates in parts of China have been found to exceed 100 per 100 000 (Enzinger & Mayer 2003; Stoner *et al.* 2007; Guo *et al.* 2008; Zheng *et al.* 2009). According to statistics released by the International Agency for Research on Cancer (IARC) (www-dep.iarc.fr), high death rates were observed in regions with high incidence rates for OSCC in 2008 (Fig. 1) (Bosetti *et al.* 2008). While OSCC is more prevalent in developing countries than adenocarcinoma, the reverse is true in developed countries. Barrets Oesophagus, (in which stratified squamous epithelial cells are replaced with columnar epithelial cells), is considered a premalignant form of AC since these patients have an increased risk for developing AC (Enzinger & Mayer 2003). Recent evidence suggests that obesity, acid reflux and Barrets oesophagus are risk factors for AC in first world nations (Tew *et al.* 2005; Layke & Lopez 2006).

Treatment for OSCC includes surgery, radiation therapy and chemotherapy which are sometimes used in combination. Surgery is only approved and advised if the cancer is localized and has not metastasized (Enzinger & Mayer 2003; Layke & Lopez 2006). Reports

have shown that patients diagnosed with early stage OSCC who have undergone surgery have 5 year survival rates between 15-24%, highlighting the poor prognosis for this disease (Enzinger & Mayer 2003). Radiotherapy can yield similar survival rates, although it is less effective as a palliative treatment compared to surgery.

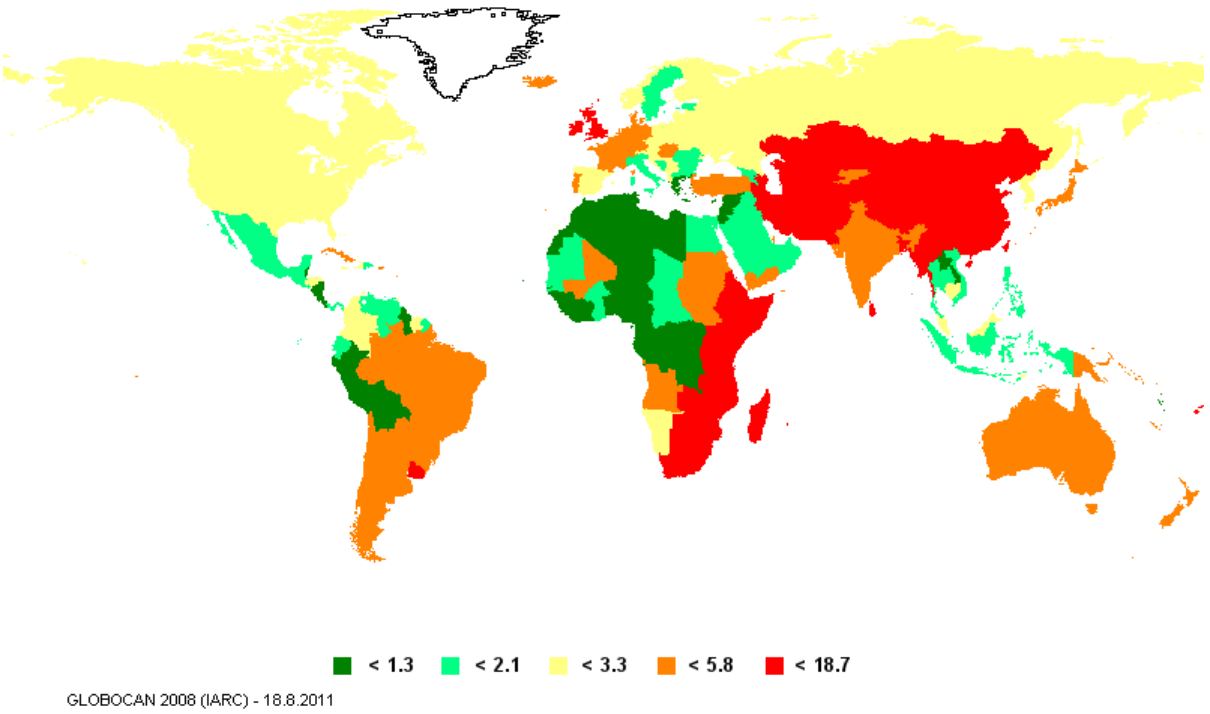

Figure 1: World-wide OSCC incidence rates

GLOBOCAN world-wide incidence rates for OSCC per 100,000 individuals in 2008. From GLOBOCAN 2008, International Agency for Research on Cancer, Lyon, France, 2004. (www-dep.iarc.fr).The figure legend depicts number of OSCC cases per 100,000 individuals. OSCC incidence is high in underdeveloped countries along the Eastern seaboard of Africa while less common in developed countries like America.

A major contributing factor to poor patient survival is the poor detection of early stage OSCC – consequently, most patients (greater than 50%) present with advanced stage III or IV OSCC, in which case the tumour is unresectable or has already metastasised (Tew *et al.* 2005; Guo *et al.* 2008). When patients with advanced disease are treated with chemotherapeutic agents such as cisplatin and 5-fluorouracil, 50-60% show initial response

for the first few months. However resistance to therapy soon develops and patients often succumb within a year. Although strategies to improve survival, in which radiotherapy and chemotherapy or pre/postoperative radio/chemotherapy are combined, the 5 year survival rate for OSCC remains unchanged, despite short term benefits (Layke & Lopez 2006). New therapeutic interventions and prognostic markers for the management of OSCC are highly sought after. Although it is recognised that certain factors like alcohol consumption, smoking, certain genetic alterations and chemical insults contribute to the development of OSCC, there is still a poor understanding of the molecular pathways responsible for the development and maintenance of oesophageal cancer. Preliminary evidence obtained in our laboratory indicated that a suite of genes including EGFR, IGF-1R and CXCR2 may be implicated in the maintenance of the cancer phenotype in OSCC (Whibley *et al.* 2005; Wang *et al.* 2006; Whibley *et al.* 2007; Wang *et al.* 2009). The signalling pathways reviewed below are frequently dysregulated in many cancers and could provide clues to the processes that operate in oesophageal cancer. This review will focus on those genes and their associated signalling pathways, to provide background for the experimental chapters that follow.

1.3 Epidermal Growth Factor Receptor (EGFR)

The epidermal growth factor receptor (EGFR) belongs to a four member family of receptors that include EGFR/ErbB1, Her2/Neu/ErbB2, Her3/ErbB3 and Her4/ErbB4 (Fig. 2) (Normanno *et al.* 2006; Bianco *et al.* 2007; Wei *et al.* 2007). The EGFR gene, located in the region of 7p13-q22, codes for a 170kDa protein that consists of an extracellular domain for ligand binding; a transmembrane domain for anchorage and a cytoplasmic domain containing an ATP binding kinase domain (Bianco *et al.* 2007; Wei *et al.* 2007). After translation of the EGFR mRNA the alpha and beta subunits dimerize with each other in a 2:2 complex containing two alpha and two beta subunits. The ErbB family receptors are highly homologous to such an extent that homo/hetero – dimerization occur between these receptors. Her2 has a constitutively active conformation, and there is no known ligand for this receptor. The conformational state of this protein, makes it the preferred dimerization partner for other ERB family members because its dimerization loop is always exposed (Wang *et al.* 2006). Her2 as the preferred dimerization partner of EGFR increases receptor stability and targets the receptor for recycling where it can be reutilized. Activation of EGFR can either occur through direct or indirect interactions. Direct activation occurs when ligands bind the extracellular ligand binding domain of the receptor. Ligands recognized by EGFR include: epidermal growth factor (EGF), transforming growth factor alpha (TGF-α), amphiregulin (AR), heparin-binding EGF-like growth factor (HB-EGF) and betacellulin (BTC) (Fig. 2) (Normanno *et al.* 2006). Indirect activation includes transactivation by other receptors like G protein coupled receptors (GPCR) or the insulin growth factor 1 receptor (IGF-1R) and external stimuli like radiation, injury and chemical insults (Thomas *et al.* 2006; Luppi *et al.* 2007).

Upon activation of the EGF receptor, homo/heterodimerization followed by autophosphorylation of tyrosine and serine residues occurs. Signalling complexes and adaptor proteins are recruited to the membrane and associate with activated EGFR (Fig. 3). Activation of the Ras/Raf/MAPK, JAK/STAT, PI3K-AKT and PLC*y* pathways then give rise to gene amplification, proliferation, survival and migration of cells (Schneider *et al.* 2009).

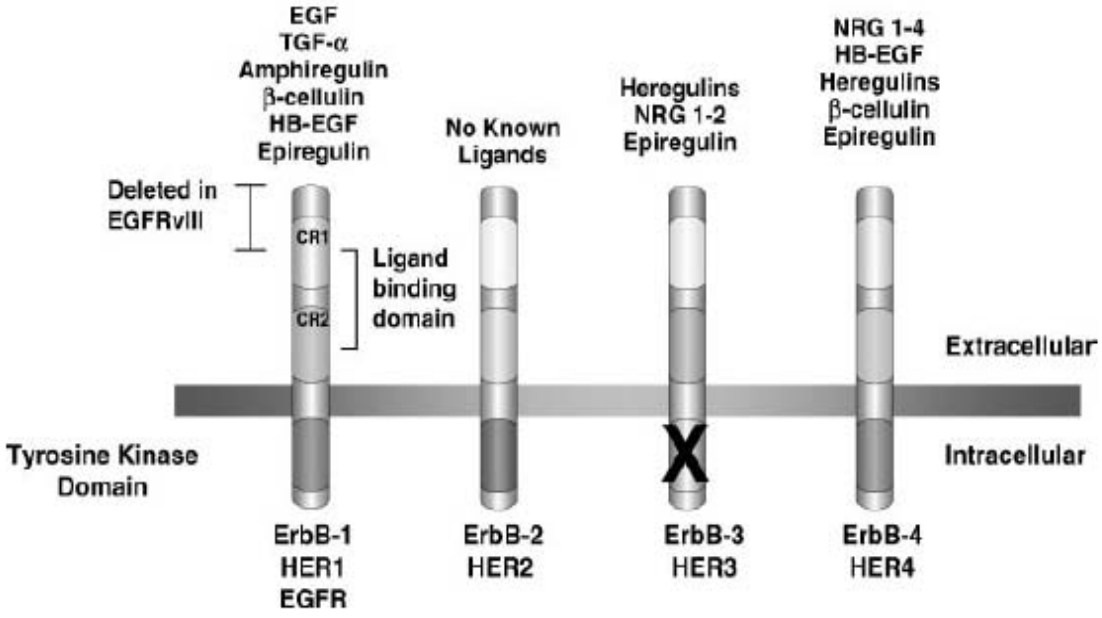

Figure 2: HER family structure and ligand identity

The HER family of receptors are divided into three domains: an extracellular ligand-binding domain with two cysteine-rich regions (CR1 and CR2), a transmembrane domain and an intracellular kinase domain. All receptors are capable of homo/heterodimerization with each other upon binding ligand. All HER receptors, with the exception of HER2, have known ligands. (EGF – epidermal growth factor, EGFR – epidermal growth factor receptor, HER – human epidermal receptor, X – kinase inactive/dead, HB-EGF heparin-binding epidermal growth factor, NRG – neuregulin and TGFα – transforming growth factor alpha). From Rowinsky (2004).

Reports have shown compelling evidence that EGFR exerts its effects mostly through the Ras/Raf/MEK/ERK1/2 pathway as this pathway is more strongly activated by EGFR than the PI3K-AKT and other pathways (Cao *et al.* 2008; Hu *et al.* 2008; Villanueva *et al.* 2010). The Ras/Raf/MEK/ERK1/2 pathway activates more than 140 target proteins, with its best known role being activation of proliferation (Khavari & Rinn, 2007). Activation of Ras leads to increased proliferation and inhibits differentiation of keratinocytes (Kern *et al.* 2011). Animal models containing constitutively activated Ras or MEK display hyperplasia in the epidermis (Kern *et al.*, 2011). Redundancies exist in this pathway since Ras and Raf have many isoforms which ensures activation of the Ras/Raf/MEK/ERK1/2 pathway. Ras isoforms include Ha-Ras, N-Ras and Ki-Ras (McCubrey *et al.* 2007).

Ras is a GTPase and can be activated by receptor tyrosine kinases like EGFR. Once EGFR is activated, adaptor proteins Grb2 and SOS bind EGFR and recruit Ras. Ras is then activated by exchanging GDP for GTP, leading to a cascade of downstream phosphorylation events, including the Raf/MEK/ERK1/2 and PI3K pathways as shown in Fig. 3 (Normanno *et al.* 2006; Khavari & Rinn 2007; McCubrey *et al.* 2007). Consistent with the importance of the Ras/Raf/MEK/ERK1/2 pathway in proliferation, it is not surprising that 25-30% of all human tumours contain activating Ras mutations (Katz *et al.* 2007; Khavari & Rinn 2007). Ras activity is also much higher in squamous cell carcinomas compared to normal cells despite the absence of mutations suggesting the presence of multiple pathways that could lead to the activation of this critical signalling pathway (Khavari & Rinn 2007). Three Raf isoforms namely; Raf1 (C-Raf), A-Raf and B-Raf are all capable of activating MEK with different affinities (Boutros *et al.* 2008). B-Raf is the most commonly mutated Raf isoform and is mutated in as much as 50% of melanomas (Villanueva *et al.* 2010). Following Raf activation, MEK is phosphorylated, which in turn activates ERK1/2. Although unphosphorylated MEK can interact with ERK1/2, phosphorylation of ERK1/2 results in a conformational change that

disrupts MEK/ERK1/2 interactions (Boutros *et al.* 2008). Activated ERK1/2 translocates to the nucleus and activates transcription factors or directly phosphorylates proteins involved in cell migration, proliferation, differentiation or apoptosis. The Ras/Raf/MEK/ERK1/2 pathway is also known to activate phosphorylation of pro-apoptotic proteins including Bad and Bim resulting in their degradation, while phosphorylation of anti-apoptotic proteins Mcl-1 and BCL-2 by ERK1/2 stabilises these proteins (McCubrey *et al.* 2007). ERK1/2 translocation to the nucleus results in stabilisation of the transcription factor c-Myc which facilitates transcription of cyclin D1 and Elk which in turn induces transcription of the c-*fos* gene. These genes are all involved in regulating cell cycle progression (Fig. 3) (Katz *et al.* 2007; Boutros *et al.* 2008). Furthermore, activation of AP-1 by ERK1/2 could lead to the transcription of matrix metalloproteases (MMPs) which are involved with extracellular remodelling and cell migration (Katz *et al.* 2007). Most receptor tyrosine kinases activate the Ras/Raf/MEK/ERK1/2 pathway because of the central role it plays in activating a multitude of important cellular events. Aberrant activation of this pathway can lead to cancer.

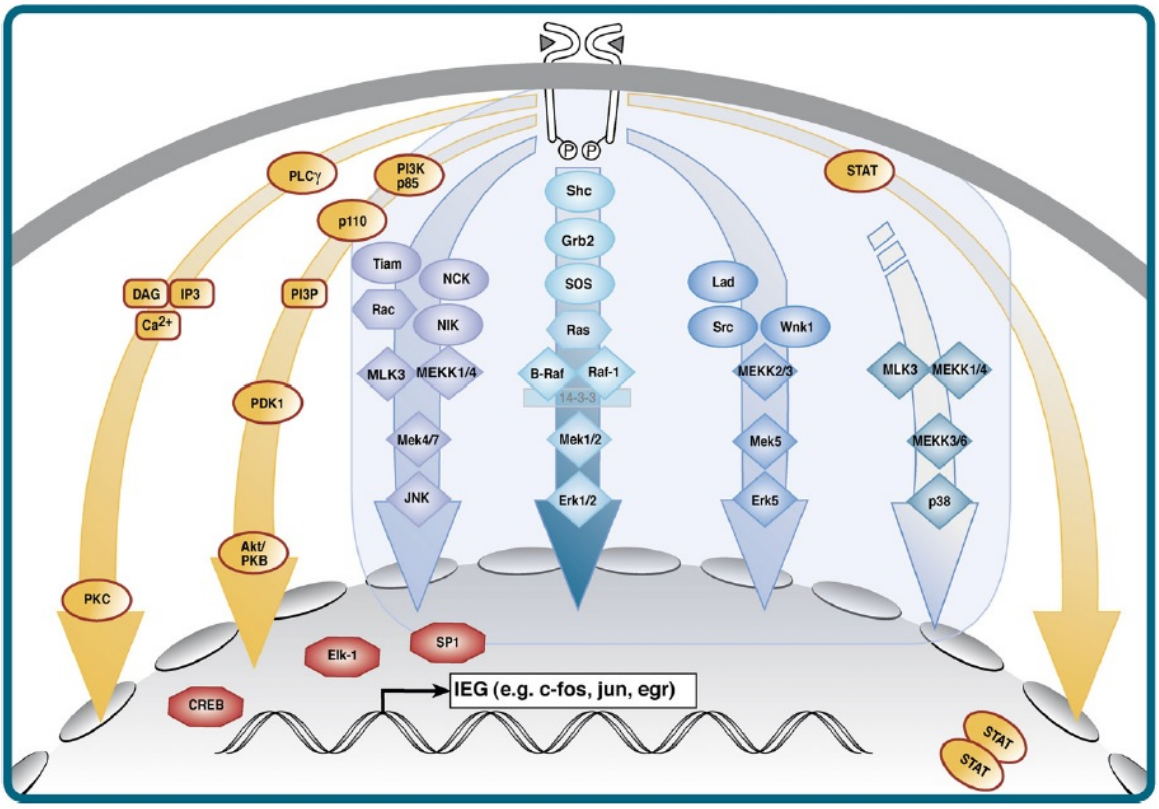

<u>Figure 3:</u> MAPK signalling

Upon binding ligand RTKs like EGFR dimerize resulting in autophosphorylation. Adapter proteins Shc, Grb2 and PI3K are recruited to the activated RTK and in turn become phosphorylated. These activated adapter proteins can then relay signals down the various MAPK pathways, by phosphorylating their substrates, resulting in activation of transcription factors which transcribe genes involved in cell cycle progression, survival and migration. Adapted from Katz et al., 2007.

1.3.1 EGFR as a target in cancer

In many cancers the EGFR has been implicated as a major contributor to tumour aggression where it is often mutated, overexpressed or transactivated in cancer cells. EGFR overexpression and mutations occur in many tumours including: oesophageal (92%), colorectal (72%), prostrate (65%) and lung (50%) cancers (Tew *et al.* 2005). Tumour aggressiveness, poor prognosis and survival also correlate with EGFR overexpression. This correlation between EGFR expression and patient survival has prompted huge investment into research in order to elucidate the structure of EGFR and develop inhibitors for this receptor. Monoclonal antibodies, like Cetuximab, targeting the extracellular domain of EGFR, and kinase inhibitors, like Erlotinib and Gefitinib (Iressa), targeting the ATP binding pocket of EGFR have subsequently been developed and approved for clinical evaluation for certain cancers. The first cancer in which EGFR targeted therapy was evaluated was in Non-small Cell Lung Cancers (NSCLC) which showed overexpression of EGFR. However, only a subset of patients showed clinical response with either tumour regression or stable disease when EGFR was specifically targeted (Sharma *et al.* 2007; Yun *et al.* 2007). It was later discovered that NSCLC patients bearing mutant EGFR (kinase domain mutations L858R and G719S) were the responders. These EGFR kinase domain mutations have been shown to be critical in tumour proliferation and survival as these tumours rely on constitutively activated EGFR and its major downstream Ras/Raf/MEK/ERK1/2 pathway (Hynes & Schlange 2006; Yun *et al.* 2007). Erlotinib was approved in 2004 for treatment of locally advanced or metastatic NSCLC patients in which chemotherapy was not effective while Gefitinib is approved only for patients who have shown response to this inhibitor (Morgillo *et al.* 2007a). Interestingly, a difference in the proportion of clinical responders has been observed in various population groups.

NSCLC patients of Asian ethnicity treated with EGFR inhibitors show response rates of 30-50% while only 10% of patients of West European or North American ethnicity show clinical response to EGFR therapy (Sharma *et al.* 2007). Further investigation revealed that most responders were non-smokers and that EGFR mutations were more frequent in the Asian population than the European population. Aside from NSCLC, EGFR inhibitors have also been approved for breast cancer, Head and Neck Squamous Cell Carcinoma and Colorectal cancer. However similar response rates are observed for these cancers as with NSCLC (Cohen *et al.* 2005; Ono & Kuwano 2006). EGFR mutations in these cancers are not the sole predictor of response to EGFR inhibitors, suggesting that other mechanisms also play a role in response. Because EGFR is commonly overexpressed in OSCC, it has been investigated as a potential target in this disease. Gefitinib treatment in advanced OSCC patients only resulted in a 10% patient response rate consistent with reports of EGFR targeted therapy in other cancers (Ferry *et al.* 2007; Sudo *et al.* 2007). Many trials and studies have shown that inhibition of EGFR has only benefited a subset of patients even though EGFR is overexpressed in many cancers.

1.4 Type-1 Insulin-like Growth Factor Receptor (IGF-1R)

The insulin-like growth factor receptor (IGF-1R) is a receptor tyrosine kinase essential for cell growth, differentiation and survival. IGF-1R is encoded by a single copy gene located on chromosome 15q25-q26 which encodes a polypeptide chain of 1367 amino acids (Hopfner *et al.* 2006; Adachi *et al.* 2010). Other family members include the Insulin receptor, which has two isoforms namely Insulin receptor A (IR-A) and Insulin receptor B (IR-B), and the type 2 Insulin-like growth factor receptor (IGF-2R) (Pandini *et al.* 2007). Both the IR and IGF-1R consist of two alpha extracellular ligand binding domain subunits and two beta subunit chains containing a juxtamembrane region embedded in the cell membrane, an intracellular cytoplasmic kinase domain and a carboxyl-terminal domain (Dupont *et al.* 2003). These two receptors are highly conserved with the greatest homology in the kinase domain (84%) (Dupont *et al.* 2003; García-Echeverría *et al.* 2004). Ligands for these 3 receptors include insulin (Ins), insulin growth factor 1 (IGF-1) and insulin growth factor 2 (IGF-2), each binding with different affinities to the respective receptors. IGF-1 and IGF-2 bind IGF-1R with an affinity 500-1000 fold higher than Ins (Hopfner *et al.* 2006). Hybrid receptors are capable of binding both Ins or IGF-1. Although the IGF-2R receptor is kinase deficient its known function is to sequester IGF-2 in order to dampen signalling by IRA and IGF-1R (Zha & Lackner 2010). The physiological role of IGF-1 is to activate cell growth and provide protective signals to enhance normal cell survival under stressful or growth factor deficient conditions. IGF-1 protects and assists normal cells in recovery after ischemia or traumatic brain injury (Kurmasheva & Houghton 2006). Secretion of Ins is tightly controlled as it is only required during periods of high blood glucose while IGF-1 production and secretion is under endocrine regulation by growth hormone (Hartog *et al.* 2007). Although IGF-1 and Ins can be produced by other tissues, the bulk of these are produced by the liver and β-cells of the

pancreas (Blakesley *et al.* 1996; Massoner *et al.* 2010; Zha & Lackner 2010). Furthermore insulin growth factor binding proteins (IGFBPs) also regulate the availability of IGFs since they bind IGF in the serum, protecting these ligands from degradation (Lee *et al.* 2002; Hartog *et al.* 2007).

The major downstream signalling pathway of the IGF-1R system is phosphatidylinositol 3-kinase (PI3K) - AKT (Hu *et al.* 2008). After binding ligand IGF-1R becomes autophosphorylated resulting in recruitment of insulin receptor substrate (IRS) and translocation of (PI3K) to the cell membrane (Fig. 4). In the process, phosphatidylinositol-3,4-bisphosphate (PIP2) is converted to phosphatidylinositol-3,4,5-triphosphate (PIP3) (Fig. 4). The presence of PIP3 attracts AKT to the plasma membrane leading to the activation of AKT by PDK1 (LoPiccolo *et al.* 2007). PTEN (phosphatase and tensin homologue deleted on chromosome ten), a lipid phosphatase which catalyses the conversion of PIP3 to PIP2, in contrast, blocks AKT activity (Fig. 4).

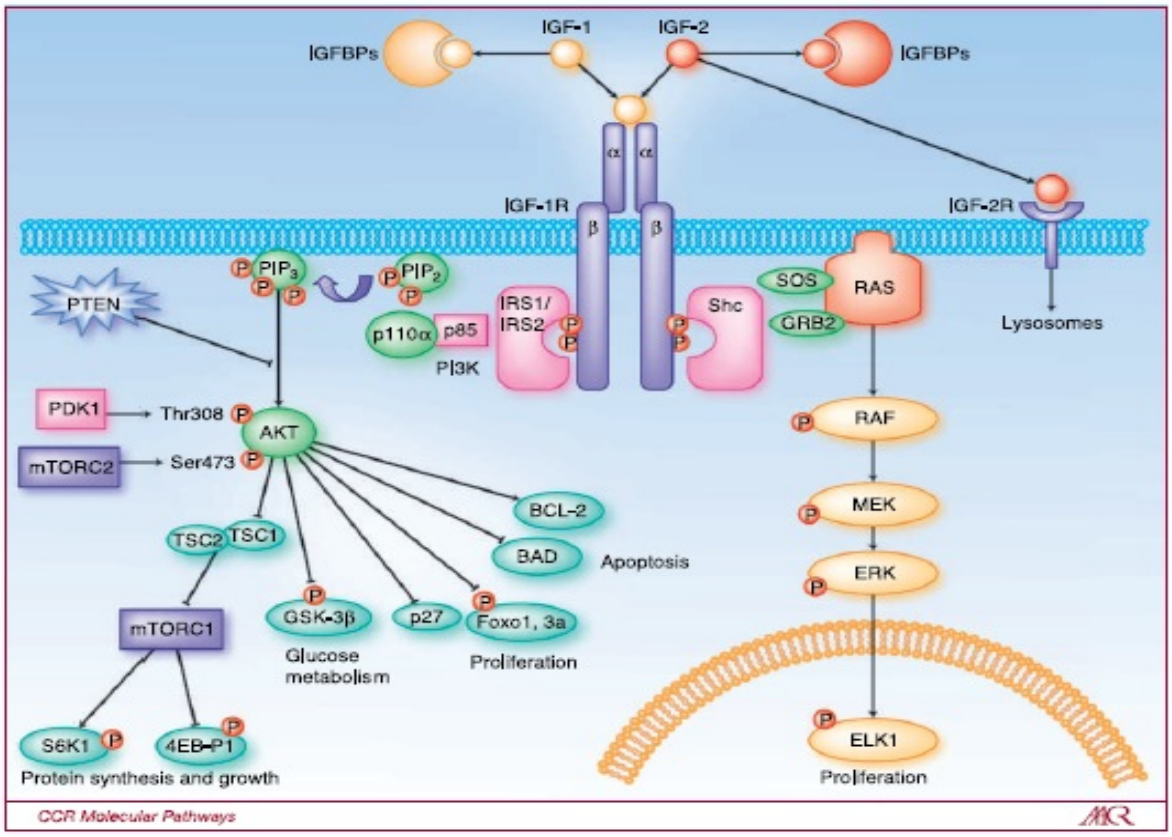

Figure 4: IGF-1R activation by ligands and downstream signalling

IGF-1R recognizes and is activated by both IGF-1 and IGF-2, however, their availability is controlled by IGFBPs and IGF-2R that bind IGF-2. Once activated by ligand, IGF-1R homo/heterodimerizes resulting in autophosphorylation and activation of downstream signal molecules IRS and Shc. Binding and phosphorylation of IRS1/2 results in activation of phosphatidyl inositol 3' kinase (PI3K). Consequently PIP2 is converted to PIP3 resulting in the recruitment of AKT to the plasma membrane where it becomes activated. AKT is then capable of phosphorylating downstream targets mTORC1, GSK-3β and others which are involved in protein synthesis, glucose metabolism, proliferation and survival. Recruitment and activation of Shc results in activation of the Ras/MAPK pathway which also stimulates cell proliferation. Adapted from Zha and Lackner 2010.

AKT plays a key role in metabolism, growth, survival and proliferation. It promotes survival by directly phosphorylating the pro-apoptotic proteins BAD (Fig. 4) and procaspase-9 resulting in their inactivation. AKT also phosphorylates MDM2, which sequesters p53 in the cytoplasm where it is degraded and, phosphorylates IKK which facilitates the activation of NF-κB resulting in the expression of pro-survival genes. Cell cycle progression is promoted

by AKT through various mechanisms: it activates β -catenin which associates with transcription factors resulting in expression of cyclin D1; it inhibits the FOXO transcription factors which are responsible for transcription of cell cycle regulatory proteins; and it also phosphorylates cell cycle inhibitors p21 and p27 leading to their translocation to the cytoplasm (Wickenden & Watson 2010; Steelman *et al.* 2011). AKT stimulates translation of protein, which is essential for growth, by phosphorylating tuberous sclerosis complex 2 (TSC2), thereby preventing the formation of the TSC1:TSC2 complex (Steelman *et al.* 2011). mTORC1 becomes activated, which signals down to S6 kinase and eukaryotic translation initiation factor 4E binding protein (4E-BP1) allowing for protein translation and cell growth (Fig. 4) (LoPiccolo *et al.* 2007; Shukla *et al.* 2008). Considering that IGF-1R plays such a crucial role in metabolism and growth a tight regulation is required to maintain homeostasis. When the activity of this receptor is deregulated, diseases like diabetes and cancer occur.

1.4.1 IGF-1R as a target in cancer

The importance of AKT in cancer cell biology is evident when considering that most cancers display dysregulation of many AKT-regulated processes, including glucose metabolism and protein synthesis. Mutations or upstream RTK activity results in deregulation and constitutive activation of the PI3K/AKT pathway facilitating the growth, proliferation and survival of numerous cancers (Chen *et al.* 2005). IGF-1R is overexpressed in breast cancer biopsies (Knowlden *et al.* 2005), in pancreatic cancer (Moser *et al.* 2008) and in >90% of colorectal cancer (CRC) (Höpfner *et al.* 2006). Expression levels of IGF-1 and IGFBP-3 were found to correlate with increased risk and poor survival of pancreatic and other cancers (Cao *et al.* 2008; Godsland 2010; Moser *et al.* 2008). Furthermore, high circulating levels of IGF-1 are

reported to increase the risk of secondary primary tumours (SPTs) in cancer of the head and neck, breast, lung, colon and prostate (Slomiany *et al.* 2006). IGF-1R has also been implicated in resistance to chemotherapeutic agents, and chemoresistant colorectal cancers display increased levels of total and activated IGF-1R (Chakraborty *et al.* 2008; Dallas *et al.* 2009).

Despite being strongly associated with transformation and drug resistance no mutations have been identified in the IGF-1R gene (Cao *et al.* 2008) and only duplication of gene copy number of IGF-1R or IGF is shown to associate with cancer (Massoner *et al.* 2010). Mutations within the PI3K pathway have been reported in roughly 30% of all cancers, with PTEN being the most common protein mutated in this pathway (Yi *et al.* 2005). Other mutations include point mutations in PI3KCA (p110α), AKT2 and 3-phophoinositide-dependent protein kinase 1 (PDK1) and amplifications of AKT2 and IRS-2 (Shaw & Cantley 2006). Aside from mutations within the PI3K pathway there are also feedback inhibitory loops which control protein expression and activity. Evidence suggests that PTEN can regulate the expression of IGF-1R, IGF-II and IGFPB3 in gastric adenocarcinoma cells (Yi *et al.* 2005). PKCδ was reported to activate mTOR, which increased IGF-1R expression in pancreatic cancer (Kwon *et al.* 2009). This activated an autocrine loop. mTOR occurs as two complexes, either the rictor mTORC2 or raptor mTORC1 complex. The rictor mTORC2 complex activates AKT and thus the balance between mTORC1/2 affects AKT activity (Kurmasheva & Houghton 2006). Cao *et al.* (2008) reported that overexpression of constitutively active AKT resulted in significantly reduced phosphorylation of endogenous AKT, suggesting AKT feedback autoinhibition. Supporting this is the observation that in the presence of nutrients when insulin activation is prolonged, PI3K and AKT activity is downregulated (Shaw & Cantley 2006). Recent evidence also suggests that AKT has feedback inhibition on other RTK including InsR and IGF-1R (Chandarlapaty *et al.* 2011).

1.4.2 IGF-1R and EGFR crosstalk and drug resistance

Aside from reports suggesting that the IGF-1R pathway can regulate itself and other RTK pathways, others indicate that IGF-1R can also transactivate and/or associate with other RTKs like EGFR. Meng *et al.*, 2007 found that in vascular smooth muscle cells (VSMC) IGF-1R activated EGFR resulting in cell proliferation and this activation was dependent on ROS production. In colon carcinoma cells, IGF stimulation activated the IGF-1R/PI3K pathway resulting in TGFα production and EGFR activation (Hu *et al.* 2008). In COS-7 cells, stimulation with IGF resulted in activation of MMPs, which consequently cleaved HB-EGF resulting activation of EGFR, this could be inhibited by MMP inhibitors and neutralizing HB-EGF antibodies (Roudabush *et al.* 2000). In breast cancer cell lines Riedemann *et al.*, (2007) observed EGFR:IGF-1R heterodimers using immunoprecipitation. IGF-1R reportedly also associated with HER2 in breast cancer cells suggesting that IGF-1R association is not restricted to EGFR (Chakraborty *et al.* 2008). Therefore considerable evidence points in the direction of RTKs, like EGFR and IGF-1R, having the ability to transactivate each other in particular cell types.

1.5 Chemokines and their cognate Receptors

Chemokines are small low molecular weight (8-17KDa) proteins that play important roles in infection, inflammation and the response of tissue to environmental external stimuli (Lazennec & Ann Richmond 2010). They serve as chemoattractants and recruit leukocytes to sites of inflammation. Chemokines can be divided into four sub families: C; CC; CXC and CX3C chemokines based on the spatial distribution of key cysteine residues in the N terminus (Bizzarri *et al.* 2006). CC and CXC chemokines comprise the majority of known chemokines (approximately 50). CXC chemokines can further be divided into two groups namely ELR+ and ELR- chemokines based on the presence of a Glutamine Leucine Arginine (ELR) motif (Addison *et al.* 2000; Keane *et al.* 2004). The ELR+ CXC chemokines promote angiogenesis, metastasis, survival and proliferation of tumour cells and include CXCL1, CXCL2, CXCL3, CXCL5, CXCL6, CXCL7, CXCL8 and CXCL12 (Table 1) (Catusse *et al.* 2003; Strieter *et al.* 2006; Balestrieri *et al.* 2008). CXC chemokines lacking the ELR motif are angiostatic, since they inhibit angiogenesis, proliferation and migration. ELR- chemokines include CXCL4, CXCL9, CXCL10 and CXCL11 while the function of the other chemokines, CXCL13-17, are less clear (Table 1) (Balestrieri *et al.* 2008). ELR+ or ELR- chemokines bind to their receptors commonly found on neutrophils; lymphocytes; endothelial and epithelial cells (Raman *et al.* 2007).

Table 1. Human chemokines and chemokine receptors

Systematic name	Synonyms	Specific receptor
CXC Chemokines		
CXCL1	Groα, MGSA-α, NAP-3	CXCR1,2
CXCL2	Groβ, MIP-2α, MGSA-β, CINC-2α	CXCR2
CXCL3	Groγ, MIP-2α, CINC-2β	CXCR2
CXCL5	ENA-78	CXCR2
CXCL6	GCP-2	CXCR1,2
CXCL7	LDGF-PBP, CTAPIII, NAP-2, PF4, MDGF, LDGF, β-TG	CXCR1,2
CXCL8	IL-8, NAP-1, MDNCF, GCP-1	CXCR1,2
CXCL4	PF4	CXCR3A, 3B
CXCL4V1		CXCR3A, 3B
CXCL9	MIG	CXCR3B
CXCL10	IP-10, CRG-2	CXCR3B
CXCL11	I-TAC, β-R1, IP-9	CXCR3B
CXCL12	SDF-1α/β, PBSF	CXCR4,7
CXCL13	BCA-1, BLC	CXCR5
CXCL14	BRAK, Bolekine	Unknown
CXCL16	SRPSOX	CXCR6
CXCL17	DMC, VCC-1	Unknown

Adapted from Balestrieri et al., 2008.

A group of plasma membrane receptor proteins termed G-protein coupled receptors (GPCRs), of which 18 have been described thus far, recognize and bind chemokines with various affinities (Kakinuma & Hwang 2006; Raman *et al.* 2007). Certain chemokines make use of the same receptors suggesting that redundancies exist in their function (Kakinuma & Hwang 2006). All angiogenic (ELR+) chemokines bind the common receptor CXCR2 with the exception of CXCL8 which binds both CXCR1 and CXCR2, and CXCL12 which binds CXCR4 and CXCR7 (Table 1) (Burger *et al.* 2005; Mestas *et al.* 2005; Balestrieri *et al.*

2008). CXCR2, a member of the GPCR family, is a 360 amino acid glycoprotein containing 7 transmembrane domains separated by 3 intracellular and 3 extracellular loops (Chapman *et al.* 2009; Lagerström & Schiöth 2008). The predicted molecular weight of CXCR2 is 40 kDa, however, when it is phosphorylated a shift in size occurs which may represent receptor degradation (Mueller *et al.* 1997; Schraufstätter *et al.* 1998). CXC receptors share 25-80% homology and CXCR2 is 78% homologous to CXCR1 at the amino acid level, with major differences located at the amino terminus, the carboxyl terminus and the second extracellular loop (Addison *et al.* 2000; Chapman *et al.* 2009). Numerous cell types including keratinocytes, fibroblasts, endothelial cells, neutrophils, macrophages, monocytes and leukocytes express CXCR2 with its functional relevance being more clearly associated with migration/chemotaxis of immune cells to an immune response and sites of inflammation (Auten *et al.* 2001; Varney *et al.* 2003; Ho *et al.* 2006; Rigamonti *et al.* 2008; Yang *et al.* 2010).

Ligand binding to CXCR2 results in the activation of guanine nucleotide-binding proteins (G proteins) associated with the receptor, which activate phospholipase C (PLC). PLC in turn catalyzes the conversion of target phospholipids to diacylglycerol and inositiol triphosphate (Fig. 5) resulting in calcium mobilisation which is important for migration of neutrophils (Yang *et al.* 1999; Fan *et al.* 2003; Sai *et al.* 2006; Chapman *et al.* 2009). G proteins (Gαβγ) also relay CXCR2 signals down the Ras/MAPK/ERK1/2 pathway resulting in translocation of ERK1/2 to the nucleus where E2F, NF-κB and activator protein transcription factors are activated leading to transcription of numerous genes involved with cell proliferation as described earlier for MAPK signalling (Fig. 5) (Waugh & Wilson 2008; Yang *et al.* 2010). Silencing of CXCR2 in ovarian cancer cells resulted in increased expression of p21 while cyclin D1, cyclin A, cyclin B1, CDK2 and CDK6 levels were decreased suggesting that CXCR2 promotes proliferation of cancer cells (Yang *et al.* 2010). PI3K/AKT activation by

CXCR2 leads to increased mTORC1 activity resulting in protein translation by 4E-BP and S6 kinase as previously described for AKT signalling (Waugh & Wilson 2008). Cell polarization towards a chemoattractant via actin nucleation and focal adhesion assembly are also important events downstream of PI3K/AKT essential for chemotaxis (Yang *et al.* 1999; Waugh & Wilson 2008). The MAPK and PI3K pathways are major downstream targets of CXCR2 since in many cell types stimulation of CXCR2 results in MAPK and PI3K signalling but barely activates stress kinases p38 and JNK (Yang *et al.* 1999; Waugh & Wilson 2008; Zhao *et al.* 2004; Sai *et al.* 2006). CXCR2 is rapidly internalized under conditions where the receptor has bound ligand, at a rate faster than that for CXCR1 (Schraufstätter *et al.* 1998; Neel *et al.* 2005). Once bound to ligand CXCR2 is internalized in clathrin-coated pits with the assistance of arrestins, and is targeted for recycling or degradation (Yang *et al.* 1999; Fan *et al.* 2003; Revankar *et al.* 2004).

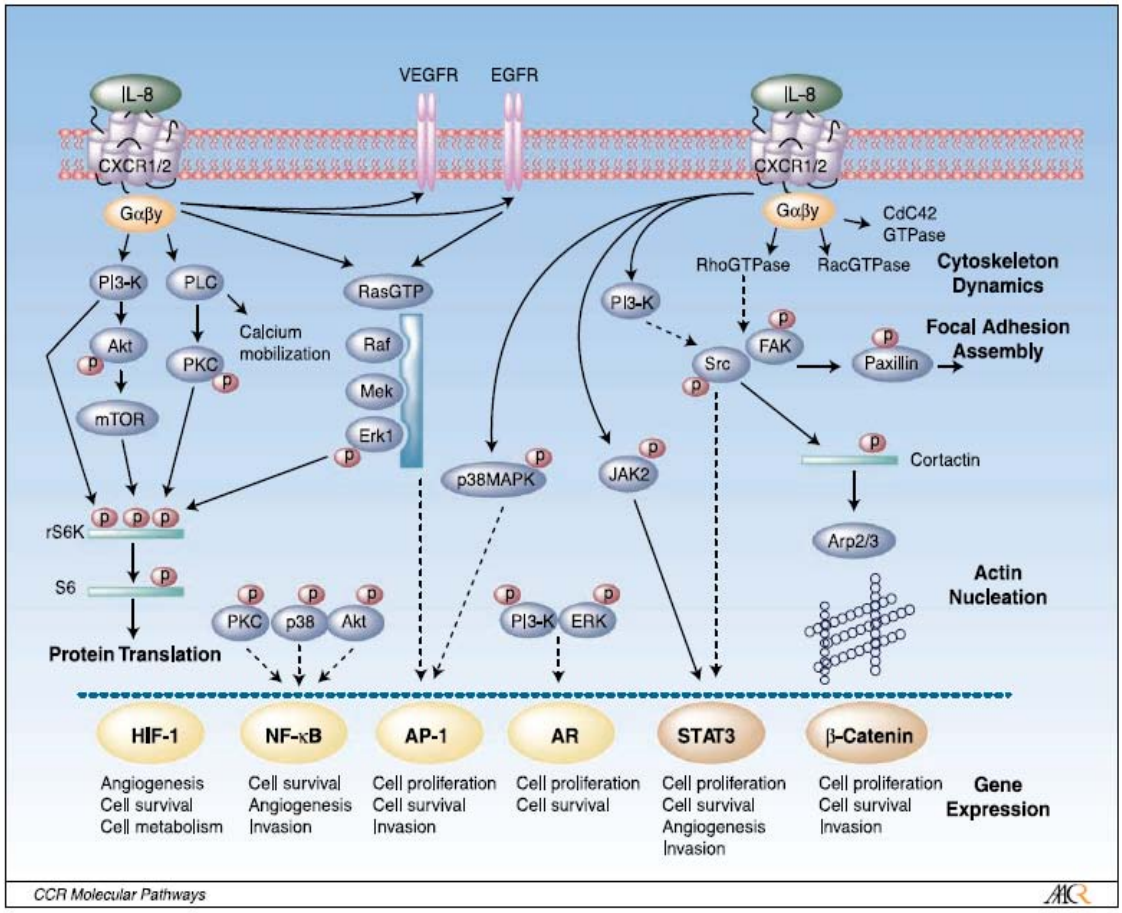

Figure 5: CXCR1/2 activation by Interleukin 8 (IL-8) and downstream signalling

Binding of IL-8 to its cognate receptors CXCR1 and CXCR2 results in phosphorylation of serine and threonine residues. This allows for the recruitment of guanine nucleotide-binding proteins (Gαβγ) which activates phosphatidyl inositol 3' kinase (PI3K), Phospholipase C (PLC) and RasGTP. Downstream signalling pathways are involved with calcium mobilization, gene expression, protein synthesis and cytoskeleton dynamics. From Waugh and Wilson 2008.

Reports have linked aberrant internalization, degradation and recycling of GPCRs to disease states. The accumulation of the GPCR v2 vassopressin receptor as a result of desensitization and internalization results in nephrogenic diabetes insipidus (Wagener *et al.* 2009). Evidence exists that CXCR2 can drive cutaneous inflammation in skin carcinogenesis by the recruitment of neutrophils (Cataisson *et al.* 2009). Overexpression of CXCR2 in NIH 3T3

cells *in vitro* leads to cell transformation (Burger *et al.* 2005). Epithelialisation and neovascularisation which involves recruitment of neutrophils are also mediated by CXCR2 during wound repair (Devalaraja *et al.* 2000). ELR+ chemokines attract leukocytes to sites of inflammation and elicit an immune response. Cells of the immune system respond to this increasing gradient of ELR+ chemokines and arrest at the site of tissue damage or infection (Svensson *et al.* 2008). Overexpression or deregulation of ELR+ chemokines has been linked to diseases such as arthritis, diabetes, Alzheimer's, asthma, pulmonary diseases and cancer (Aggarwal *et al.* 2006). Chronic inflammation of the intestine termed ulcerative colitis (UC) involves accumulation of leukocytes in the mucosa of the colon. Not surprisingly, CXCL8 and CXCR1/2 expression was found elevated in patients with UC (Bizzarri *et al.* 2006). Pulmonary diseases such as cystic fibrosis and asthma have an increased concentration of neutrophils associated with the inflammatory environment of the disease. Elevated levels of CXCL8 and CXCR2 have been linked to pulmonary diseases (Chapman *et al.* 2009). Evidence suggests that CXCR2 promotes autosomal dominant polycystic kidney disease (ADPKD) and liver cyst growth (Amura *et al.* 2008). The irregular production of chemokines and their receptors in the tumour environment results in recruitment of leukocytes which can contribute as much as 70% of the tumour mass (Yan *et al.* 2006). Chemokine receptors found associated with tumours include: CXCR2 important for angiogenesis; CCR2 responsible for recruitment of macrophages in the tumour micro environment; CCR7 which aids metastasis into sentinel lymph nodes which produce CCR7 ligand CL21; and CXCR4 involved in metastatic spread of numerous tumours (Raman *et al.* 2007). There is strong evidence that deregulation of chemokines and their receptors play a role in the onset of many diseases including cancer.

1.5.1 Chemokines and CXCR2 in Cancer

Chemokines and their receptors are important in host mediated defence against infections, environmental stimuli and mechanical injury by eliciting an inflammatory response. Furthermore, numerous reports strongly suggest that inflammation and cancer are closely related processes, since tumours are often surrounded by cells of the immune system and chemokine ligands, and/or receptors are elevated in most cancers (Aggarwal *et al.* 2006; Wislez *et al.* 2006; Acosta & Gil 2009; Cataisson *et al.* 2009; Varney *et al.* 2011). Chemokine expression has also been linked to tumourogenesis and angiogensis of tumours. The chemokines IL-1, IL-6 and IL-8 are reported to promote growth and metastasis of various cancers, and inhibition of IL-8 in NSCLC xenografts was shown to reduce vascular density and tumour volume by 40% (Watanabe *et al.* 2002; Aggarwal *et al.* 2006). In a murine squamous cell carcinoma model, overexpression of GROα resulted in increased infiltration of leukocytes to the tumour site and increased vascularity (Loukinova *et al.* 2000). The evidence that ELR+ chemokines are associated with cancer growth and angiogenesis suggests that their receptors also play a role linking autocrine or paracrine ligand cues with intracellular signalling. Most ELR+ chemokines bind the common receptor CXCR2 and reports have observed a functional role of CXCR2 in certain cancers.

ELR+ chemokines can act in an autocrine loop in melanoma and pancreatic cancer where NF-κB drives transcription of IL-8 which activate the receptors CXCR1/2 (Wente *et al.* 2006; Luppi *et al.*, 2007). Melanoma cells displaying elevated levels of IL-8 and CXCR2 have reduced proliferation and angiogenesis when targeted with CXCR2 small molecule inhibitors (Singh *et al.* 2009; Yang *et al.* 2010). In pancreatic cancer patients, CXCL5 and CXCL8 are elevated with expression correlating with tumour aggression, whereas inhibition of CXCR2

in pancreatic cancer xenografts resulted in significantly reduced tumour volume and microvessel density (Matsuo *et al.* 2009). Mestas *et al.*, (2005) observed elevated CXCR2 ligands in the plasma of renal cell carcinoma (RCC) patients versus that of healthy control individuals. Furthermore, this group showed that RCC tumour volume is significantly reduced when xenografted into CXCR2-/- vs CXCR2+/+ mice. A similar observation was reported for lung cancer xenografts in CXCR2-/- mice (Keane *et al.* 2004). A previous study in our laboratory suggested the presence of a CXCR2/GROβ autocrine loop in oesophageal cancer cells since silencing GROβ expression resulted in reduced cell proliferation *in vitro* (Wang *et al.* 2006).

This review has shown that EGFR, IGF-1R and CXCR2 are frequently dysregulated in many cancers, and that they may contribute to the tumourigenic state. The aim of this study was to characterise the role of EGFR, IGF-1R and CXCR2 in OSCC cultured cells with the following main objectives being:

- determining the expression of EGFR, IGF-1R and CXCR2 in OSCC cell lines
- verify whether receptors are functional and activate downstream MAPK and AKT pathways
- evaluate the effect of receptor inhibition or silencing on cell proliferation and survival
- assess the potential of these three receptors as therapeutic targets for the management of OSCC.

Chapter 2

Epidermal Growth Factor Receptor and Type-1 Insulin-like Growth Factor Receptor as potential therapeutic targets for Oesophageal Cancer

2.1 Introduction

The epidermal growth factor receptor (EGFR) is commonly overexpressed in 30-80% of OSCC cases as well as in other cancers of epithelial origin (Tew *et al.* 2005; Weihua *et al.* 2008). Overexpression of EGFR in oesophageal cancer correlates with poor patient survival and increased tumour aggressiveness making it an interesting target for OSCC therapy. However this receptor has been targeted in other cancers with patients showing limited response to therapy (Cohen *et al.* 2005; Ono & Kuwano 2006; Sharma *et al.* 2007). A few clinical trials have explored the potential of EGFR as a target in OSCC but these results are difficult to interpret given that most patients in these studies present with advanced stages of disease, and some had already undergone surgery or chemotherapy as a first line of treatment. Furthermore, patient numbers are often small, patient cohorts frequently consist of both SCC and AC, and EGFR expression levels were not assessed in patients prior to initiation of treatment (Janmaat *et al.* 2006; Ferry *et al.* 2007; Sudo *et al.* 2007; Dragovich & Campen 2009). The general poor response to EGFR targeted therapy suggests that there may be other underlying processes either compensating for loss of EGFR function or that EGFR contributes to tumour proliferation but that it is not crucial for tumour survival.

In numerous cancers the insulin-like growth factor receptor (IGF-1R) has been implicated in the development of drug resistance both in cancer cell line models and in the clinical setting. Non-small cell lung cancer (NSCLC) patients resistant to EGFR-targeted therapy, gefitinib and erlotinib, reportedly display elevated levels of active IGF-1R, and inhibition of IGF-1R has been found to restore sensitivity to gefitinib or erlotinib in resistant NSCLC cell lines (Morgillo *et al.* 2007a; Morgillo *et al.*, 2007b). Similar observations have been reported in breast cancer patients resistant to the HER2 monoclonal antibody, transtuzumab (Chakraborty *et al.* 2008). Although elevated levels of IGF-1R correlated with poor survival in OSCC patients, little is known regarding its potential as a target in OSCC (Sutter *et al.* 2006). Evidence in the literature regarding the important role that EGFR and IGF-1R play in several cancers highlights the need for a better understanding of these receptors in OSCC.

2.2 Results

2.2.1 EGFR and IGF-1R expression and signalling

Since many studies reported that EGFR and IGF-1R are overexpressed in OSCC tissue compared to adjacent normal tissue (Imsumran *et al.* 2007; Sutter *et al.* 2006) we proceeded to determine the expression of EGFR and IGF-1R in a panel of cultured OSCC cell lines. Oesophageal cancer cell lines, established from primary OSCC tumours, were cultured and the protein harvested for western blot analysis. As observed in Figure 2.1, EGFR and IGF-1R were expressed in all cell lines albeit at different levels. WHCO1 and WHCO6 were chosen as model cell lines to explore EGFR and IGF-1R and their associated signalling pathways since these cell lines have been routinely used in our laboratory to further our understanding of OSCC cell biology (Whibley *et al.* 2005; Wang *et al.* 2006; Whibley *et al.* 2007; Wang *et al.* 2009).

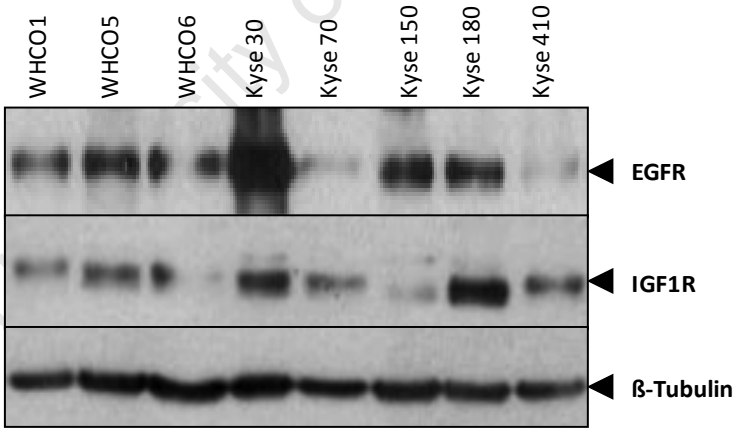

Figure 2.1: EGFR and IGF-1R expression in OSCC cell lines.

OSCC cells were cultured to 60-70% confluency and protein was harvested. A total of 40 µg of protein lysate from each cell line was separated by SDS-PAGE electrophoresis and transferred to nitrocellulose membrane. The membrane was probed with antibodies recognizing total EGFR and IGF-1R. Beta-tubulin was used as a loading control for all subsequent experiments unless stated otherwise and each figure is a representative of 3 experiments.

Since both receptors were present in the cell lines, we next determined if these receptors were functional and capable of activating their downstream targets. WHCO1 and WHCO6 cells were stimulated with 20 ng/ml EGF or 50 ng/ml IGF-1 for the indicated time periods and protein was harvested for western blot analysis. Receptor activation was visualised by probing with antibodies directed to the phosphorylated forms of EGFR (anti-pTyr1173) and IGF-1R (anti-pTyr1131). EGFR was rapidly activated by EGF and its activity could be measured up to 1 hour post-treatment, after which activity was lost (Fig. 2.2A). This was consistent with reports for EGFR activation and desensitization after stimulation with ligand (Burke *et al.* 2001). Similarly, ERK1/2 was strongly activated by EGF treatment while AKT activation increased slightly, similar to previous reports that EGFR strongly regulates ERK1/2 activity compared to AKT activity (Cao *et al.* 2008; Hu *et al.* 2008; Villanueva *et al.* 2010). Total EGFR levels were also reduced by 3 hr and 8 hr post-EGF treatment in both WHCO1 and WHCO6 cells, suggesting that prolonged stimulation with EGF resulted in EGF receptor degradation (Appendix Fig. A1). Protein levels of IGF-1R, AKT and ERK1/2 remained unchanged when cells were treated with EGF (Appendix Fig. A1). The signalling results observed here, suggested that functional EGFR was capable of relaying signals down the MAPK-ERK1/2 and PI3K-AKT pathway (Fig. 2.2A).

Stimulation with IGF-1 resulted in a sustained activation of IGF-1R and its downstream target AKT indicating that this receptor was also functional in the model OSCC cell lines WHCO1 and WHCO6 (Fig. 2.2B). The sustained IGF-1R activity is consistent with reports that IGF-1R activation is stable (Hansen *et al.* 1996). Furthermore, total IGF-1R levels also remained unchanged in the presence of IGF-1 treatment (Appendix Fig. A1). Several interesting observations were noted in the response of the cells to treatment with EGF and IGF. Firstly, EGF stimulation resulted in the early transient activation of IGF-1R – more noticeable in WHCO1 than WHCO6 cells (Fig. 2.2A). IGF-1 stimulation had no effect on the

activation of EGFR (Fig. 2.2B). Lastly, a strong decrease in pERK1/2 was noted when cells were stimulated with IGF-1 (Fig. 2.2B). These observations were further addressed to determine if there were any interactions between the EGFR and IGF-1R pathways in OSCC cell lines, as suggested by literature reports for other tissues (Roudabush *et al.* 2000; Meng *et al.* 2007; Riedemann *et al.* 2007; Hu *et al.* 2008).

A

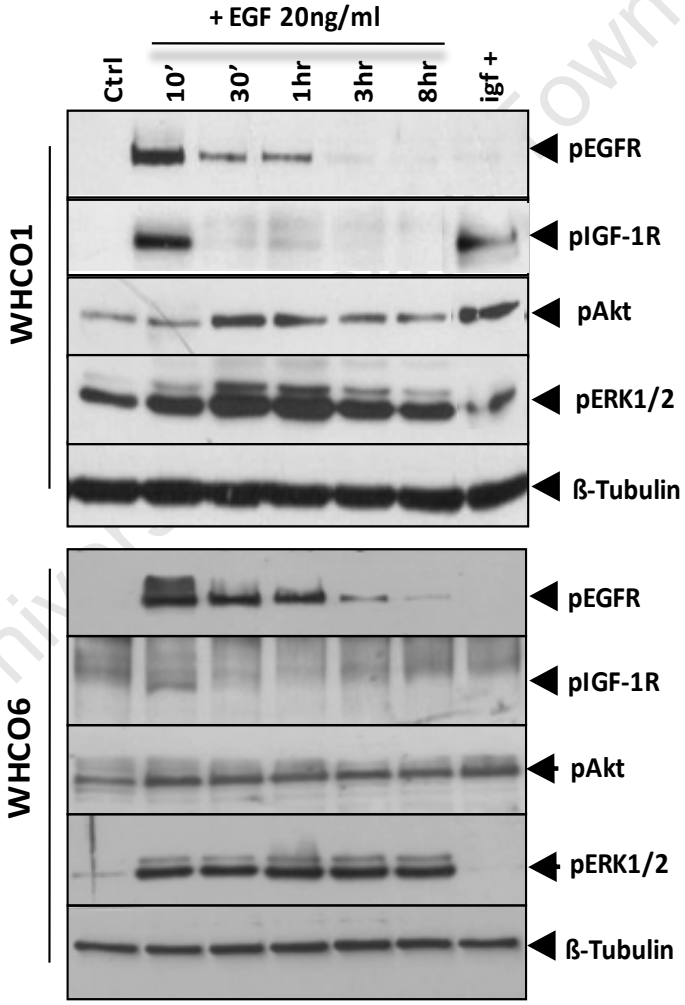

B

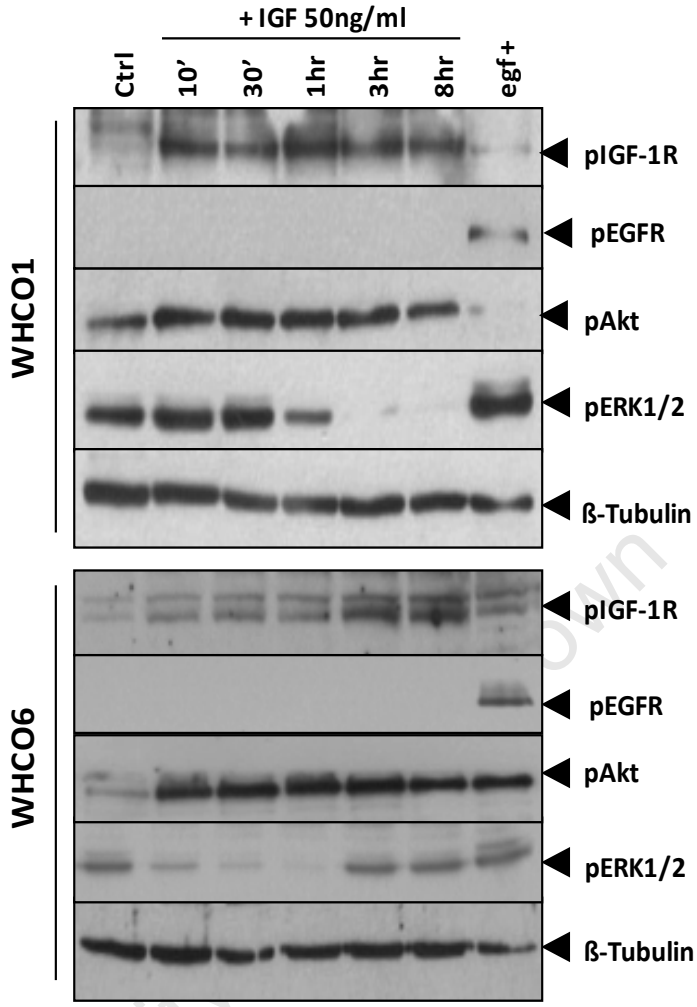

Figure 2.2: EGF and IGF-1 stimulation in OSCC cell lines.

WHCO1 and WHCO6 cells were seeded at 3 x 10^5 cells per 60 mm dish. Cells were serum starved for 1hr in serum free DMEM followed by stimulation with 20 ng/ml EGF or 50 ng/ml IGF-1 in serum free DMEM for the indicated times. Protein was harvested and subjected to western blot analysis using antibodies specific for pIGF-1R, pEGFR, pAKT and pERK1/2 (A and B). The last lane in A and B represents cells stimulated with either 20 ng/ml EGF (egf+) or 50 ng/ml IGF-1 (igf+) for 10 min and served as a positive control to detect pEGFR or pIGF-1R.

Crosstalk from IGF-1R to EGFR has been reported in other cancers as mentioned earlier. However, when OSCC cells were stimulated with IGF-1 we could not detect an increase in pEGFR despite the positive response observed in the lane of EGF-stimulated cells (Fig 2.2B). Ligand binding to EGFR results in dimerization and autophosphorylation of Tyr residues, with pTyr1173 being the major phosphorylation site indicative of fully active EGFR (Mandic *et al.* 2006). Seeing that the pEGFR antibody used here only recognised pTyr1173, we could not exclude the possibility that EGFR may be phosphorylated at other sites in response to IGF-1 treatment. To address this problem, WHCO1 cells were stimulated with IGF-1 for 10 min or 3 hr; and with EGF ligand for 10 min as a positive control. Protein was harvested and subjected to immunoprecipitation using anti-EGFR, followed by western blotting. A pan-pTyr antibody, readily detected pEGFR in the EGF stimulated cells (Fig. 2.3, lane 2), however, no increase in pEGFR was observed in the IGF-1 treated cells (Fig. 2.3, lanes 3 and 4). EGFR was present at approximately equal levels in all lanes indicating that the receptor was successfully immunoprecipitated in each pull down experiment. This result confirmed that IGF-1 treatment was not associated with activation of EGFR in OSCC cells.

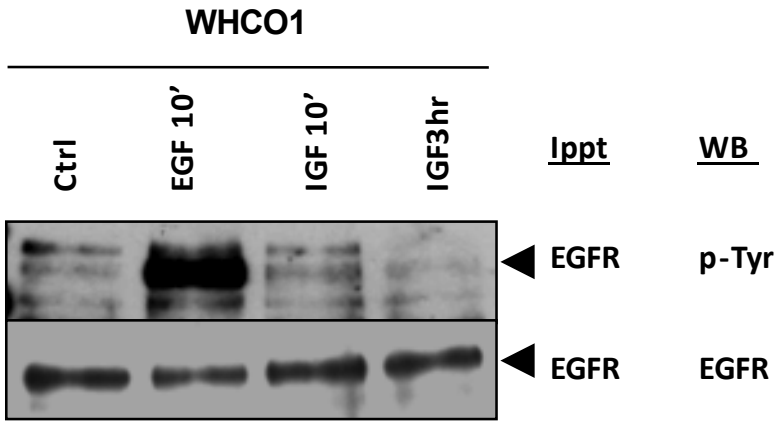

Figure 2.3: EGFR activity in the presence of EGF or IGF-1 in WHCO1 OSCC cells.

A total of 3 x 10^5 WHCO1 cells were serum starved followed by treatment with either 20 ng/ml EGF or 50 ng/ml IGF-1 for the indicated time points in 60 mm dishes. Protein was harvested and 300 µg of protein was subjected to EGFR immunoprecipitation (Ippt). EGFR immunoprecipitates were subjected to western blotting, probing with EGFR or pan-pTyr specific antibodies.

Our observation that IGF-1R was rapidly phosphorylated in response to EGF treatment in OSCC cell lines (Fig. 2.2A) has not been reported previously. We observed the same result in two other OSCC cell lines (WHCO5 and KYSE 180), suggesting that this phenomenon was not an artefact associated with specific cell lines (appendix Figure A2). We thus sought to determine if the activation of IGF-1R was dependent on the activation of EGFR or if EGF directly activated IGF-1R. Cells were pre-treated with the EGFR kinase domain inhibitor, AG1478, for 30 min followed by stimulation with EGF. Protein was harvested and analysed by western blot analysis using antibodies specific for pEGFR and pIGF-1R. EGF-induced phosphorylation of EGFR was completely abrogated in the presence of AG1478 indicating that the concentration of inhibitor used was sufficient to inhibit EGFR activity (Fig. 2.4). Furthermore co-treatment of cells with EGF and AG1478 also prevented the transient EGF-induced phosphorylation of IGF-1R, indicating a requirement for EGFR activity in this crosstalk.

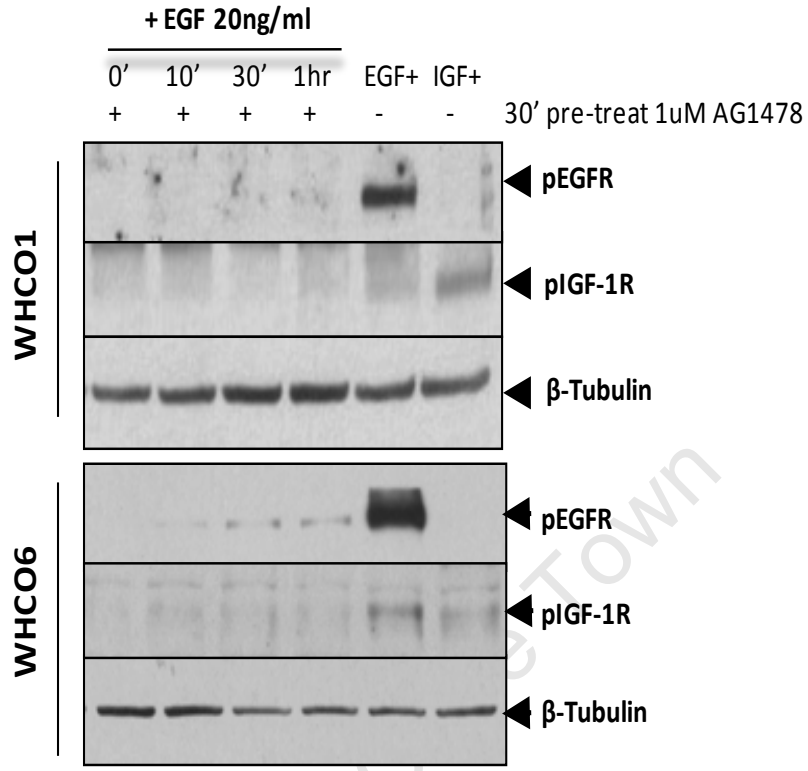

Figure 2.4: EGFR and IGF-1R activity in the presence of EGF and EGFR kinase inhibitor AG1478.

WHCO1 and WHCO6 cells were pre-treated with 1 μM EGFR kinase inhibitor AG1478 for 30 min followed by stimulation with 20 ng/ml EGF for the indicated time period. Cell lysates were subjected to western blot analysis using antibodies towards pEGFR and pIGF-1R. Cells stimulated with either 20 ng/ml EGF (EGF+) or 50 ng/ml IGF-1 (IGF+) for 10 to 30 min were used as positive controls.

The observation that IGF-1R was rapidly phosphorylated in response to EGF treatment, and that this phosphorylation was dependent on activated EGFR, suggested that EGFR could directly activate IGF-1R. Riedemann *et al.*, (2007) reported the presence of EGFR/IGF-1R dimers in breast cancer cells. A similar interaction between these receptors in OSCC cells could in part, explain the EGF-induced phosphorylation of IGF-1R that we observed. To further investigate an association between EGFR and IGF-1R, cells were cultured to 70% confluency and protein was harvested and incubated with an EGFR antibody overnight. EGFR was pulled down with protein-A agarose beads and subjected to western blot analysis using antibodies against EGFR and IGF-1R. We performed EGFR immunoprecipitations in several OSCC cell lines to determine the presence of EGFR/IGF-1R hetero-dimers. When protein lysate was incubated with beads only, as a negative control, we observed no non-specific bands corresponding to EGFR and IGF-1R. Both EGFR and IGF-1R were present in all EGFR immunoprecipitates suggesting that these receptors associate with each other in all of the OSCC cell lines tested (Fig. 2.5).

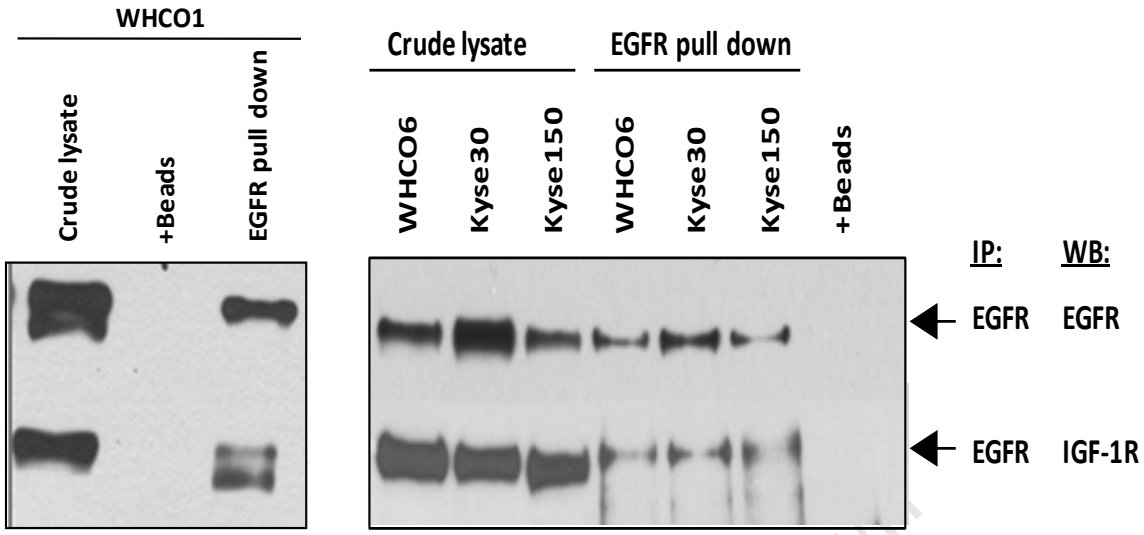

Figure 2.5: EGFR immunoprecipitation in OSCC cell lines.

Protein harvested from OSCC cell lines was subjected to EGFR immunoprecipitation (IP). Protein lysate (300 µg) was incubated with EGFR primary antibody overnight at 4°C with rotation. Protein-A agarose beads was added and incubated for 4 hr with rotation, EGFR was pulled down by centrifugation and analysed by western blotting using antibodies to EGFR and IGF-1R as indicated. A negative control (+Beads), consisting of protein lysate incubated with protein A beads in the absence of EGFR antibody, was performed in parallel to rule out non-specific binding of target proteins to the beads.

2.2.2 IGF-1R-AKT negatively regulates the EGFR-ERK1/2 axis

As previously mentioned, activation of the IGF-1R pathway with IGF-1 resulted in a sharp decrease in pERK1/2 levels in WHCO1 and WHCO6 OSCC cells (Fig. 2.2B). This observation was reproducible in multiple experiments and in another OSCC cell line, WHCO5 (Appendix Fig. A3). This suggested that activation of the IGF-1R pathway negatively regulated ERK1/2 activity under these conditions. Considering this observation,

we questioned whether the inverse was true, hypothesising that inhibition of basal IGF-1R activity would result in increased levels of pERK1/2. At the time when these experiments were conducted most IGF-1R inhibitors that were commercially available were not very specific, and cross-reacted with the insulin receptor while the more specific inhibitors were under patent rights and could not be obtained. For this reason, cells that stably expressed IGF-1R shRNA or control non-specific shRNA were generated using a lentiviral system. WHCO1 and WHCO6 cells were infected with lentiviral particles containing IGF-1R specific shRNA or random shRNA, and transfected cells were selected by FACS analysis based on GFP positivity (as described in methods section). Cells were cultured and protein harvested under normal unstimulated culture conditions for western blot analysis. Total IGF-1R and pAKT levels were reduced by ≥50%, and both EGFR and ERK1/2 levels displayed increased phosphorylation whereas total EGFR levels were reduced (Fig. 2.6).

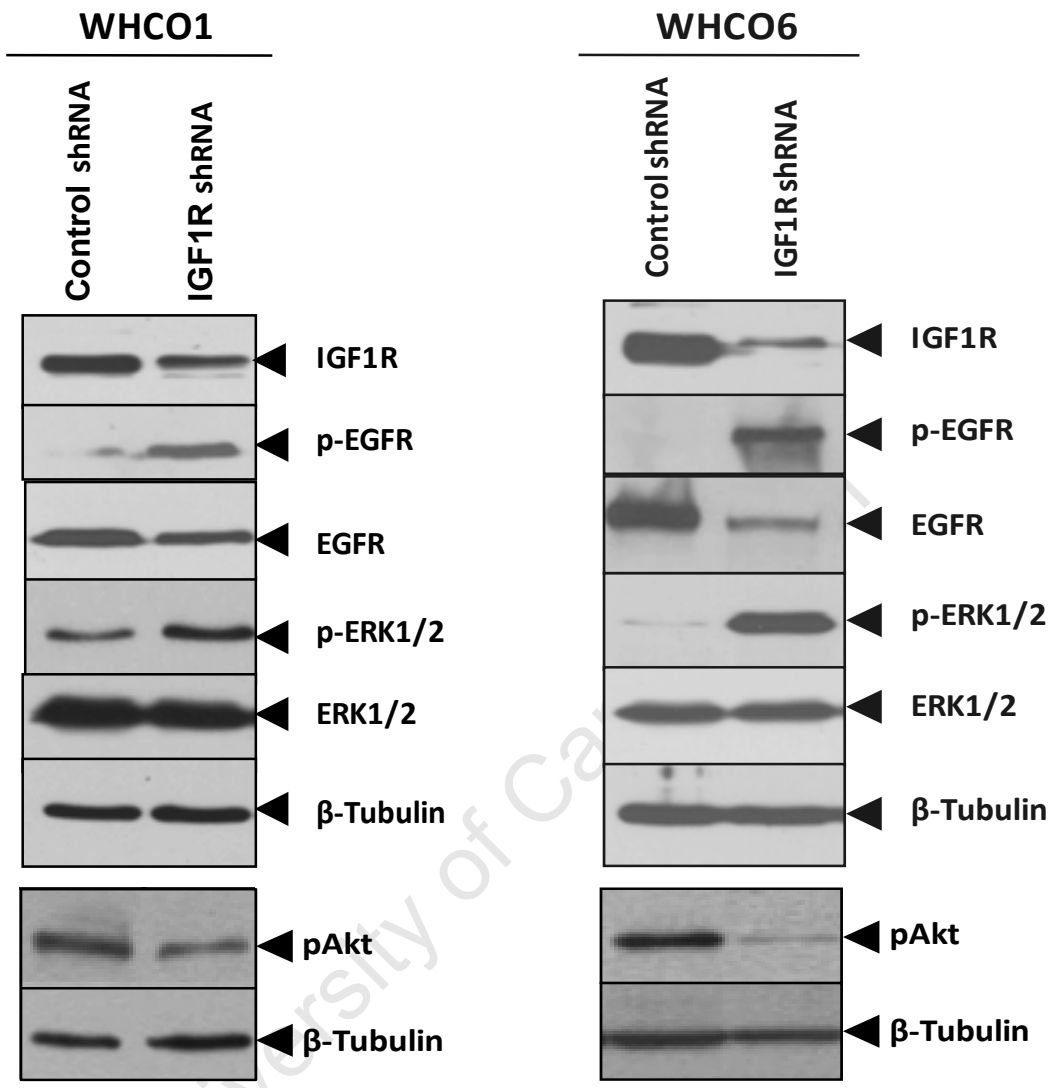

Figure 2.6: IGF-1R knockdown in WHCO1 and WHCO6 OSCC cell lines.

WHCO1 and WHCO6 cells were infected with lentiviral particles containing either Ctrl or IGF-1R shRNA expression vectors and transfected cells were collected using a cell sorter. Protein was harvested from Ctrl and IGF-1R shRNA cells and analyzed by western blot analysis using antibodies to IGF-1R, pEGFR, EGFR, pERK1/2, ERK1/2 and pAKT.

The decrease in pERK1/2 levels associated with IGF-1 treatment, and the increase in pERK1/2 levels observed when IGF-1R was knocked down suggested the presence of an IGF-1R driven, negative feedback loop impinging on the Ras/ERK1/2 MAPK pathway. Recent evidence has implicated AKT in negatively regulating receptor tyrosine kinases that include Her3, Her4 and InsR (Chandarlapaty *et al.* 2011). Furthermore, evidence suggests that AKT activity negatively regulates Raf, one of the upstream signalling molecules in the Ras-Raf-Mek-ERK1/2 pathway (Moelling *et al.* 2002; McCubrey *et al.* 2007). We used another approach (an AKT inhibitor) to further explore the link between the IGF-1R/AKT and EGFR signalling pathways in OSCC. Parental WHCO1 and WHCO6 cells were treated with 20 μM AKT VIII trifluoroacetate salt for the indicated time points, protein was harvested and analysed by western blot analysis using antibodies to pEGFR and pERK1/2.

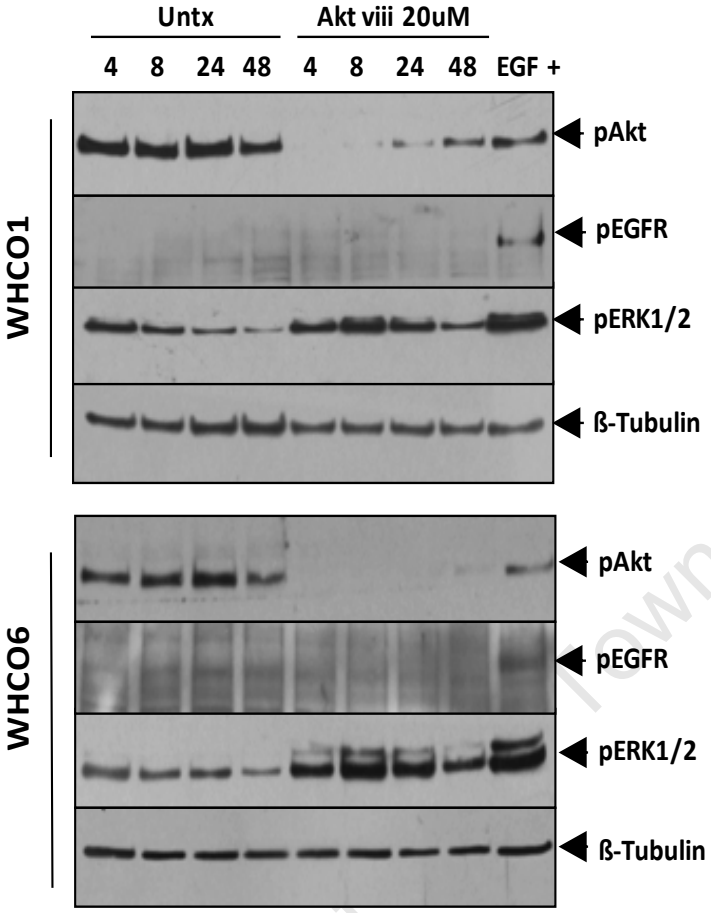

Figure 2.7: Effect of AKT inhibitor (AKT VIII trifluoroacetate salt) on pEGFR and pERK1/2 in WHCO1 and WHCO6 OSSCC cell lines.

WHCO1 and WHCO6 cells (3 x 10^5 cells per 60 mm dish) were treated with 20 μM AKT inhibitor (AKT VIII trifluoroacetate salt) for the indicated times and protein was harvested. The cell lysates were analyzed by western blot analysis using antibodies specific for pAKT, pEGFR and pERK1/2.

The AKT inhibitor clearly blocked the activation of AKT for at least 24 hr in WHCO1 cells and for 48 hr in WHCO6 (Fig. 2.7). AKT inhibition was associated with a significant increase in pERK1/2 levels in both cell lines. However AKT inhibition had no effect on pEGFR levels. This suggested that in OSCC cells AKT signalling regulated ERK1/2 activity but exerted no inhibition on EGFR activity or expression.

To exclude the possibility that IGF-1R knockdown cells secreted elevated levels of EGFR ligand, hence activating EGFR as observed in Figure 2.6, we treated wild type WHCO1 and WHCO6 cells with conditioned medium from the IGF-1R knockdown cells. Briefly, WHCO1 and WHCO6 cells expressing Ctrl or IGF-1R shRNA were cultured to 60-70% confluency. The conditioned medium harvested from WHCO1 and WHCO6 Ctrl and IGF-1R shRNA cells was transferred to WHCO1 and WHCO6 parental cell lines respectively. In both WHCO1 and WHCO6 parental cells no increase in pEGFR was observed following incubation in conditioned medium from Ctrl or IGF-1R shRNA transfected cells (Fig. 2.8). This suggests that the IGF-1R shRNA cells do not produce increased levels of EGFR ligands, and indicates that the process responsible for increased EGFR activation in IGF-1R knockdown cells does not involve upregulation of EGFR ligands.

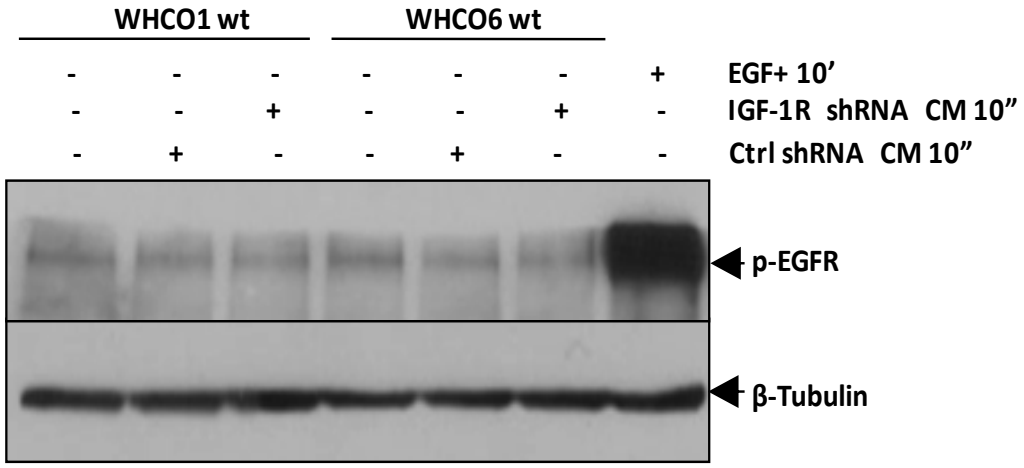

Figure 2.8: EGFR activity in parental WHCO1 and WHCO6 cells in the presence of Ctrl or IGF-1R shRNA conditioned medium.

WHCO1 and WHCO6 Ctrl and IGF-1R shRNA cells were grown to 60-70% confluency and cells were incubated for 16 hr with serum-free DMEM medium. Conditioned media (CM) (serum free DMEM) from WHCO1 and WHCO6 Ctrl and IGF-1R shRNA transfected cells were added to the respective parental (wt) WHCO1 and WHCO6 cells for 10 min and protein was harvested. Cell lysate was analyzed by western blot probing for pEGFR. WHCO1 cells treated with 20 ng/ml EGF for 10 min was used as a positive control for pEGFR (EGF+ 10').

The work described thus far has characterized a part of the EGFR and IGF-1R signalling pathway in OSCC cell lines, allowing the following important observations: EGFR and IGF-1R are functional and co-associate in several OSCC cell lines; EGFR rapidly activates IGF-1R within ten min when cells are stimulated with EGF and this activation requires EGFR kinase activity; lastly IGF-1R signalling negatively regulates EGFR/ERK1/2 activity as IGF-1 treatment reduced pERK1/2 levels and IGF-1R knockdown resulted in increased pEGFR and pERK1/2 levels. This evidence of significant cross-talk between the EGFR and IGF-1R pathways in OSCC prompted us to investigate the potential of EGFR and IGF-1R, as drug targets in OSCC cell lines.

2.2.3 EGFR and IGF-1R as drug targets in OSCC

After incubating OSCC cultured cells and normal cultured skin fibroblast cells with varying concentrations of AG1478 for 48 hr, the IC_{50} was determined using the MTT assay. An IC_{50} value of 13.6 µM for WHCO1 and 11.9 µM for WHCO6 OSCC cells was obtained while normal skin fibroblasts were >6-fold more resistant to drug (Table 2).

Cell Line	IC_{50} in µM	Confidence interval
WHCO1	13.6	10.8 -17.2
WHCO6	11.9	7.4 - 19
DMB	>100	undefined
FG^0	75	43.2 - 130

Table 2: Drug sensitivity of OSCC cells and normal fibroblast cells to AG1478

WHCO1 (A) and WHCO6 (B) OSCC cells, and normal skin fibroblasts DMB (C) and FG^o (D) were plated at a density of 5000 cells per well in 96 well plates and were treated with a range of concentrations of AG1478 to determine the IC_{50} values. Cells were incubated with AG1478 for 48 hr followed by the MTT assay. The absorbance was read with a multi plate reader at 595 nm and data was analysed using GraphPadPrism v3®.

Previously we showed that 1 μM of AG1478 was sufficient to inhibit EGFR activation in the presence of EGF (Fig. 2.4) and we thus determined the effect of low concentrations of AG1478 on the cell cycle and proliferation. Cells were treated with 1 μM AG1478 and proliferation was monitored by MTT assay. Cell proliferation was reduced by 30-40% in WHCO1 and WHCO6 cells treated with inhibitor compared to untreated cells ($p \leq 0.005$) (Fig. 2.9). The decrease in cell proliferation was consistent with the strong cell cycle arrest observed when the cell cycle profile was analysed. The results in appendix Figure A4, show that 1 μM AG1478 induces a G1 cell cycle block after 48 hr, with a nearly complete loss of the S and G2 cell cycle phases.

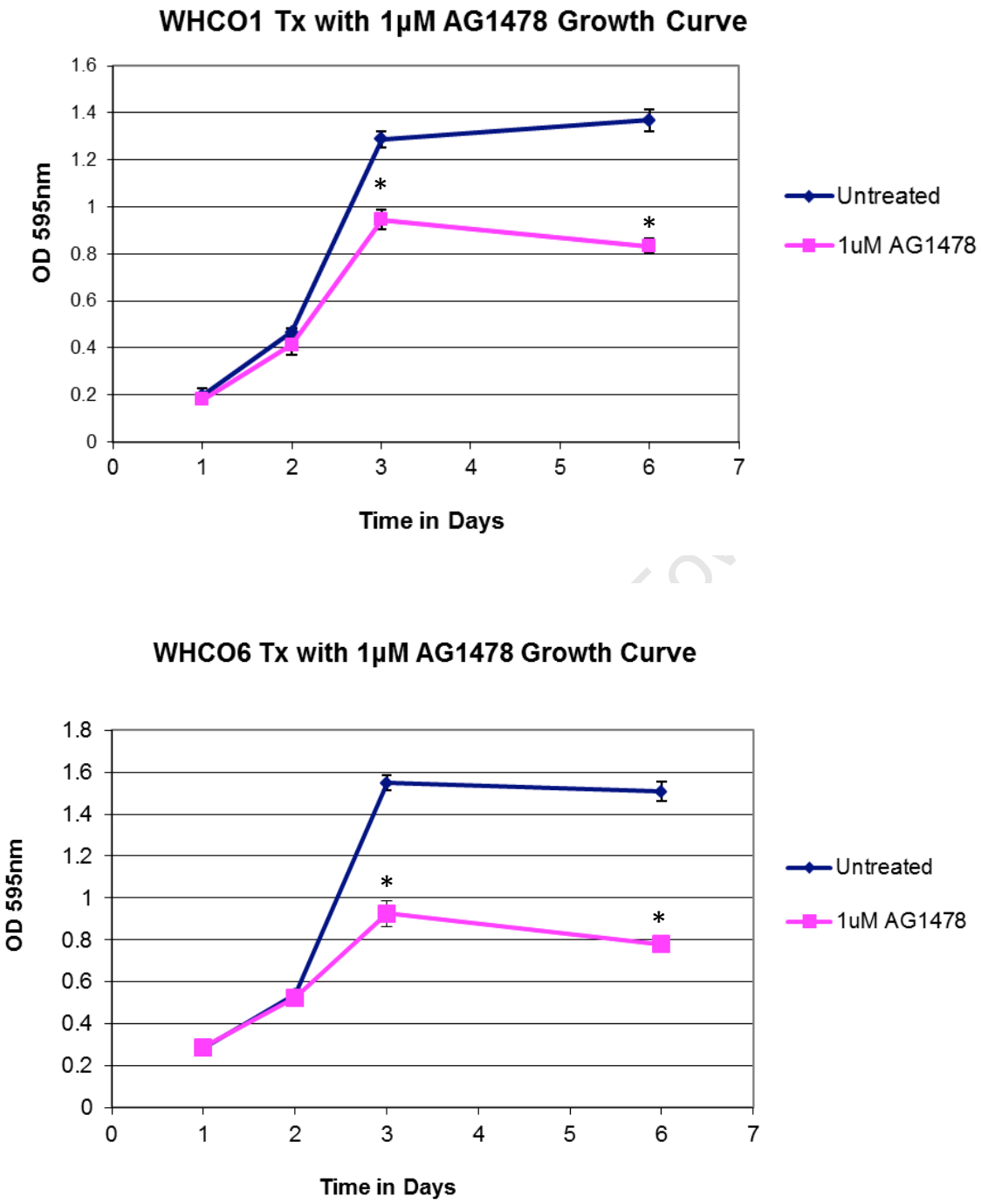

Figure 2.9: Cell proliferation of WHCO1 and WHCO6 OSCC cells in the presence of AG1478

WHCO1 and WHCO6 cells were plated at a density of 1500 cell per well in 96 well plates and treated with 1 µM AG1478 in triplicate. Growth was monitored over a 6 day time period by means of the MTT assay and the corrected absorbance values of untreated and treated cells were plotted in a line graph in Microsoft Excel®. Each point represents a triplicate with error bars displaying STDEV. (* $p \leq 0.005$)

To confirm that the growth inhibitory effects of AG1478 were due to inhibition of EGFR, an siRNA approach was also used. WHCO1 cells were treated with control or EGFR siRNA over a period of three days to transiently reduce levels of EGFR protein. EGFR levels were significantly reduced for 48 hr but returned to normal levels after 72 hr in WHCO1 cells transfected with EGFR siRNA (Fig. 2.10). This is consistent with the transient nature of siRNA transfection.

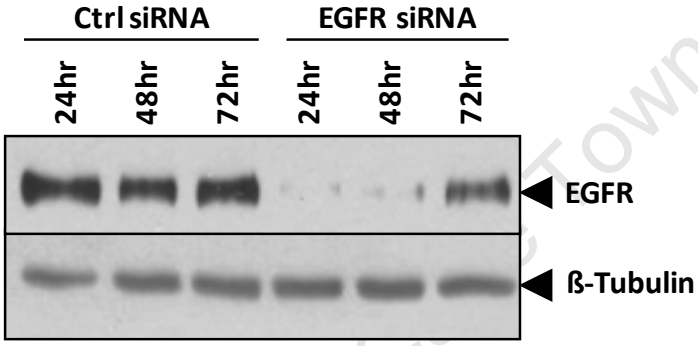

Figure 2.10: EGFR transient knockdown

WHCO1 cells were seeded in 35 mm dishes at a density of 1.2 x 10^5 cells per dish. The following day cells were transfected with 20 nM control or EGFR siRNA and protein was harvested at 24, 48 and 72 hr post-transfection. Western blot analysis of 40 µg of protein lysate was performed using an antibody specific for EGFR.

WHCO1 and WHCO6 cells were treated with Ctrl or EGFR siRNA and growth was monitored by MTT assay over a period of time. EGFR siRNA transfected cells displayed a transient reduction in proliferation compared to cells transfected with control siRNA (Fig. 2.11). The transient nature of the reduction in proliferation could be attributed to the re-expression of EGFR protein after 72 hr (Fig. 2.10).

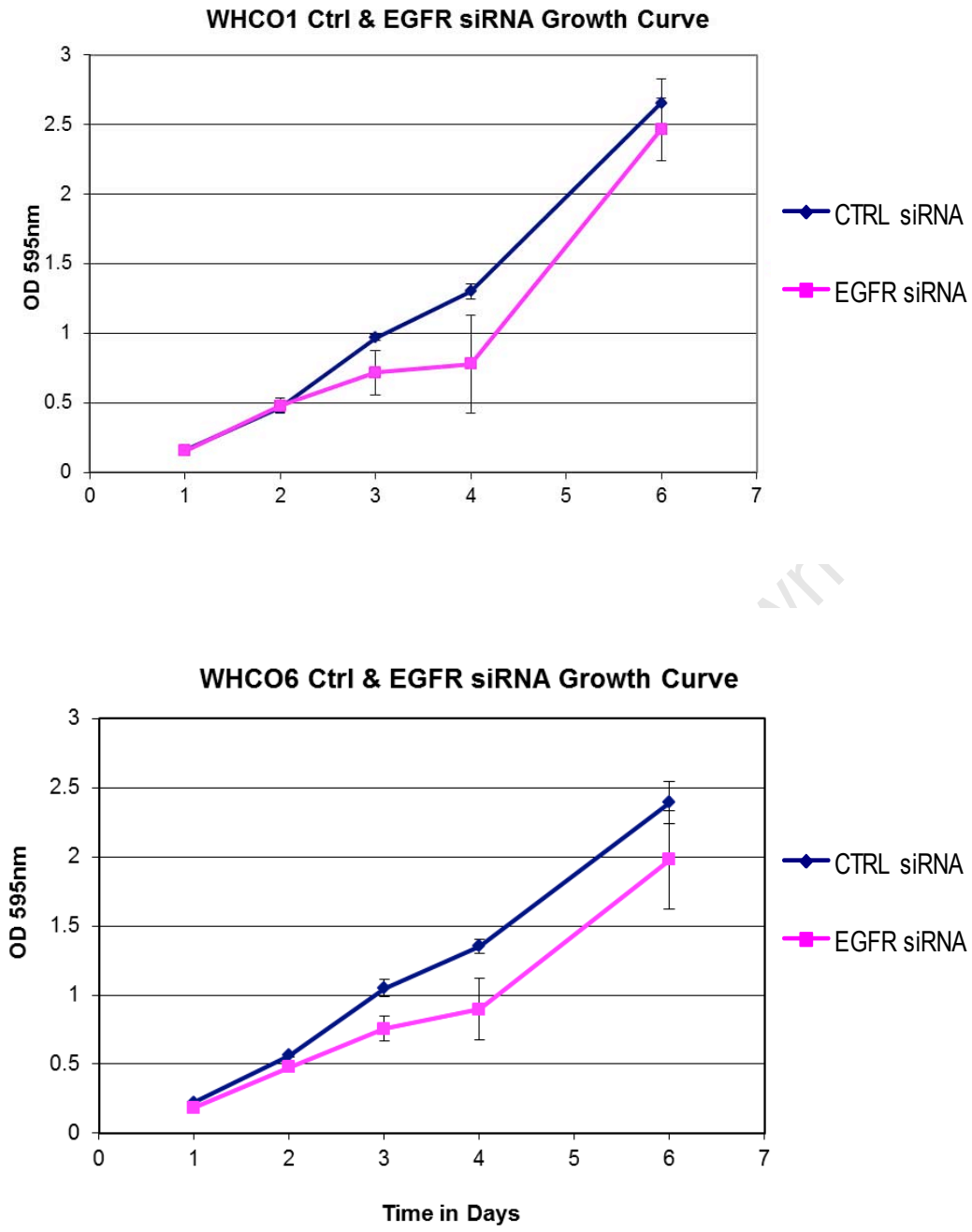

Figure 2.11: Proliferation of WHCO1 and WHCO6 cells treated with Ctrl or EGFR siRNA

WHCO1 and WHCO6 cells were transfected with 20 nM Ctrl or EGFR siRNA in 60 mm dishes. The following day cells were re-plated at a density of 1500 cells per well in 96 well plates and cell proliferation was determined over a period of time using the MTT assay. The absorbance of Ctrl and EGFR siRNA treated cells was determined using a plate reader and plotted as a line graph in Microsoft Excel®. Each point was performed in triplicate and error bars represent STDEV.

Taken together, results with the EGFR inhibitor and EGFR knockdown suggest that EGFR does contribute to proliferation of OSCC cells to some extent. However, whether or not EGFR is important for OSCC cell survival is still debatable, since cells were still viable when EGFR expression was knocked down, or when treated with sufficient AG1478 to completely abolish EGFR activation for six days.

Given the cross-talk between EGFR and IGF-1R identified in the first part of this chapter, we proceeded to investigate the simultaneous targeting of EGFR and IGF-1R using the IGF-1R knockdown cells as a model. IGF-1R knockdown cells displayed a ≥50% reduction in levels of total IGF-1R with reduced downstream pAKT levels (Fig. 2.6). When cell proliferation was determined by means of the MTT assay similar growth rates were observed in IGF-1R shRNA transfected cells and Ctrl shRNA transfected cells (Fig. 2.12). Cell cycle analysis also revealed no significant changes in G1/S/G2 phases and these cells were indistinguishable from control cells in viability assays (data not shown).

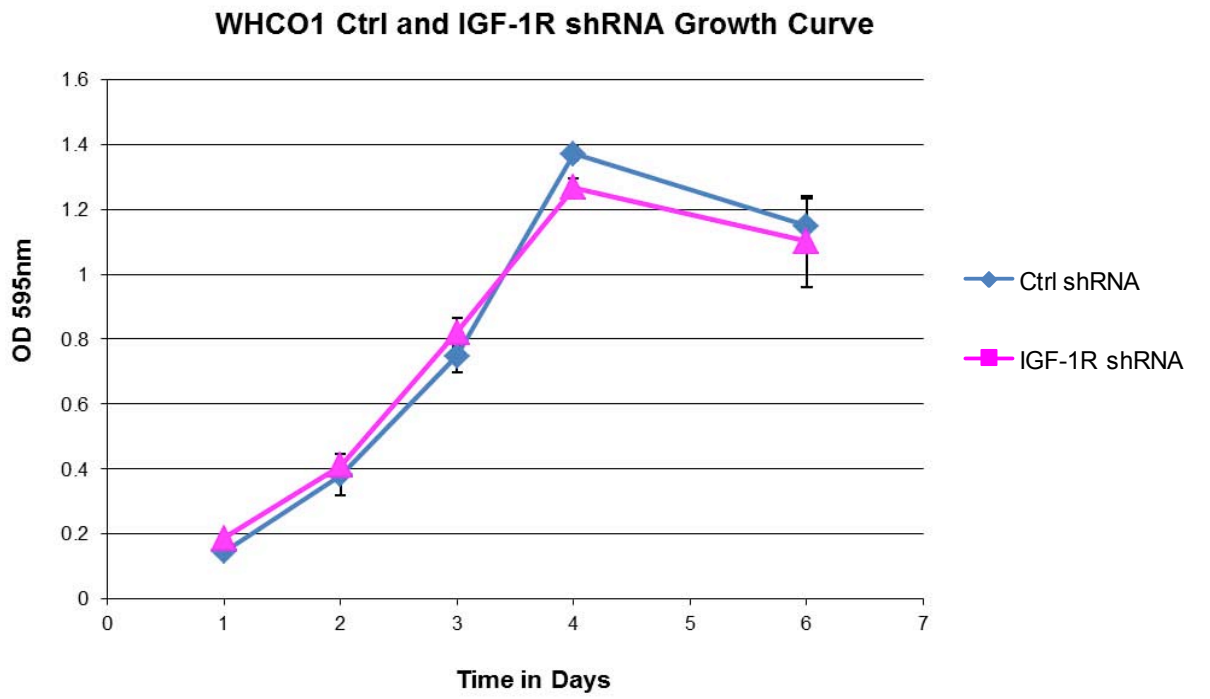

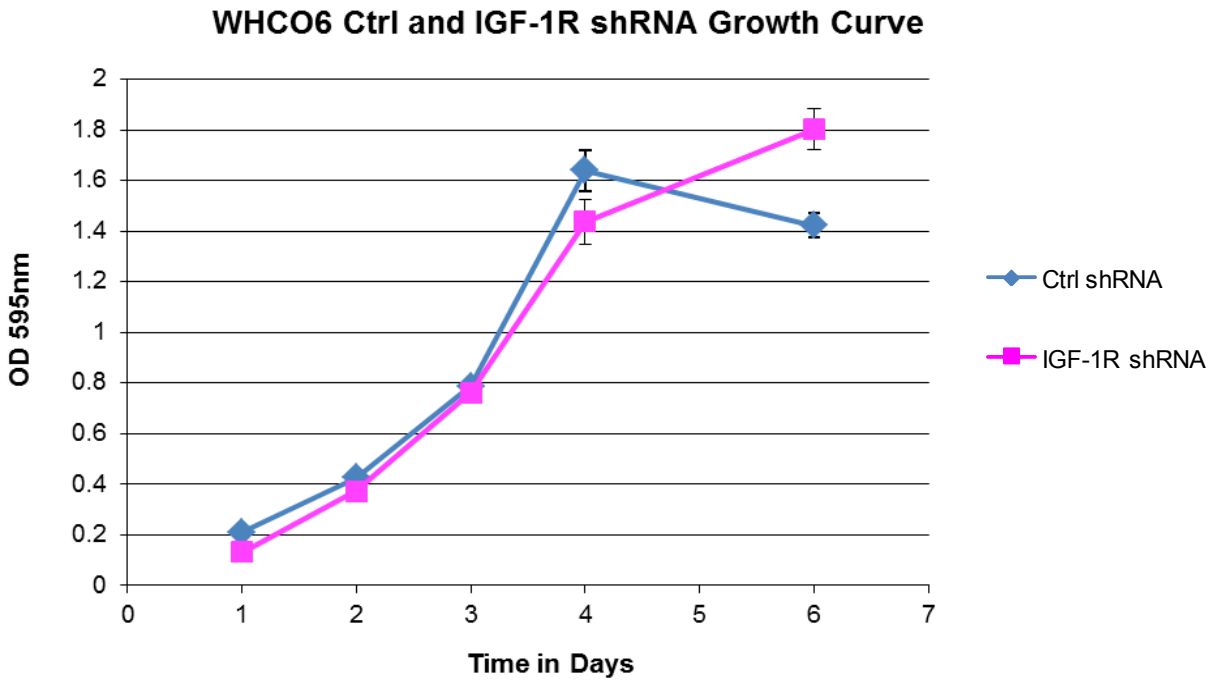

Figure 2.12: Proliferation of Ctrl and IGF-1R shRNA cells

WHCO1 and WHCO6 cells stably expressing Ctrl or IGF-1R shRNA were seeded at a density of 1500 cells per well in 96 well plates and proliferation was measured by means of MTT assay. The absorbance of WHCO1 and WHCO6 Ctrl and IGF-1R shRNA cells was determined using a plate reader and plotted as a line graph in Microsoft Excel®. Each point was performed in triplicate and error bars represent STDEV.

Our observation that IGF-1R knockdown cells displayed similar proliferation rates as control cells (Fig. 2.12), while displaying elevated EGFR/ERk1/2 pathway activity (Fig. 2.6) provided an interesting phenotype for further investigation using the EGFR inhibitor, AG1478. The MTT assay was conducted treating WHCO1 and WHCO6 Ctrl and IGF-1R shRNA cells with AG1478 to determine drug sensitivity. IGF-1R shRNA cells displayed a two- to three- fold increase in sensitivity to AG1478 compared to Ctrl shRNA cells (Fig. 2.13). Furthermore when PARP cleavage (an indicator of apoptosis) was measured in cells treated with 3 μM AG1478, a similar two- to three-fold increase in PARP cleavage was observed in IGF-1R knockdown cells compared to control cells (Fig. 2.14).

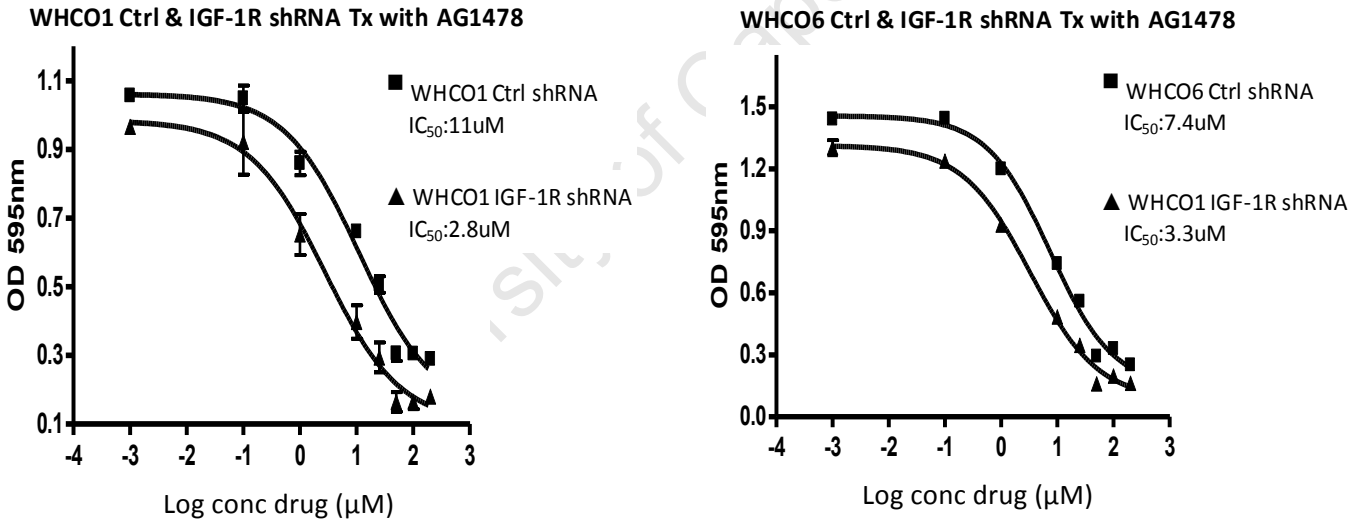

Figure 2.13: Drug sensitivity of WHCO1 and WHCO6 Ctrl and IGF-1R shRNA transfected cells to AG1478

WHCO1 and WHCO6 Ctrl and IGF-1R shRNA cells were plated at a density of 5000 cells per well in 96 well plates and were treated with a range of concentrations of AG1478 and drug sensitivity was determined after 48 hr by means of the MTT assay. The absorbance was read with a multi plate reader at 595 nm and data was analysed using GraphPadPrism v3®. Each point was performed in triplicate and error bars represent STDEV.

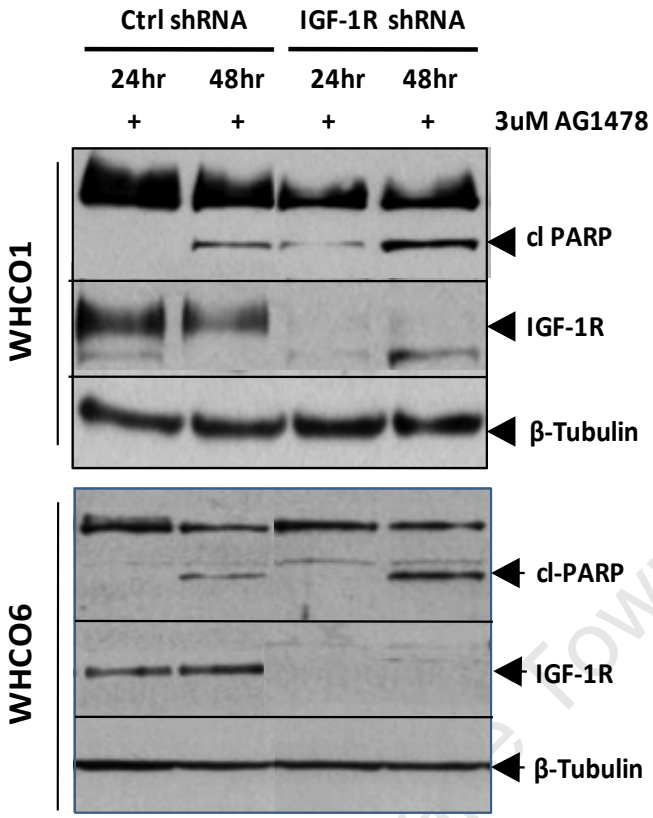

Figure 2.14: Effect of AG1478 on apoptosis in WHCO1 and WHCO6 Ctrl and IGF-1R shRNA cells

A total of 3 x 10^5 WHCO1 and WHCO6 Ctrl and IGF-1R shRNA cells were seeded in 60 mm dishes. The following day cells were treated with 3 μM AG1478 for 24 and 48 hr. Protein was harvested and IGF-1R and cleaved PARP (cl-PARP) levels was measured by western blotting.

Previous reports have implicated IGF-1R in providing survival signals to chemo-resistant cells (Chakraborty, Liang, & DiGiovanna, 2008; Dallas *et al.*, 2009) which could explain the observed increased sensitivity of IGF-1R knockdown cells to AG1478 (Fig. 2.14). We hypothesized that if IGF receptors were providing survival signals in OSCC cells, IGF-1R shRNA cells should also display an increased sensitivity to other chemotherapeutic compounds. WHCO1 control and IGF-1R shRNA cells were treated with cisplatin to determine the sensitivity to this drug (Fig. 2.15). Control and IGF-1R knockdown cells

displayed similar sensitivity to cisplatin (18.5 μM vs. 20.8 μM respectively) suggesting that reduction in IGF-1R expression had not sensitized the cells to cisplatin. Furthermore when WHCO1 and WHCO6 Ctrl and IGF-1R shRNA cells were treated with 10 μM cisplatin or 5 μM doxorubicin for 24 or 48 hr, no further increase in PARP cleavage was observed in IGF-1R knockdown cells (Fig. 2.16 A and B). Our data suggest that simultaneous disruption of EGFR and IGF-1R function could be more effective than inhibition of IGF-1R combined with other chemotherapeutic agents such as cisplatin or doxorubicin. However, this novel targeted therapeutic approach for the treatment OSCC still needs further *in vivo* characterization.

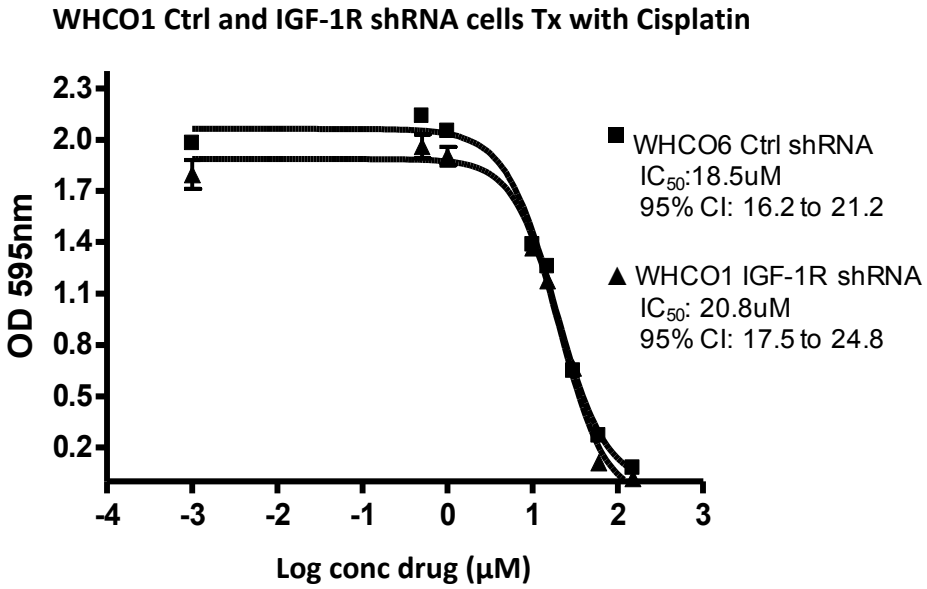

Figure 2.15: Drug sensitivity of WHCO1 Ctrl and IGF-1R shRNA transfected cells to cisplatin

WHCO1 Ctrl and IGF-1R shRNA cells were treated with a range of concentrations of cisplatin for 48 hr and drug sensitivity was determined by the MTT assay. The absorbance was read with a multi plate reader at 595 nm and data was analysed using GraphPadPrism v3®. Each point was performed in triplicate and error bars represent STDEV.

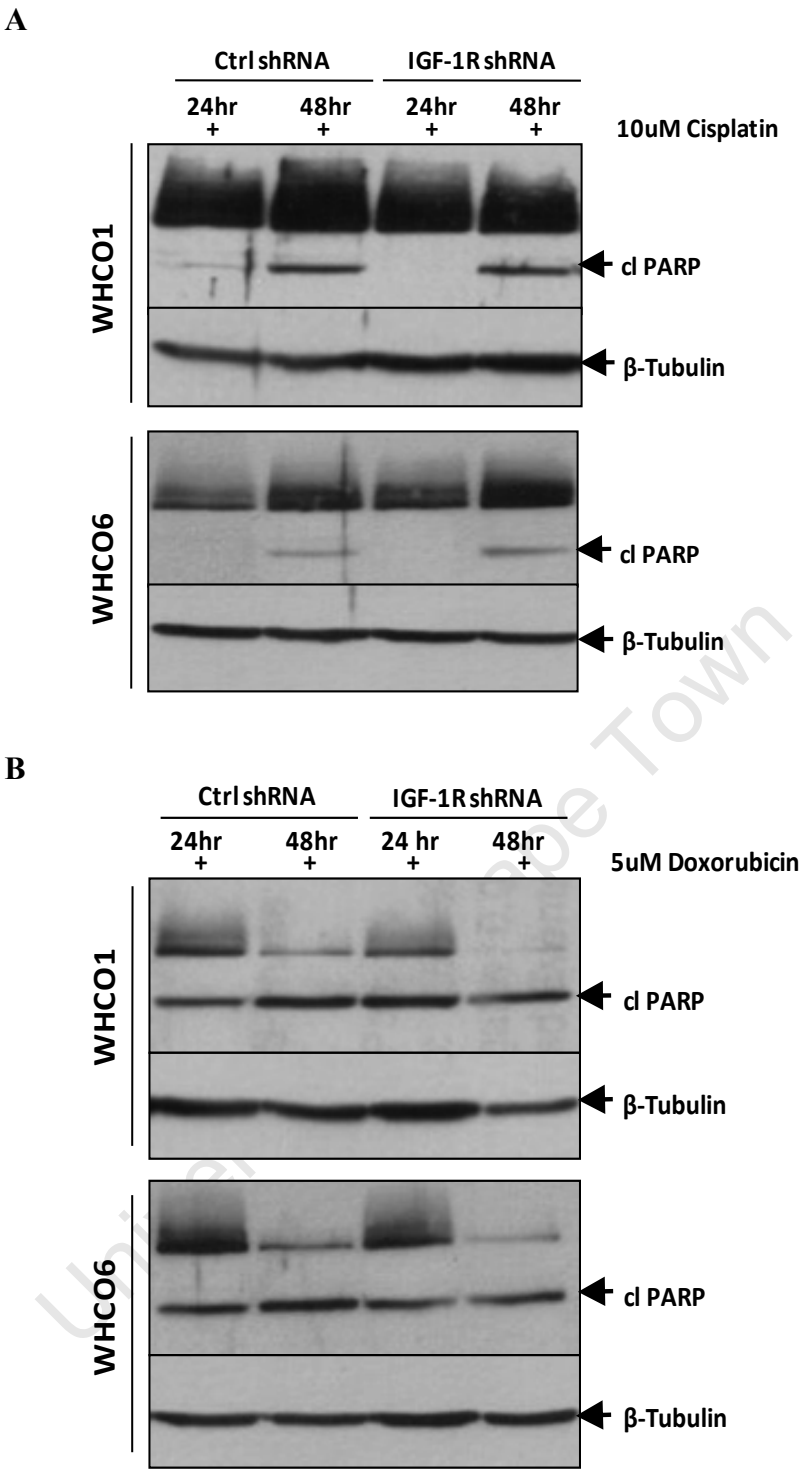

Figure 2.16: Effect of cisplatin or doxorubicin on apoptosis in WHCO1 and WHCO6 Ctrl and IGF-1R shRNA cells

WHCO1 and WHCO6 Ctrl and IGF-1R shRNA cells were seeded in 60 mm dishes at a density of 3 x 10^5 cells per dish. The following day cells were treated with 10 μM Cisplatin (A) or 5 μM Doxorubicin (B), and incubated with drug for 24 or 48 hr. Apoptosis was determined by western blot, probing cell lysates for cleaved PARP.

2.3 Discussion

EGFR and IGF-1R both play important roles in cancer biology with overexpression of EGFR associated with poor prognosis in oesophageal and head and neck cancers (Tew *et al.* 2005) and IGF-1R overexpression associated with resistance to chemotherapeutic agents (Dallas *et al.*, 2009). Furthermore, overexpression of EGFR in the normal immortalised epithelial keratinocyte cell line, EPC2 is sufficient to transform cells *in vitro* and *in vivo* (Kim *et al.* 2006). EGFR overexpression in epithelial tissue of the epidermis results in hyperplasia and abnormal growth of cells (Okawa *et al.* 2007). However, understanding the biology of these receptors is complex, as a recent study revealed, with EGFR knockout mice dying soon after birth but transgenic mice expressing kinase deficient EGFR remaining fully viable (Weihua *et al.* 2008). A deeper understanding of the role of these receptors in oesophageal cancer is required before we can consider clinical applications of receptor targeting. In this study we investigated the role of EGFR and IGF-1R in OSCC cell biology evaluating their function and potential as drug targets. The focus of this study was to attain a better understanding of the role of EGFR and IGF-1R in OSCC as studies in other cancers provided evidence that co-targeting these receptors simultaneously might be more beneficial than individual targeting.

We demonstrated that both EGF and IGF-1 receptors were expressed in a panel of our OSCC cell lines. WHCO1 and WHCO6 cells were chosen as model cell lines as they have been extensively studied in our laboratory. Analysis of receptor functionality by means of ligand stimulation revealed that these receptors were functional in WHCO1 and WHCO6 cells with overlapping interactions either between receptors or regulation of their downstream signalling pathways. EGF treatment resulted in a rapid but transient activation of IGF-1R suggesting crosstalk. Studies have reported crosstalk between EGFR and IGF-1R where IGF-1R

transactivates EGFR (Thomas *et al.* 2006; Meng *et al.* 2007; Hu *et al.* 2008). However, to our knowledge, no previous reports described EGFR as being capable of activating IGF-1R, making this a novel finding. Furthermore we observed that activation of the EGFR kinase domain was critical for IGF-1R activation by EGF, which suggested that EGFR and IGF-1R may associate with each other accounting for the rapid activation of IGF-1R. EGFR and IGF-1R, despite belonging to different RTK families have been shown to associate when co-expressed (Riedemann *et al.* 2007). Elevated receptor expression increases the likelihood of their association which has been observed in breast cancer and NSCLC, although in some breast cancers, EGFR and IGF-1R do not associate despite being expressed at elevated levels (Morgillo *et al.* 2007b; Riedemann *et al.* 2007). Furthermore, the association between EGFR and IGF-1R also occurs in non-cancerous tissue (e.g. mammary epithelial cells) and this association is involved with activating cell proliferation (Ahmad *et al.* 2004; Meng *et al.* 2007; Jin & Esteva 2008). We observed that EGFR and IGF-1R co-immunoprecipitate in several OSCC cell lines under basal conditions, suggesting that association between EGFR and IGF-1R may commonly occur in OSCC. In cancer cells which often display elevated levels of these receptors, it is possible that dimerization may be advantageous by conferring increased sensitivity to bio-available ligands.

We also observed that IGF-1 stimulation strongly reduced pERK1/2 levels in three of our OSCC cell lines suggesting that IGF-1R negatively regulates ERK1/2 activity. This was supported by our observation that inhibition of AKT resulted in increased pERK1/2 levels and knockdown of IGF-1R increased pEGFR and pERK1/2 levels. Our data suggests that in OSCC cells the processes regulating EGFR/ERK1/2 activity may involve (at least in part) the IGF-1R/AKT axis. Recent evidence supports this theory that the IGF-1R/AKT pathway can regulate the EGFR/MAPK pathway as AKT was shown to exert feedback inhibition on RTKs

including the HER family of receptors, erlotinib potentiated mTOR regulated translation of EGFR, loss of IGF-R increased expression of other kinases including EGFR, and IGF-1R activity was suggested to block basal pEGFR (Kuribayashi *et al.* 2004; Morgillo *et al.* 2007a; Huang *et al.* 2009; Chandarlapaty *et al.* 2011). The activation of EGFR in IGF-1R knockdown cells was not attributed to increased levels of EGFR ligands considering that parental cells displayed no increase in pEGFR when treated with IGF-1R knockdown conditioned medium. Morgillo *et al.*, (2007b) also observed increased pEGFR levels when IGF-1R was inhibited. However, they do not explain this observation. Their reported observation, that IGF-1R inhibition resulted in increased pEGFR, could be in line with our data suggesting that IGF-1R activity regulates the EGFR/ERK1/2 axis. Furthermore, the observation that inhibition of AKT resulted in increased expression and activation of EGFR (Chandarlapaty *et al.* 2011) might be specific to certain cancers, since pEGFR levels did not increase in our cells when AKT was inhibited. Our data could suggest that IGF-1R regulates EGFR activity upstream of AKT.

EGFR has been the focus of numerous studies over the past 20 years and inhibitors of this receptor were approved for clinical treatment of certain cancers. Epithelial cancers often display elevated EGFR expression but only in certain types of cancers like NSCLC and HNSCC has EGFR targeted therapy proven successful (Cohen *et al.* 2005; Ono & Kuwano 2006; Sharma *et al.* 2007; Weihua *et al.* 2008). In this study we investigated the potential of EGFR as a target in OSCC cell lines because its overexpression was reported to correlate with patient survival. OSCC cells displayed drug sensitivity to AG1478 in the range of 10 μM while normal skin fibroblasts were much less sensitive. Proliferation of cells using low concentrations of AG1478 or transient knockdown of EGFR resulted in a 30-40% reduction in cell growth. Our *in vitro* data correlate well with observations from clinical settings, since

10-30% of OSCC patients treated with EGFR inhibitors displayed stable disease for 2-3 months followed by tumour progression (Dragovich & Campen 2009). Similarly our observation that inhibition of EGFR activity, with low concentrations of AG1478 or siRNA, resulted in reduced proliferation but not significant apoptosis suggested that EGFR may contribute to proliferation but not be critical for OSCC cell survival.

IGF-1R is commonly overexpressed in OSCC and evidence has implicated it in drug resistance (Mitsiades *et al.* 2004; Chakraborty *et al.* 2008). IGF-1R has been assessed as a target *in vitro* and *in vivo* in other cancers with promising results. Small molecule inhibitors, NVP-AEW541 and NVP-ADW742, directed against IGF-1R kinase domain displayed potent activity *in vitro* and *in vivo* in fibrosarcomas, multiple myeloma, colorectal cancer and pancreatic cancer (García-Echeverría *et al.* 2004; Mitsiades *et al.* 2004; Höpfner *et al.* 2006; Moser *et al.* 2008). The concern with IGF-1R targeted therapy is the potential of impaired glucose metabolism - fortunately most studies observe no adverse side effects and no real difference in plasma glucose levels in *in vitro* and *in vivo* cancer models (García-Echeverría *et al.* 2004; Mitsiades *et al.* 2004). The long term effects of IGF-1R inhibition still need to be determined. Knockdown of IGF-1R in OSCC cell lines WHCO1 and WHCO6 resulted in an interesting phenotype, with a 50% reduction in IGF-1R level, elevated pEGFR and pERK1/2 levels despite these cells growing similar to control cells. When EGFR was inhibited in these cells a 2-3 fold increase in sensitivity to AG1478 compared to control cells was observed. Recalling that our data suggested an IGF-1R/AKT negative feedback regulatory loop opposing EGFR/ERK1/2 activity in OSCC cells, this observation suggested that cells became more reliant on active EGFR when this feedback loop was disrupted. This is consistent with reports which observed that co-targeting EGFR and IGF-1R in other cancers led to increased apoptosis (Morgillo *et al.* 2007; Huang *et al.* 2009; Villanueva *et al.* 2010). When IGF-1R

knockdown cells were treated with cisplatin, doxorubicin and novel gold-based organometallic compounds (data not shown) no further increase in drug sensitivity was observed, which was consistent with a report that colorectal cancer cells showed no increased sensitivity to 5-fluorouracil or oxaliplatin combined with IGF-1R inhibition (Dallas *et al.* 2009). This suggested that the increased sensitivity observed when co-targeting EGFR and IGF-1R in WHCO1 and WHCO6 OSCC cells was specific for these two receptors.

The relevance of EGFR and IGF-1R receptor interaction in cancer biology is not clear but as these receptors are commonly overexpressed it suggests that cancer cells exploit multiple pathways to survive, since targeting of a single receptor is often not sufficient to kill tumour cells. Our data suggests that in OSCC which overexpress EGFR and IGF-1R, targeting both receptors with specific inhibitors may represent a rational therapeutic option that should be explored further.

.

Chapter 3

Chemokine CXC Receptor 2 as a target in Oesophageal Cancer

3.1 Introduction:

The role of CXCR2 in chemotaxis of immune cells (neutrophils, macrophages and leukocytes) and capillary formation in endothelial cells has been well documented and characterised (Raman *et al.* 2007; Waugh & Wilson 2008; Matsuo *et al.* 2009). Dysregulation of components of the chemokine pathway can result in chronic inflammation, which can lead to various disease states, including cancer (Raman *et al.* 2007). Evidence in the literature has linked CXCR2 expression with cancer, but its exact role in this disease is unclear. CXCR2 overexpression in NIH 3T3 cells resulted in transformation *in vitro* and promoted tumour development and metastasis in nude mice (Burger *et al.* 2005). Elevated expression of CXCR2, which correlated with tumourigenesis, angiogenesis and metastasis, was reported in prostate, lung, melanoma and pancreatic cancer. CXCR2 was reported to be pro-tumourogenic in melanoma, and its expression was found to correlate with melanoma stage, tumour aggression and metastasis (Singh *et al.* 2009) while in normal skin fibroblasts and benign lesions, CXCR2 expression correlated with oncogene induced senescence (Acosta *et al.* 2008; Acosta & Gil 2009; Matsuo *et al.* 2009; Singh *et al.* 2009; Yang *et al.* 2010). Although reports are contradictory regarding CXCR2 function in tumourogenesis or senescence, *in vivo* targeting of CXCR2 has highlighted its role in tumour proliferation, angiogenesis and metastasis. In pancreatic and skin carcinogenesis, inhibition of CXCR2 *in vivo* with either neutralising antibody or by CXCR2 knockdown resulted in significantly reduced tumour size and blood vessel density (Cataisson *et al.* 2009; Matsuo *et al.* 2009). Lung cancer cells xenografted into CXCR2-/- mice or treated with anti-CXCR2 antibody in

wild-type mice displayed substantially reduced tumour growth and metastasis (Keane *et al.* 2004). The reduced tumour volume, angiogenesis and metastasis observed when targeting CXCR2 *in vivo* was attributed to the involvement of CXCR2 in angiogenesis. A study performed in our laboratory found that CXCR2 and its ligands GROα and GROβ were overexpressed in OSCC tissue compared to adjacent normal epithelial tissue (Wang *et al.* 2006; Wang *et al.* 2009). In this study we evaluated the potential of CXCR2 as a target in OSCC cells since we have previously reported evidence of its role in OSCC proliferation.

3.2 Results:

3.2.1 CXCR2 expression and signal inhibition with anti-CXCR2 antibody or stable knockdown in OSCC cells

We had previously shown in our laboratory that CXCR2 and its ligands GROα and β may play a role in the proliferation and survival of OSCC cells. This data suggested that CXCR2 may serve as a potential therapeutic target for OSCC. Our first objective was to confirm the expression of CXCR2 in cultured OSCC cell lines. Protein was harvested from cultured OSCC cell lines, and subjected to western blot analysis using an antibody which recognizes total CXCR2. All OSCC cells, except KYSE 70, expressed CXCR2 by western blot analysis (Fig. 3.1). CXCR2 was detected as two distinct bands at a molecular weight of 48 kDa and 40 kDa respectively. Others have reported that phosphorylation of CXCR2 results in degradation of the receptor which results in two bands being detected by western blot (Mueller *et al.*, 1997 and Schraufstatter *et al.*, 1998). WHCO1 and WHCO6 cells were chosen as model cell lines as these cells have routinely been used in previous studies in our laboratory (Whibley *et al.* 2005; Wang *et al.* 2006; Whibley *et al.* 2007; Wang *et al.* 2009).

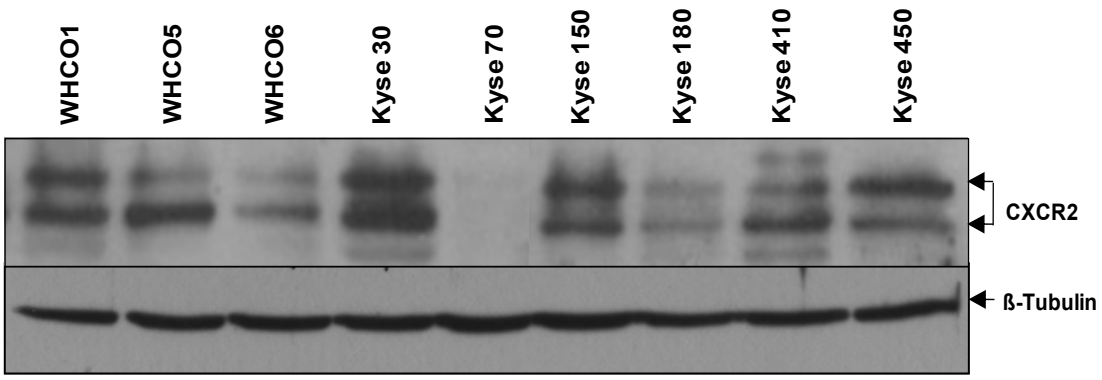

Figure 3.1: CXCR2 expression in OSCC cell lines.

OSCC cells were cultured to 60-70% confluency and protein was harvested. A total of 40ug of protein lysate from each cell line was separated by SDS-PAGE and transferred to nitrocellulose membrane. The membrane was probed with antibodies recognizing total CXCR2. β-tubulin was used as a loading control for all further experiments unless stated otherwise and each figure is representative of 3 independent experiments.

To test the activity of CXCR2, cells were stimulated with GROβ which binds specifically to CXCR2. At the time of this study antibodies that specifically recognized phosphorylated CXCR2 were not available, and we thus measured AKT and ERK1/2 activity as these are known downstream targets of activated CXCR2 (Fan *et al.* 2003; Sai *et al.* 2006). WHCO1 cells were cultured in 60mm dishes and serum starved for 1 hr. Following serum starvation cells were treated with 100ng/ml GROβ for ten min (Fig. 3.2A). GROβ treated cells displayed an increase in pERK1/2 and pAKT levels compared to untreated cells suggesting that CXCR2 was functional in our model system. To investigate basal CXCR2 activation, WHCO1 cells were incubated with 1ug/ml CXCR2 neutralising monoclonal antibody for one hr and pAKT and pERK1/2 levels were measured by western blotting (Fig. 3.2B). A substantial reduction in basal pERK1/2 levels was observed while pAKT levels were only slightly reduced in WHCO1 cells treated with neutralizing antibody compared to untreated cells.

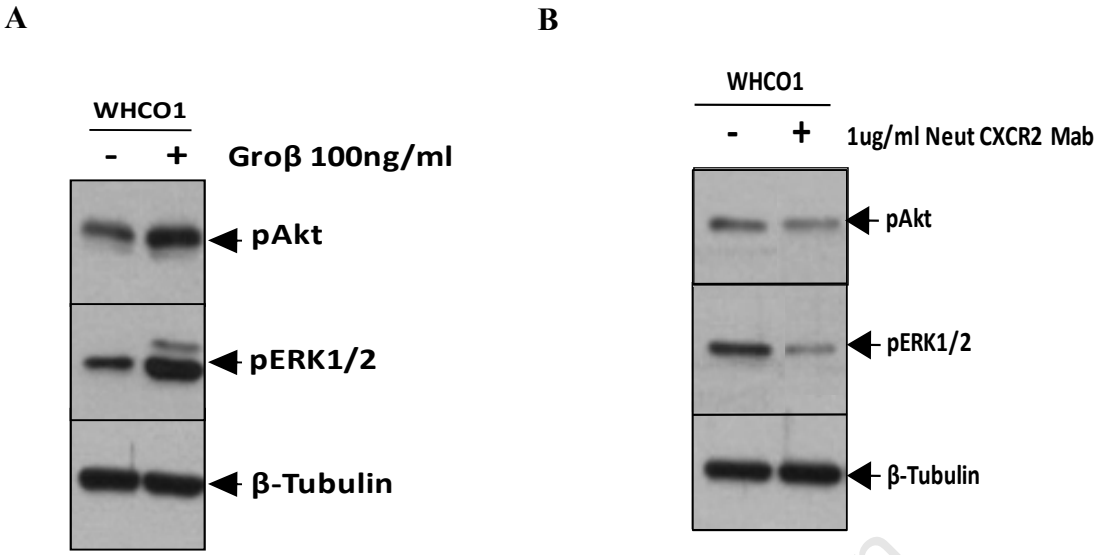

Figure 3.2: Effect of Groβ and CXCR2 neutralising antibody on pAKT and pERK1/2 levels in WHCO1 cells.

WHCO1 cells were seeded at a density of 3 x 10^5 cells per 60 mm dish and stimulated with 100 ng/ml Groβ ligand for ten min (A) or treated with 1 µg/ml neutralising CXCR2 monoclonal antibody (Mab331) for 1 hour (B) and protein was harvested. A total of 40 µg of protein lysate from each cell line was separated by SDS-PAGE and transferred to nitrocellulose membrane. The membrane was probed with antibodies recognizing pAKT and pERK1/2.

The effect of neutralizing CXCR2 MAb on OSCC proliferation was tested in WHCO1 and WHCO6 cells. Cells were seeded at 1500 cells per well in triplicate in 96 well plates and proliferation was determined in the presence of 2 µg/ml CXCR2 neutralizing antibody supplemented every 24 hr over a period of 4 days. No significant decrease in proliferation was observed despite treating cells with 2 fold more neutralising antibody than is required to reduce pERK1/2 levels by >50% (Fig. 3.3).

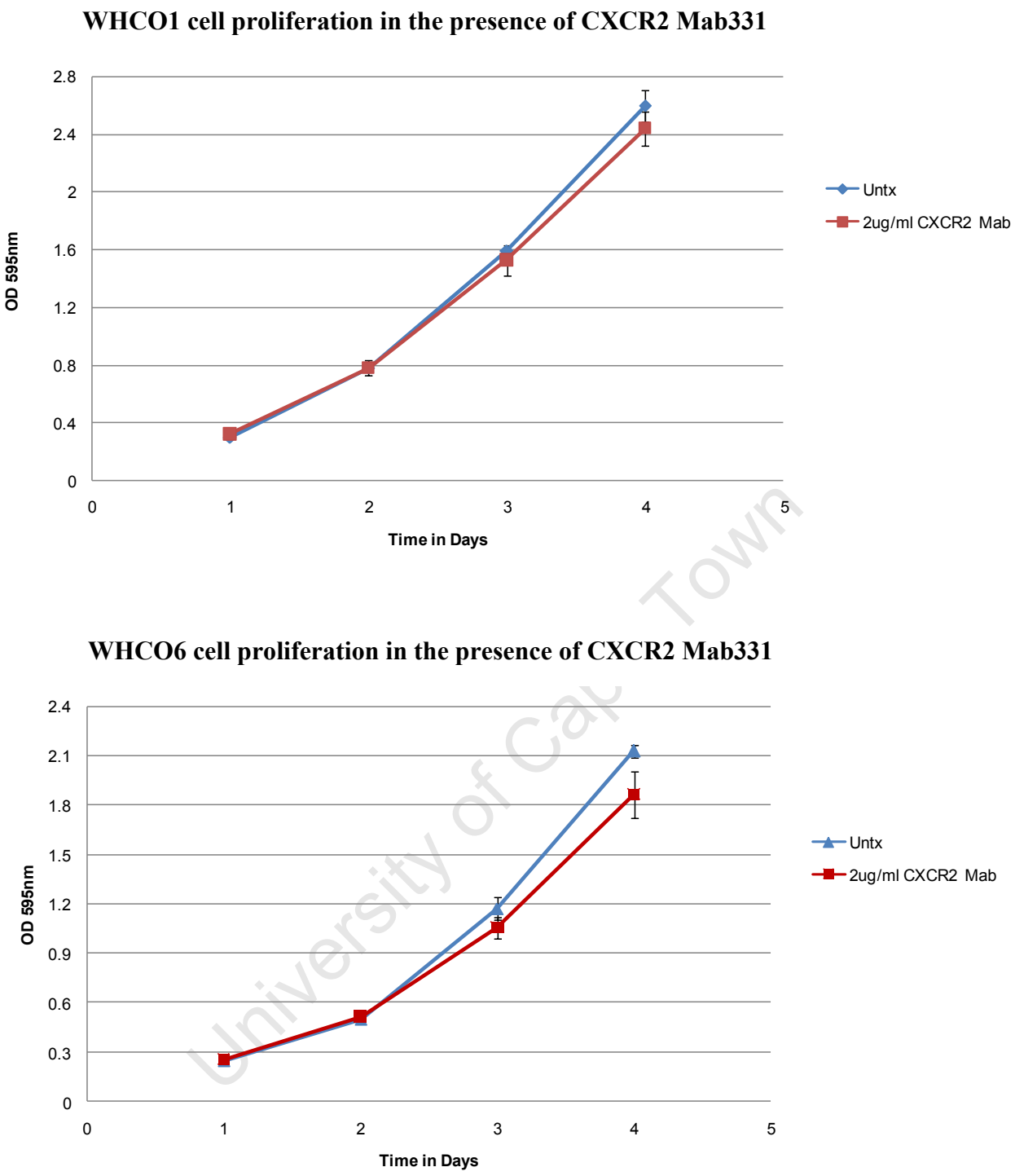

<u>Figure 3.3:</u> Effect of CXCR2 Mab331 on WHCO1 and WHCO6 OSCC cell proliferation

WHCO1 and WHCO6 OSCC cells were seeded at 1500 cells per well in a 96 well plate in triplicate. Cells were treated with 2 µg/ml neutralising CXCR2 monoclonal antibody supplemented every 24 hr for the indicated time periods. Cell proliferation was determined by MTT assay. The absorbance of WHCO1 and WHCO6 cells was determined using a plate reader and plotted as a line graph in Microsoft Excel®. Each point was performed in triplicate and error bars represent STDEV.

Considering that treatment with neutralising CXCR2 Mab had no effect on proliferation, even at a concentration sufficient to reduce pERK1/2 signalling, we used a CXCR2 knockdown system to further explore the role of CXCR2 in OSCC cells. WHCO1 and WHCO6 cells were infected with lentiviral particles containing CXCR2 shRNA or control shRNA, and pools of cells with greater than 95% GFP positivity (lentiviral vectors used contained GFP) were used for further studies. WHCO1 and WHCO6 CXCR2 knockdown cells were cultured and RNA and protein was harvested for real-time PCR and western blot analysis of CXCR2. The mRNA levels of CXCR2 were significantly reduced by >80% ($p \leq 0.0005$) in WHCO1 and WHCO6 CXCR2 knockdown cells compared to control cells (Fig. 3.4).

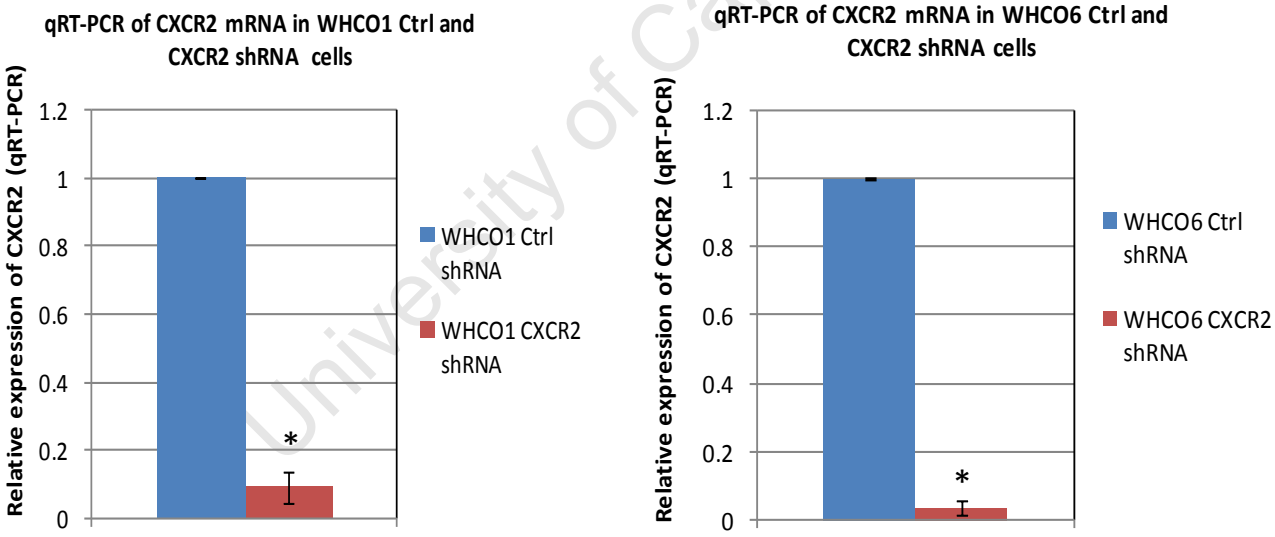

Figure 3.4: CXCR2 mRNA expression in WHCO1 and WHCO6 Ctrl and CXCR2 shRNA cells.

WHCO1 and WHCO6 Ctrl and CXCR2 shRNA cells were seeded at 3 x 10^5 cells per 60 mm dish and cultured overnight. RNA was extracted the following day and cDNA was synthesized and subjected to real-time PCR. Primers specific for CXCR2 was used to amplify CXCR2 and GUSB primers were used as a control. Relative expression of CXCR2 was calculated using the delta-delta CT method. Each point was performed in triplicate and error bars represent STDEV. (* $p \leq 0.0005$)

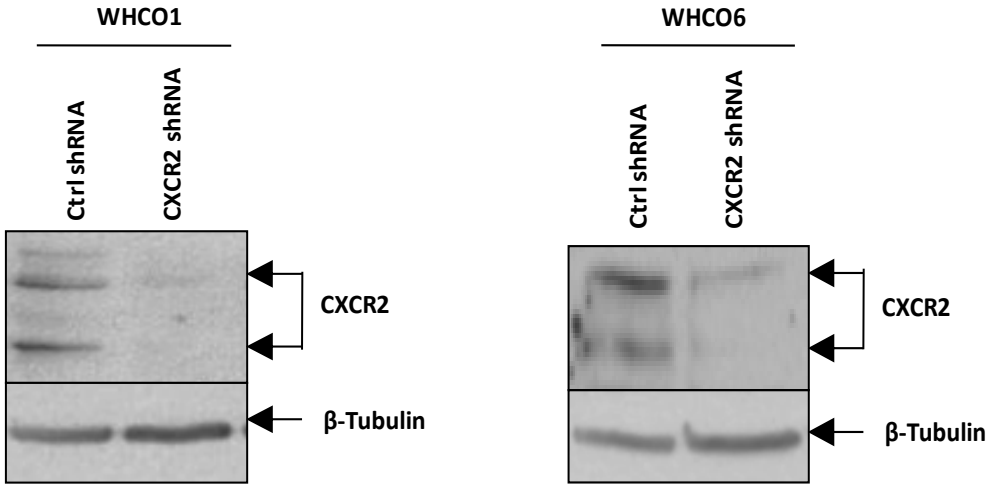

Figure 3.5: CXCR2 protein expression in WHCO1 and WHCO6 Ctrl and CXCR2 shRNA cells

WHCO1 and WHCO6 Ctrl and CXCR2 shRNA cells were seeded at 3 x 10^5 cells per 60 mm dish and allowed to settle overnight. Protein was harvested and 40 µg of each sample was separated by SDS-PAGE and transferred to nitrocellulose membrane. The membrane was probed with antibody specific to CXCR2.

Analysis of CXCR2 protein levels in CXCR2 knockdown cells, by western blotting, revealed substantial reduction in CXCR2 levels (Fig. 3.5). The proliferation of WHCO1 and WHCO6 CXCR2 knockdown cells compared to control cells was next determined. WHCO1 and WHCO6 control and CXCR2 knockdown cells were seeded in 96 well plates at 1500 cells per well and growth was measured by the MTT assay over the indicated time period. CXCR2 knockdown cells grew at the same rate as control cells with no detectable differences in proliferation (Fig. 3.6), consistent with our previous results using the neutralising antibody. Our observation is also consistent with reports that inhibition of CXCR2 has no impact on cell growth under *in vitro* conditions (Mestas *et al.* 2005; Wislez *et al.* 2006; Cataisson *et al.* 2009; Matsuo *et al.* 2009).

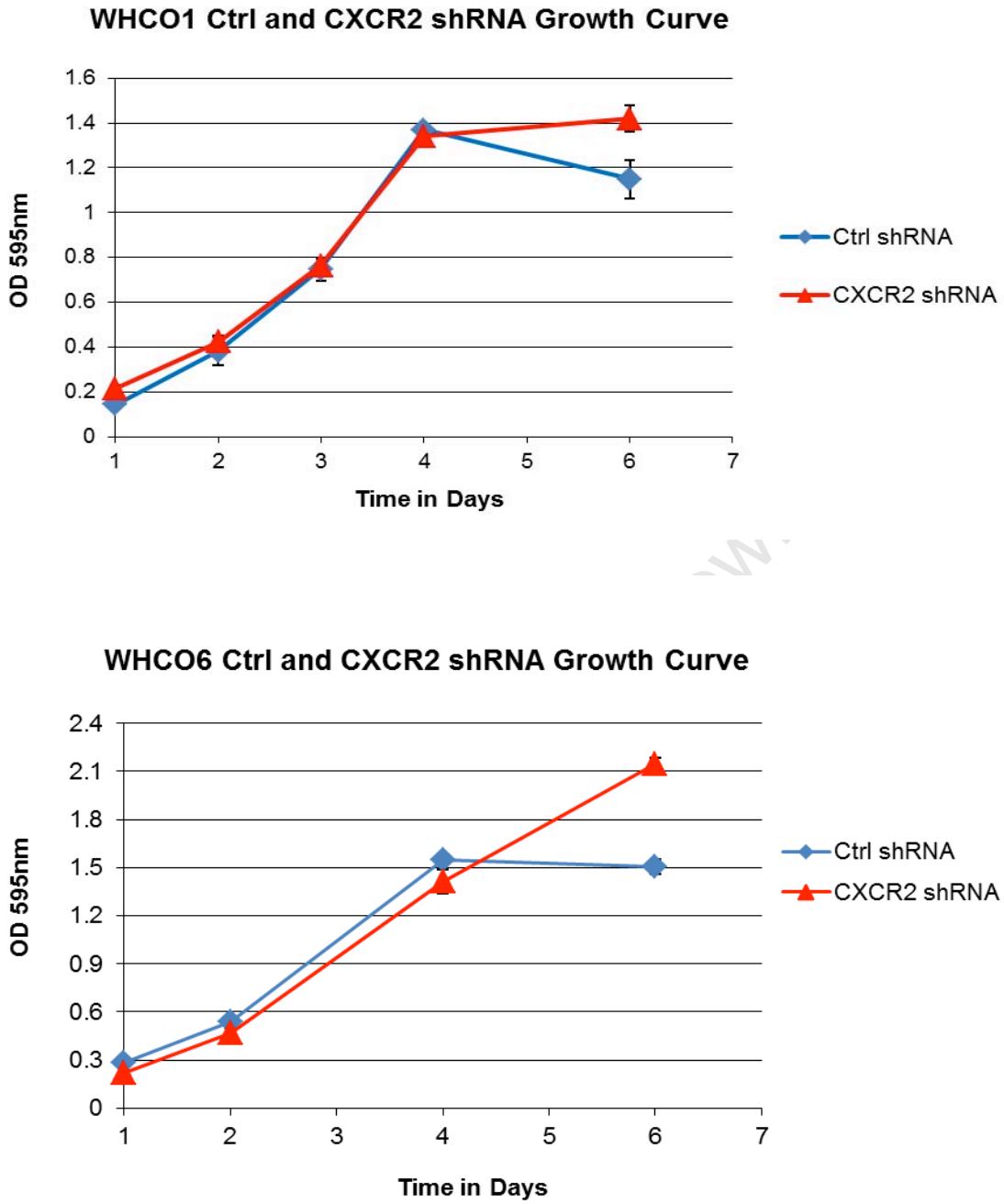

Figure 3.6: Proliferation of WHCO1 and WHCO6 control and CXCR2 knockdown cells

WHCO1 and WHCO6 control and CXCR2 knockdown cells were seeded at 1500 cells per well in triplicate in 96 well plates and cultured for the indicated time periods. Cell proliferation was determined by means of MTT assay. The absorbance of WHCO1 and WHCO6 control and CXCR2 shRNA cells was determined using a plate reader and plotted as a line graph in Microsoft Excel®. Each point was performed in triplicate and error bars represent STDEV.

Thus far our data suggested that inhibition of CXCR2 with a neutralizing antibody or CXCR2 knockdown had no significant impact on cell proliferation. This was contradictory to our previous observation which demonstrated that knockdown of GROβ with shRNA was associated with a decrease in cell proliferation (Wang *et al.* 2006). Another strategy using CXCR2 inhibitor SB225002, was employed to determine the effect of CXCR2 inhibition on cell proliferation.

3.2.2 Effect of CXCR2 inhibitor SB225002 in OSCC cells

Previously we had shown that 200 nM SB225002 was capable of reducing cell proliferation by 50% (Wang *et al.* 2006). Here the IC_{50} for SB225002 of two normal fibroblast cells, DMB (skin) and WI38 (lung) and two OSCC cell lines, WHCO1 and WHCO6 was determined. Cells were plated at a density of 5000 cells per well in 96 well plates, treated with the indicated concentrations of SB225002 and the MTT assay was performed. The OSCC cells WHCO1 and WHCO6 showed IC_{50} values of 2.5 μM and 2.4 μM respectively (3.7C and D) while no IC_{50} value could be determined for the normal fibroblast cells, DMB and WI38 since they appeared resistant to the effects of SB225002 (Figure 3.7A and B). The observation that CXCR2 inhibition had no effect on DMB and WI38 cell survival and proliferation is consistent with a recently published report (Acosta *et al.* 2008). The authors found that CXCR2 activates senescence in DMB fibroblasts which was alleviated when CXCR2 was knocked down or inhibited by SB225002 (Acosta *et al.* 2008). We observed that lower concentrations of SB225002 (0-10 μM) had no effect on DMB and WI38 metabolism/viability after 48 hr while the increase in OD at the higher concentration of drug (>10 μM) suggested an increase in cell number (Fig 3.7A and B). This was not explored further.

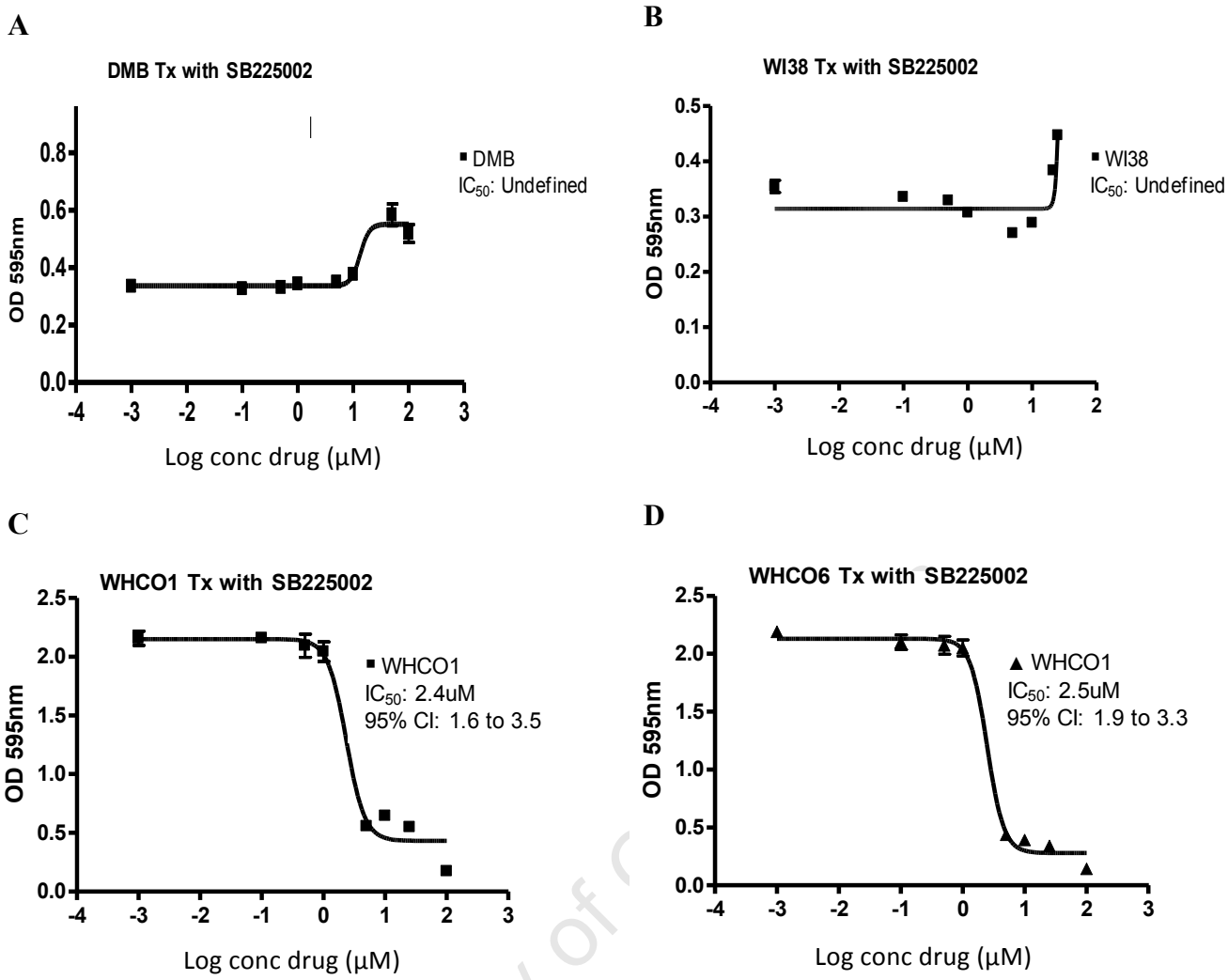

Figure 3.7: Drug sensitivity of OSCC and normal fibroblast cell lines to SB225002

Normal skin fibroblast cells DMB (A) and normal lung fibroblasts WI38 (B) and WHCO1 and WHCO6 OSCC cells (C and D) were seeded at a density of 5000 cells per well in triplicate in 96 well plates. Cells were treated with a range of concentrations of SB225002 to determine the IC_{50} after 48 hr by the MTT assay. Absorbance was read with a multi-plate reader at 595 nm. Each point was performed in triplicate and error bars represent STDEV.

The effect of 2 µM SB225002 on proliferation of OSCC cells was determined based on the IC_{50} values obtained earlier in Figure 3.7. WHCO1 and WHCO6 cells were seeded in 96 well plates and treated with 2 µM SB2205002 over the indicated time period (Fig. 3.8). SB225002 treatment completely inhibited cell proliferation in WHCO1 and WHCO6 cells ($p \leq 0.0005$), suggesting that CXCR2 activity was required for cell proliferation in these cells.

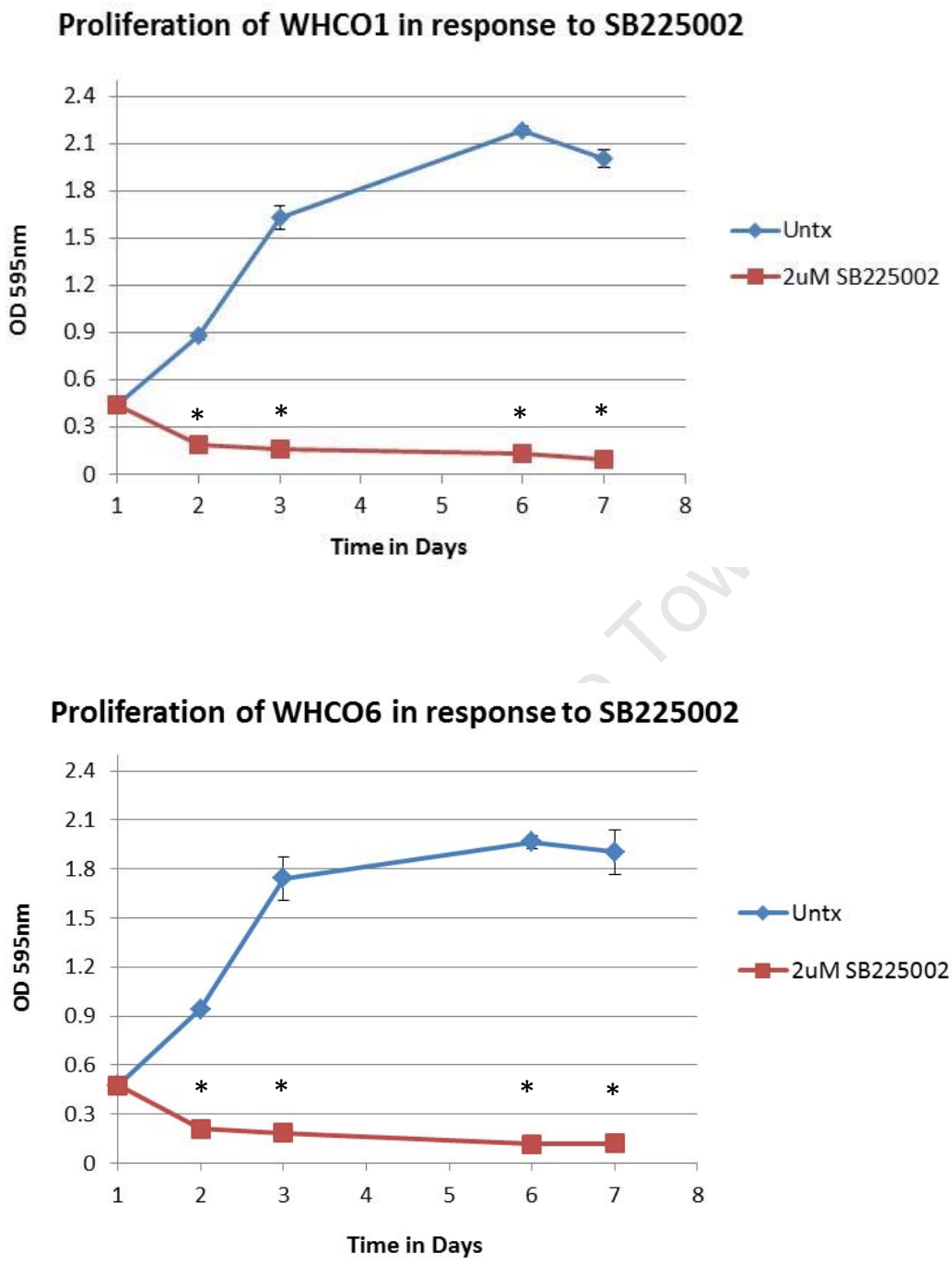

Figure 3.8: Effect of SB225002 on WHCO1 and WHCO6 cell proliferation

WHCO1 and WHCO6 OSCC cells were seeded at 1500 cells per well in triplicate in 96 well plates. The following day cells were treated with 2 µM SB225002 over the indicated time period and cell proliferation was measured by MTT assay. Absorbance was read with a multi-plate reader at 595 nm. Each point was performed in triplicate and error bars represent STDEV. (* $p \leq 0.0005$)

Our results (Fig. 3.7 and 3.8) clearly indicated that SB225002 inhibited proliferation of WHCO1 and WHCO6 cells. We next determined the effect of SB225002 treatment on the cell cycle profile of cells to better understand the mechanism of action of this compound. WHCO1 and WHCO6 cells were seeded in 60 mm dishes in triplicate and treated with 2 μM SB225002 for 8, 24 and 48 hr. Cells were trypsinized, stained with propidium iodide and was analyzed by flow cytometry. A significant G2/M arrest was observed as early as 8 hr in cells treated with SB225002, with 64% of WHCO1 and 48% of WHCO6 cells ($p \leq 0.005$), respectively, blocked in the G2/M phase, compared to untreated cells (14% for WHCO1 and 13% for WHCO6) (Fig. 3.9). However this arrest was lost at the 24 hr and 48 hr time points. The loss of the G2/M arrest at the 24 hour and 48 hour point was associated with a substantial increase in the sub G1 population ($p \leq 0.005$), suggesting that a significant proportion of cells were dying. The increase in sub G1 was observed in both WHCO1 and WHCO6 cells.

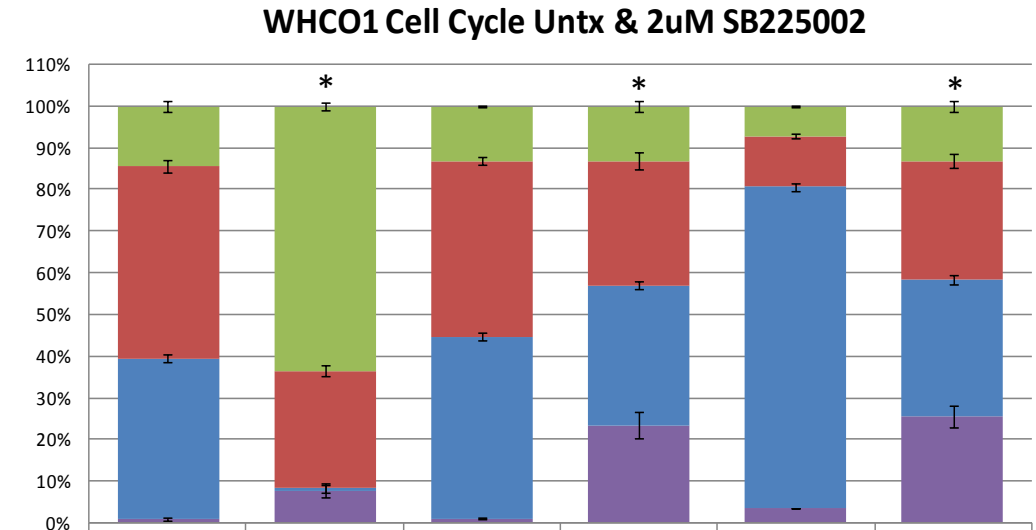

	WHCO1 Untx 8Hr	WHCO1 2uM SB225002 8Hr	WHCO1 Untx 24Hr	WHCO1 2uM SB225002 24Hr	WHCO1 Untx 48Hr	WHCO1 2uM SB225002 48Hr
G2	14.38	63.63	13.05	13.02	7.23	13.04
S	46.23	28.32	42.29	30.05	12.12	28.63
G1	38.60	0.40	43.75	33.58	77.22	32.90
Sub G1	0.79	7.65	0.91	23.35	3.42	25.43

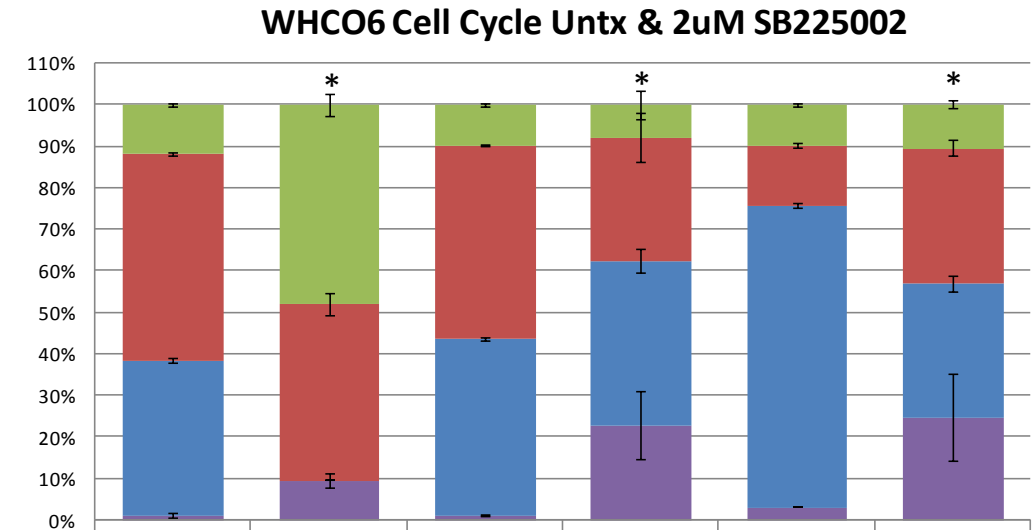

	WHCO6 Untx 8Hr	WHCO6 2uM SB225002 8Hr	WHCO6 Untx 24Hr	WHCO6 2uM SB225002 24Hr	WHCO6 Untx 48Hr	WHCO6 2uM SB225002 48Hr
G2	11.72	47.94	9.64	7.83	9.68	10.42
S	49.82	42.44	46.73	29.56	14.50	32.66
G1	37.16	0.00	42.42	39.69	72.58	32.21
Sub G1	1.30	9.62	1.21	22.91	3.23	24.71

Figure 3.9: Cell cycle profile of OSCC cells treated with SB225002.

WHCO1 and WHCO6 cells were seeded at a density of 3x105 cells per 60mm dish in triplicate and cultured for 24 hr. The following day cells were treated with 2uM SB225002 for 8, 24 and 48 hr. Cells were processed for flow cytometry and stained with propidium iodide. The cell cycle profile of cells was analysed on a FACS Calibur machine. Each point was performed in triplicate and error bars represent STDEV. (* $p \leq 0.05$)

The cell cycle is tightly regulated by cyclins (cyclin A, cyclin B and cyclin D); cyclin dependent kinases (CDK4, CDK6, CDK2) and cell cycle check point proteins including p21, p27 and p53 (Stark & Taylor 2006). The G2/M arrest observed in cells treated with SB225002 at the 8 hr time point may be associated with an alteration in cyclin protein levels that can be detected by western blot. WHCO1 and WHCO6 cells were plated in 60 mm dishes and treated with SB225002 for 4 and 8 hr respectively. Protein was harvested, subjected to western blotting and probed with specific antibodies for p27 and cyclin B. Cyclin B is essential for orchestrating the progression from G2 to mitosis while p27 is one of the important cell cycle inhibitors of G2/M (Mukherjee *et al.*, 2010). Consistent with the G2/M arrest observed in Figure 3.9, cyclin B levels were increased at the 4 and 8 hour time points (Fig 3.10). No change was observed for p27 suggesting no involvement with the cell cycle arrest.

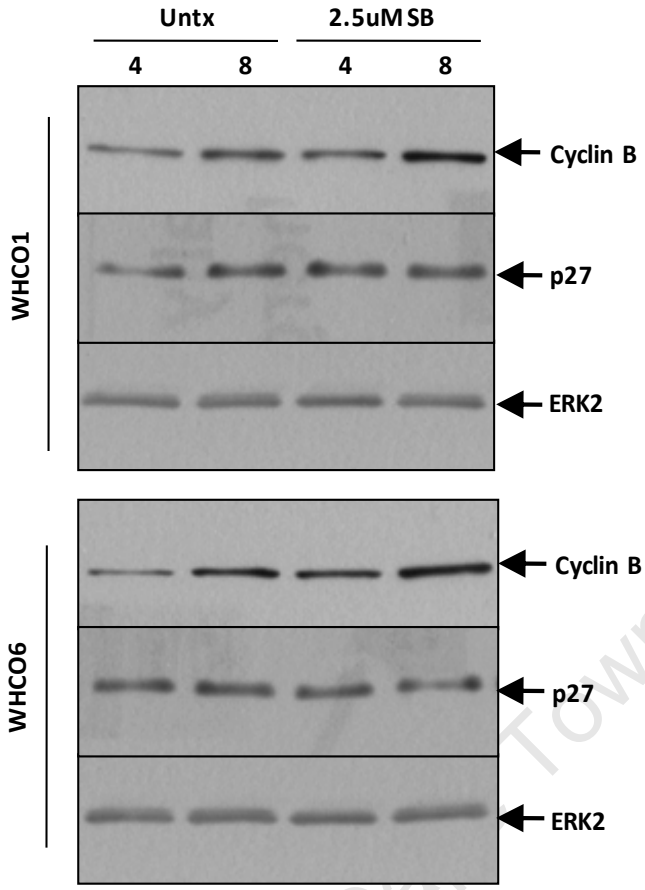

Figure 3.10: **Effect of SB225002 on cell cycle proteins cyclinB and p27 in OSCC cells**

WHCO1 and WHCO6 cells were plated in 60 mm dishes at 3 x 10^5 cells. Cells were treated with 2.5 µM SB225002 for the indicated times (in hr) and protein was harvested. A total of 40 µg of each sample was separated by SDS-PAGE and transferred to nitrocellulose membrane. The membrane was probed with antibody specific to cyclinB and p27 with total ERK2 used as a loading control.

The increase in the sub G1 population observed in the cell cycle analysis experiments (Fig. 3.9) at the later time points following the G2/M arrest suggested that cells were undergoing cell death. To further understand this observation cells were seeded in 60 mm dishes, treated with 2.5 µM SB225002 and protein was harvested. Western blot analysis was conducted using antibodies specific to pH2AX and PARP. When double strand DNA breaks occur histone 2AX becomes phosphorylated. These double-strand DNA breaks can indirectly be detected by western blot analysis as an increase in pH2AX positivity. A significant increase

in DNA damage was observed at the later time points in cells treated with 2.5 µM SB225002 compared to untreated cells (Fig 3.11) and apoptosis observed as cleaved PARP was evident at 24 hr with increased levels observed at 48 hr after drug treatment.

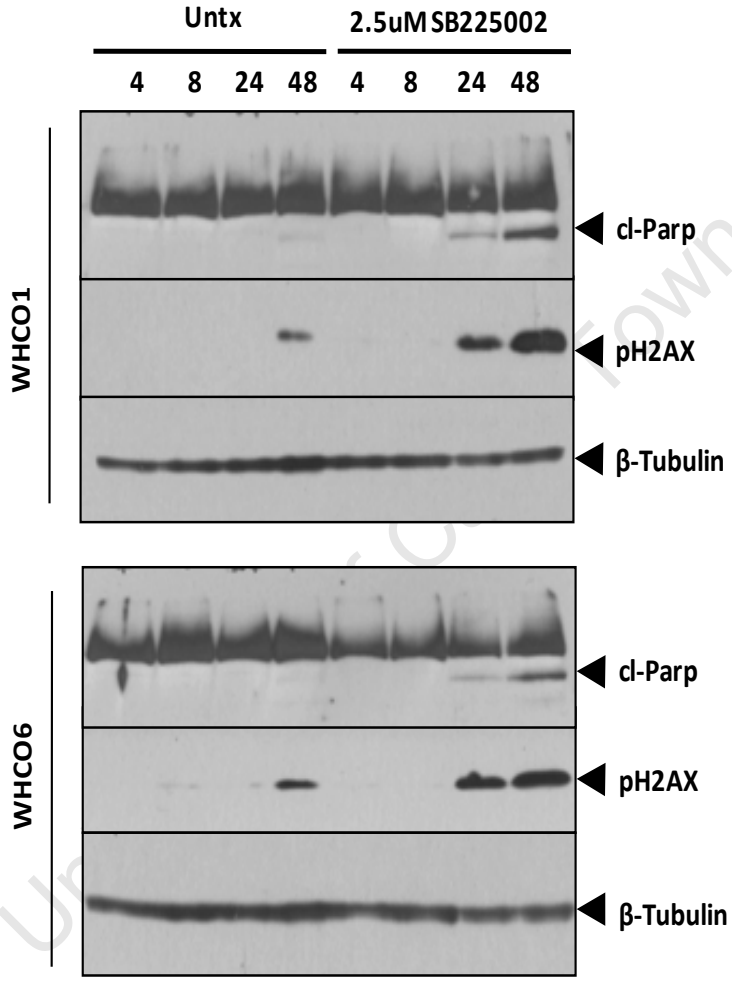

Figure 3.11: Effect of SB225002 on DNA damage and apoptosis in OSCC cells

WHCO1 and WHCO6 cells were plated in 60 mm dishes at 3 x 10^5 cells. Cells were treated with 2.5 µM SB225002 for the indicated times and protein was harvested. A total of 40 µg of each sample was separated by SDS-PAGE and transferred to nitrocellulose membrane. The membrane was probed with antibodies specific for cl-PARP and pH2AX.

Considering that the effect of SB225002 is mediated by the CXCR2 receptor, we wanted to determine whether the CXCR2 knockdown cells displayed resistance to SB225002. CXCR2 knockdown cells were plated at 1500 cells per well in 96well plates and treated with 1.5 μM SB225002 over a period of days. WHCO1 and WHCO6 CXCR2 knockdown cells treated with 1.5 μM SB225002 grew similar to untreated CXCR2 knockdown and control cells despite being challenged with drug (Fig 3.12). Proliferation of control cells, which expressed CXCR2, was significantly reduced compared to WHCO1 and WHCO6 CXCR2 shRNA cells treated with SB225002 ($p \leq 0.005$).

Proliferation of WHCO1 Ctrl and CXCR2 shRNA cells in response to SB225002

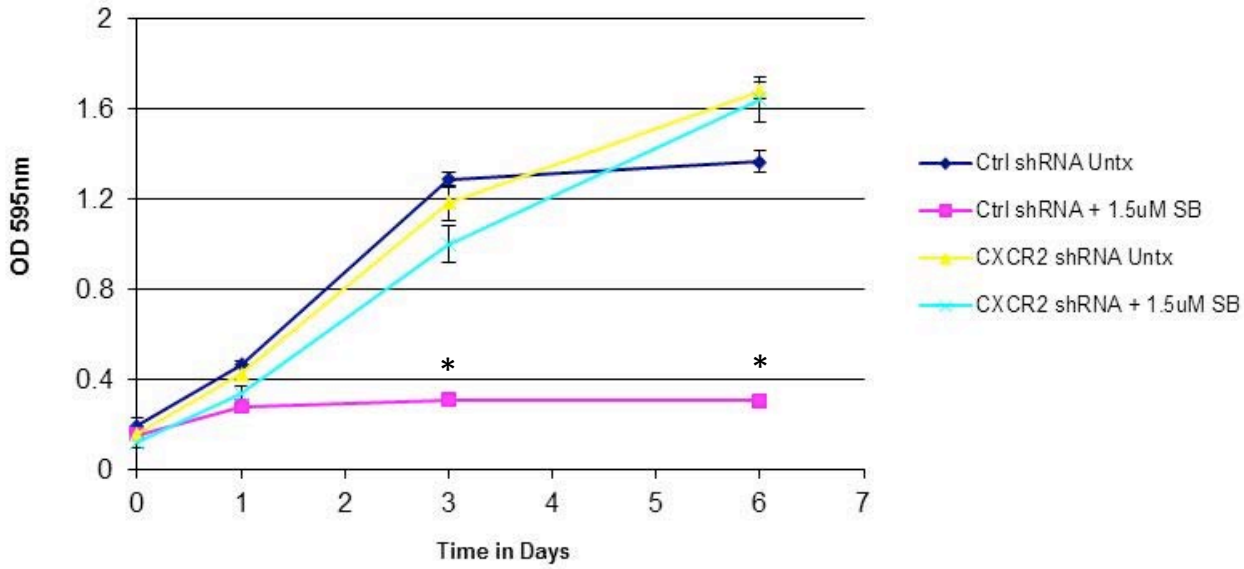

Proliferation of WHCO6 Ctrl and CXCR2 shRNA cells in response to SB225002

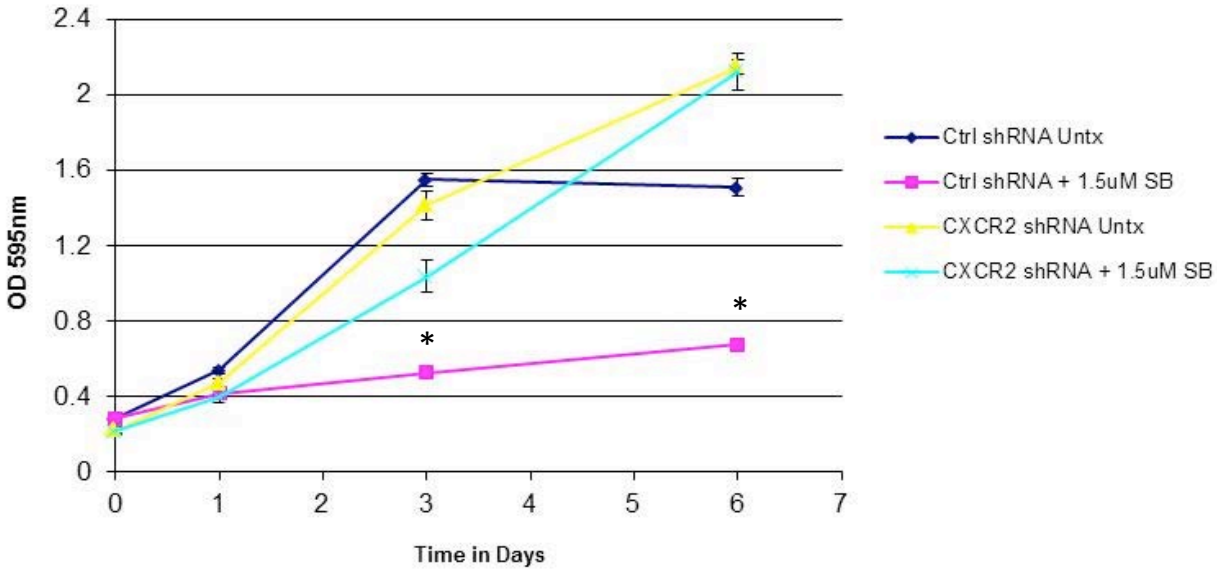

Figure 3.12: Effect of SB225002 on control and CXCR2 knockdown cell proliferation

WHCO1 and WHCO6 control and CXCR2 knockdown cells were seeded at 1500 cells per well in triplicate in 96 well plate. Cells were treated with 1.5 µM SB225002 and proliferation was monitored by MTT assay over the indicated times. Absorbance was read with a multi-plate reader at 595 nm. Each point was performed in triplicate and error bars represent STDEV. (* $p \leq 0.005$)

We have previously shown that SB225002 induces a G2/M arrest at the 8 hr time point in wild-type WHCO1 and WHCO6 cells. We wanted to investigate the effect of SB225002 on the cell cycle of CXCR2 knockdown cells at a density of 3 x 10^5 cells per dish, followed by treatment with 2 μM SB225002 for 8 hr. Cells were harvested, stained with propidium iodide and their cell cycle profile was determined. We observed a G2/M arrest in the control cells treated with SB225002 ($p \leq 0.0005$), however, CXCR2 knockdown cells displayed no G2/M arrest suggesting that CXCR2 was involved with mediating the SB225002-induced G2/M arrest in cells expressing CXCR2 (Fig. 3.13). Our data suggest that CXCR2 could be a good drug target for the management of OSCC, using SB225002 as an inhibitor.

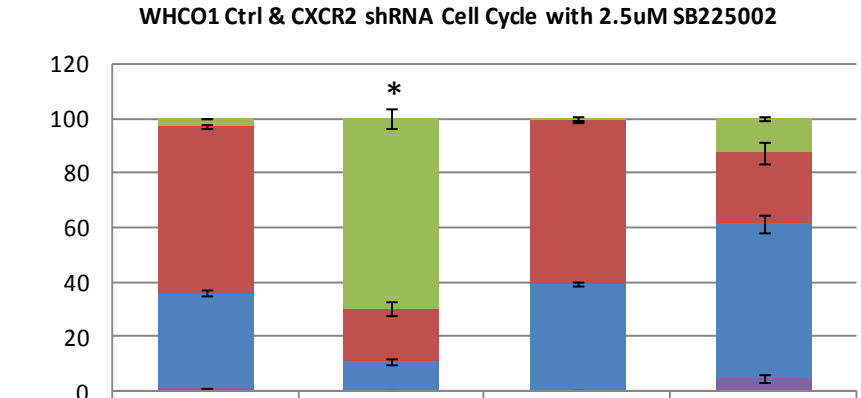

	WHCO1 Ctrl shRNA Untx 8Hr	WHCO1 Ctrl shRNA 2.5uM SB225002 8Hr	WHCO1 CXCR2 shRNA Untx 8Hr	WHCO1 CXCR2 shRNA 2.5uM SB225002 8Hr
G2	2.94	69.61	0.81	12.34
S	61.01	19.32	59.59	26.04
G1	34.76	10.72	39.15	56.72
Sub G1	1.29	0.35	0.45	4.90

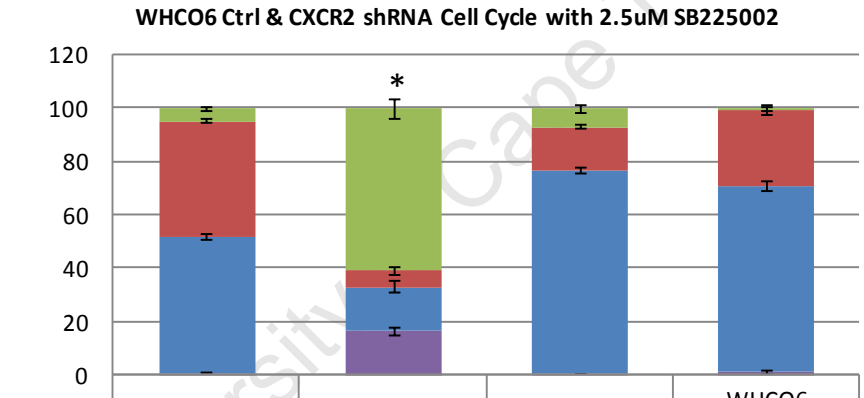

	WHCO6 Ctrl shRNA Untx 8Hr	WHCO6 Ctrl shRNA 2.5uM SB225002 8Hr	WHCO6 CXCR2 shRNA Untx 8Hr	WHCO6 CXCR2 shRNA 2.5uM SB225002 8Hr
G2	4.56	60.50	6.72	0.40
S	43.48	6.24	16.15	28.58
G1	51.24	16.47	76.37	69.80
Sub G1	0.71	16.80	0.76	1.22

<u>Figure 3.13:</u> Cell cycle profile of CXCR2 knockdown cells treated with SB225002.

WHCO1 and WHCO6 control and CXCR2 knockdown cells were seeded at a density of 3 x 10^5 cells per 60 mm dish in triplicate and left to settle overnight. The following day cells were treated with 2.5 µM SB225002 for 8 hr. Cells were processed for FACS analysis and stained with propidium iodide. The cell cycle profile of cells was analysed on a FACS Callibur machine. Each point was performed in triplicate and error bars represent STDEV. (* $p \leq 0.00005$)

3.3 Discussion:

Our original observations (Wang *et al.* 2006) suggested that CXCR2 signalling contributed to survival and proliferation in OSCC cells, since a knockdown of GROβ in these cells, or treatment with an inhibitor of CXCR2 SB225002, reduced cell proliferation by approximately 50%. These observations were consistent with reports that described functional CXCR2/ligand signalling loops in melanoma cell lines, and that these contributed to proliferation (Singh *et al.* 2009; Yang *et al.* 2010). The involvement of CXCR2 in OSCC proliferation and survival suggested that these receptors may represent feasible targets in the treatment of OSCC, an attractive option considering our observation that CXCR2 was overexpressed in 88% of primary OSCC tissue examined by IHC (Wang *et al.* 2006).

In this study we demonstrated that most OSCC cell lines examined (8/9) express CXCR2 that was functional, based on the phosphorylation of AKT and ERK1/2 in response to GROβ treatment. Furthermore, treatment of cells with a neutralizing antibody to CXCR2, resulted in decreased basal pAKT and pERK levels, suggesting that CXCR2 signalling contributed to basal pAKT and pERK levels in OSCC cell lines. Signalling from CXCR2 to the MAPK/ERK1/2 and PI3K/AKT pathways is important for the activation of genes involved with cell cycle progression and proteins involved with protein translation and cell polarization respectively (Yang *et al.* 1999; Zhao *et al.* 2004; Sai *et al.* 2006; Chapman *et al.* 2009). Contrary to our previous observation, blockade of CXCR2 using two different approaches - either neutralizing antibodies to CXCR2, or CXCR2 knockdown with shRNA, had no effect on cell proliferation. This result was observed in two OSCC cell lines, suggesting that we were not observing cell line specific artefacts. Although the level of CXCR2-neutralizing antibody used in the cell proliferation experiments (Fig. 3.3) was 2-fold

higher than that required to reduce pAKT and pERK1/2 levels by >50% (Fig. 3.2), and even if antibody levels were supplemented every 24 hr, it is still possible that this may not have been sufficient to block CXCR2 activity. Although numerous reports show that inhibition of CXCR2 *in vivo* with neutralizing antibody results in decreased angiogenesis and ultimately reduced tumour volume - consistent with our data, no observable changes in cell proliferation have been reported when targeting CXCR2 *in vitro* with an anti-CXCR2 antibody (Karl *et al.*, 2005; Keane, Belperio, Ying Y Xue, Marie D Burdick, & Robert M Strieter, 2004; Matsuo *et al.*, 2009). However, it is very difficult to rationalize the CXCR2 knockdown experiments. Our results convincingly demonstrates a substantial reduction in CXCR2 mRNA levels in both WHCO1 and WHCO6 cell lines (>95%), and also shows a substantial reduction in CXCR2 protein levels. Despite this evident depletion of CXCR2 activity, the CXCR2 shRNA expressing cells show proliferation values similar to control cells (for both cell lines). These results are consistent with our findings showing no effect of neutralising antibody on proliferation, and suggest that the absence of CXCR2 does not reduce cell proliferation or survival in OSCC cells. This is in contrast to results obtained previously in our laboratory showing that GROβ knockdown resulted in a 50% reduction in cell proliferation (Wang *et al.* 2006). The two experimental systems are very different. In the earlier system, knockdown of GROβ was presumably associated with unoccupied CXCR2 located on the plasma membrane, bound to accessory proteins, whereas in the current experimental system, no, or very little CXCR2 was located at the plasma membrane. Altered CXCR2 signalling to arrestins and adaptor-protein 2, crucial for receptor desensitization and controlled signalling, can result in apoptosis of cells (Revankar *et al.* 2004; Wagener *et al.* 2009). This may explain the reduced proliferation in the GROβ knockdown cells, but not CXCR2 knockdown OSCC cells, as CXCR2 signalling to arrestins may have been defective. It is also possible that the GROβ shRNA sequences could have non-specific toxic effects on the cells, although this is

less likely since two different sequences were used, with similar results observed. Maybe some of these differences underlie the contradictory effects of these two approaches on cell proliferation, but they require further investigation before this conundrum can be resolved.

We have consistently demonstrated that the CXCR2 inhibitor, SB225002, strongly inhibits OSCC cell proliferation, with an IC_{50} of about 2 μM, whereas the proliferation of fibroblasts was unaffected by SB225002, even at concentrations of 100 – 200 μM. Likewise, Acosta *et al.*, (2008) had observed that normal skin fibroblast cells (DMB cells) were insensitive to SB225002 and that inhibition of CXCR2 in these cells increased their proliferative ability. Our observation that inhibition of CXCR2 in OSCC cells results in cell death compared to normal cells, which are insensitive to CXCR2 inhibitor is consistent with reports that CXCR2 has opposing roles in cancers compared to normal cells (Acosta *et al.* 2008; Acosta & Gil 2009). CXCR2 is suggested to activate proliferation, angiogenesis and metastasis in cancer cells while in normal cells it can activate senescence (Acosta & Gil 2009; Cataisson *et al.* 2009; Matsuo *et al.* 2009; Singh *et al.* 2009).

Further investigation of the toxic effect of SB225002 in OSCC cells, revealed that relatively low concentrations of this CXCR2 inhibitor caused a strong G2/M block at 8 hr after treatment, and that this was associated with elevated levels of cyclin B. G2/M arrest in cells is frequently associated with defects in DNA repair mechanisms, aberrant spindle attachment and altered polarization of spindle microtubules (Mukherjee *et al.* 2010). A review of the cell cycle by Stark and Taylor (2006) suggested p53 involvement in maintaining the G2/M arrest in cells treated with radiation (Stark & Taylor 2006). The G2/M block observed at the 8 hour point after SB225002 treatment, was not observed at the 24 hour and 48 hour point (post SB225002 treatment), but substantial amounts of sub G1 debris was observed. Indeed, PARP cleavage analysis confirmed that the debris observed at the 24 hour and 48 hour time points

were due to apoptosis, suggesting that cells were either undergoing apoptosis directly in the G2/M phase, or that they first exited G2/M, then undergo apoptosis.

Seeing that the G2/M arrest and apoptosis induced by SB225002 was dependent on CXCR2 presence but knockdown of CXCR2 or inhibition by neutralizing antibody had no effect on OSCC cell biology, it suggests to us that the drug when bound to CXCR2 results in aberrant receptor function. When neutralizing antibody is bound to receptor, receptor levels are decreased as a result of internalization and degradation (Rowinsky 2004), while in CXCR2 knockdown cells only low levels of receptor are present. We hypothesise that the CXCR2 knockdown cells and cells treated with neutralizing antibody are thus similar in this regards, hence no effect on proliferation was observed. When cells were treated with SB225002, it is possible that this compound interferes with the normal processing of CXCR2, leading to apoptosis. CXCR2 could be trapped at the cell membrane when bound to SB225002 as reported by Acosta *et al.* (2008). Localization of CXCR2 bound to SB225002 at the cell membrane may have resulted in association of arrestins with CXCR2 which has been reported to activate apoptosis when its function is impaired (Revankar *et al.* 2004; Wagener *et al.* 2009). Alternatively, if CXCR2 bound to inhibitor was internalized, this could result in accumulation of drug in intracellular compartments or endosomes resulting in deregulated endosomal pathways leading to cell death.

Our data suggests that CXCR2 is overexpressed in OSCC cell lines and OSCC patient tissue compared to normal cells and adjacent tissue (Wang *et al.* 2006). Furthermore CXCR2 inhibition with inhibitor results in apoptosis of OSCC cells that display receptors, however, OSCC cells which lack CXCR2 were insensitive to inhibitor. This highlights the importance of CXCR2 as a potential therapeutic target in OSCC. Normal cells which express little to no receptor would not be adversely affected by CXCR2 inhibition. The results observed here are

novel, and in fact, the induction of apoptosis by SB225002 has only very recently been observed in head and neck cancer cells (Romanini *et al.* 2011). There is thus precedent for the observation that SB225002, can kill cancer cells (albeit very recent evidence), and strongly supports our case that SB225002, could be a very useful drug in our limited arsenal of compounds that we can use to treat oesophageal cancer.

Chapter 4

Conclusion:

OSCC currently presents a significant health burden in many developing countries and will continue to do so for the foreseeable future. We could reduce the morbidity and mortality associated with this disease if better therapeutic options for these patients could be developed. Of course, the discovery and implementation of more effective early diagnostic measures could be equally, if not more effective in this regard, and it is important that research in this area continue unabated.

This project, however, focussed on the identification and characterisation of potential therapeutic targets in OSCC. Here we demonstrated that OSCC cells show increased sensitivity to AG1478 (the EGFR inhibitors) when IGF-1R is blocked, suggesting that the simultaneous targeting of EGFR and IGF-1R may be a promising strategy to follow in OSCC patients. In this project, simultaneous targeting of these two receptors was associated with increased apoptosis. These results seem very promising and they suggest a course of action that could be considered. It would be interesting to test some of the newer specific IGF-1R inhibitors, and determine if the simultaneous targeting of IGF-1R and EGFR in parental OSCC cell lines kill these cancer cells more efficiently than separate treatment. If the simultaneous targeting of EGFR and IGF-1R in cultured OSCC cells lead to the more effective induction of apoptosis, the next step should be to test the effect of these compounds, individually or in combination on the growth of OSCC human xenografts in a nude mouse model. A successful study using xenografts in a nude mouse model would be a very strong incentive to consider initiating clinical trials in OSCC patients, whose tumours display

positivity for both EGFR and IGF-1R. This approach seems reasonable considering the clinical implications of the results reported here for EGFR and IGF-1R.

However, the results of this study also raise interesting questions about the biology of EGFR and IGF-1R function. The knockdown of IGF-1R show that reduced IGF-1R levels on the plasma membrane of OSCC cell lines, is associated with elevated levels of pEGFR, and that this result is not mediated through AKT, but possibly directly through IGF-1R (considering the effects of the AKT inhibitor). It would be very interesting to determine how this phenomenon is mediated. Furthermore, the functional significance of the transient activation of IGF-1R observed in response to EGF treatment is also an interesting observation that could be investigated further.

As mentioned before, it is difficult to rationalise the results observed earlier in our laboratory where knockdown of GROα and GROβ was associated with a reduction in cell proliferation in OSCC cell lines, with the present results which indicate that a CXCR2 neutralising antibody, and CXCR2 knockdown, both had no measurable effect on cell proliferation. These divergent observations require further investigation.

Our results observed for CXCR2 also have potentially important clinical implications. The induction of apoptosis in OSCC cells by relatively low levels of SB225002 (IC_{50} of 2 – 3 μM), combined with the observation that 5 – 10 fold this concentration had no inhibitory effect on fibroblast proliferation, suggest that SB225002, should be tested in a OSCC xenograft model in nude mice. A positive response in a xenograft mouse model should be followed by clinical trials of SB225002 in OSCC patients positive for CXCR2, to determine the efficacy of this drug. Reports in the literature suggest that CXCR null mice show no

defects in development (Keane *et al.* 2004; Svensson *et al.* 2008), suggesting that this therapeutic approach may have minimal side effects.

Although our results here show that treatment of OSCC cell lines with SB225002 was associated with an early cell cycle disruption (G2/M block at 8 hr), DNA damage (H2AX phosphorylation) and the induction of apoptosis (PARP cleavage), it would be interesting to determine how SB225002 triggers this response in OSCC cells, and not fibroblasts for example. Is ROS production involved in this process, and is this associated with the DNA damage observed? These questions are currently being explored in our laboratory, so that we can understand how the effects of SB225002 are mediated in OSCC cells.

We highlighted the potential of three receptors as therapeutic targets for the management of OSCC with novel findings including a negative regulatory IGF-1R/AKT loop, increased cell death when specifically targeting EGFR and IGF-1R simultaneously and specific killing of CXCR2 positive cancer cells verses CXCR2 negative or CXCR2 expressing normal fibroblast cells. Our data should be considered for further *in vivo* evaluation as we have provided good *in vitro* evidence for the potential of targeting EGFR, IGF-1R and CXCR2.

Chapter 5

Materials and Methods:

5.1.i Cell culture

Oesophageal squamous cell carcinoma (OSCC) cell lines, WHCO1, WHCO5 and WHCO6 were obtained as a generous gift from Dr Veale (Veale and Thornley 1984) and KYSE30, KYSE70, KYSE150, KYSE180, KYSE410 and KYSE450 were obtained from Dr Shimido – Japan and purchased from the DSMZ cell bank. Normal skin fibroblast cell lines, FG^0 and DMB were obtained as a generous gift from Dr A. D. Marais (Groote Schuur Hospital, Cape Town) and normal lung fibroblast cell line, WI38, were purchased from the American Type Culture Collection (ATCC) (Rockville, MD, USA). All the above cell lines were cultured at 37°C in a humidified atmosphere of 5% CO_2 and 95% air in Dulbecco's modified Eagle medium (DMEM) containing 10% heat inactivated foetal calf serum, penicillin (100U/ml) and streptomycin (100 µg/ml). HEK293T cells (Invitrogen) were cultured at 37°C in a humidified atmosphere of 5% CO_2 and 95% air in DMEM containing 10% heat inactivated foetal calf serum (Gibco), 0.1 mM MEM Non-Essential Amino Acids (Sigma), 2 mM L-glutamine, penicillin (100U/ml) (Gibco), streptomycin (100 µg/ml) (Gibco), and 500µg/ml Geneticin (Sigma).

5.1.ii Thawing Cells

Culture medium was pre-warmed in a 37°C water-bath and 3 ml of pre-warmed media was added to a 60 mm dish. Cells were collected from liquid nitrogen tanks and thawed in a 37°C water-bath. Once cells were thawed the cells were transferred to a 10ml tube containing 3 ml of media. Cells were pelleted by centrifuging at 1000 rpm for 5 min. The supernatant was

removed, the cell pellet was resuspended in 1 ml of media and the cell suspension was added to the 60 mm dish. Cells were placed in the 37°C incubator and were cultured for further experiments.

5.1.iii Freezing Cells

Cells were grown to 80% confluency, medium was removed and the dish was rinsed with 2 ml of warm trypsin/EDTA (Difco). Another 2 ml of trypsin was added and incubated with cells for 1-2 min. Following incubation with trypsin/EDTA, cells were aspirated and then transferred to a 10 ml tube containing 4 ml of media. Cells were centrifuged at 1000 rpm for 5 min, the supernatant was removed and the cell pellet was resuspended in a total of 5 ml of media. An aliquot of the cell suspension (10 µl) was counted by means of a haemocytometer to determine cell number. Medium, foetal calf serum and DMSO was added to the cell suspension so that the final concentration of cells per ml was $1x10^6$, foetal calf serum 20%, DMSO 10%. One ml aliquots of cells were added to cryotubes and placed at -80^oC for 2 days and then transferred to liquid nitrogen for long term storage.

5.2 Protein Extraction and Processing

Cells were seeded at a density of 3 x 10^5 cells per 60 mm and left overnight to settle. 24 hr later, cells were treated with various agents as indicated: EGF (Sigma); IGF-1 (Sigma); SB225002 (TOCRIS Bioscience); AG1478 (CalBiochem); cisplatin (TOCRIS Bioscience); AKT VIII trifluoroacetate salt (Sigma); doxorubicin (Sigma) at the indicated concentrations for the indicated time periods and protein was harvested. Media was collected from cells, followed by 2 washes with 2 ml of 1 x PBS which was also collected and this was centrifuged at 1000 rpm for 5 min in 12 ml tubes. RIPA buffer and the indicated additives were added to

cells (60-100 µl) and cells were scraped using a cell scraper. Cell protein was then collected in eppendorf tubes. Media was removed from the 12 ml tubes containing a cell pellet obtained from the floating cells. The pellet was resuspended in Ripa buffer and the indicated additives and transferred to the corresponding eppendorf tube. Protein concentration was determined using the bicinchoninic acid (BCA) Protein Assay kit (Pierce, Thermo Scientific) as described by the manufacturers and then stored at -80^{o}C. Protein (20 – 40 µg per sample) was prepared for SDS-PAGE by adding loading dye and heating samples at 85^{o}C for 5 min, followed by loading samples on 10% SDS poly-acrylamide gels.

5.3 Immunoprecipitation

Cells were seeded in 100 mm dishes at a density of 1x10^{6} cells. Protein was harvested in RIPA buffer as described above and quantified using the BCA kit. Protein (300 µg) was incubated with 2 µg EGFR antibody overnight at 4^{o}C on a circular rotor. The next day 50 µl of protein-A agarose beads (Calbiochem) was added to each sample and incubated for 4 hr with agitation on a circular rotor at 4^{o}C. Samples were centrifuged at 12000 rpm for 5 min, the supernatant removed and the pelleted beads were washed three times with 300 µl 1xPBS. After the final centrifugation PBS was removed so that a final volume of 25 µl remained, 6 µl of 5 x loading dye was added to samples, which were then heated at 85^{o}C for 5 min and subjected immediately to Western blotting using 10% SDS-PAGE gels.

5.4 Western Blot Analysis

Ten or twelve percent SDS-PAGE gels were cast in either 1 mm or 1.5 mm glass plates using the BioRad Western blotting system. Resolving and stacking gel solutions were prepared as specified in the tables 1 and 2 below. First, the resolving gel was poured between the glass

plates, water was added and this was allowed to set. Protein samples were prepared by thawing the samples on ice, determining the amount of sample required for 20-40 µg, and adding the appropriate amount of 5 x loading dye the prepared samples were heated to 85^{o}C for 5 min and subjected to a pulse spin for 20 sec. The water was poured off the resolving gel, the stacking gel was added on top of the resolving gel and a 10 or 15 well comb was inserted. This was allowed to set followed by gel assembly.

Table 1:

Resolving Gel Solution	10% (1.5 mm gel)	12% (1.5 mm gel)	10% (1 mm gel)	12% (1 mm gel)
Resolving Buffer	3 ml	3 ml	2 ml	2 ml
Acrylamide	3 ml	3.75 ml	2 ml	2.75 ml
dH_2O	3 ml	2.25 ml	2 ml	1.25 ml
10% APS	150 µl	150 µl	100 µl	100 µl
TEMED	15 µl	15 µl	10 µl	10 µl

Table 2:

Stacking Gel Solution (5%)	**1.5 mm gel**	**1 mm gel**
Stacking buffer	1.5 ml	750 µl
Acrylamide	1 ml	500 µl
dH_2O	3.5 ml	1.75 ml
10% APS	60 µl	30 µl
TEMED	6 µl	3 µl

Protein was loaded alongside a protein ladder (Fermentas Spectra Multicolor Broad Range Protein ladder) for sizing and gels were electrophoresed at 150 V for 1 hr and 15 min. Following electrophoresis, proteins were transferred onto nitrocellulose membrane (Amersham Hybond ECL). An ice pack was placed in the tank which was subsequently filled with 1x transfer buffer. Protein transfer was carried out at 100 V for 90 min. Membranes were subsequently washed with 1x TBST and blocked for one hour in 5% non-fat powder milk made with 1x TBST. The blocking solution was removed, primary antibody was added (see Table 3 for concentrations) and membranes were incubated overnight at 4^{o}C with shaking. The next day membranes were washed 3 x 5 min with 1x TBST and incubated with secondary antibody for 1hour at room temperature with shaking (see Table 3 for concentrations).

Following this, membranes were washed 3 x 5 min with 1x TBST, placed on transparency film, incubated with chemiluminescence detection reagent (see table 3) and exposed to X-ray film in a dark room. The film was developed and fixed, rinsed with water and left to dry in a 37^{o}C incubator.

Table 3: Antibody Conditions

Antibody (Ab)	Company and Cat no.	1° Ab Conditions	2° Ab Conditions	Substrate
pEGFR (Tyr 1173)	Santa Cruz sc-12351	1:1000 TBS-Tween	1:2000 2.5% BSA DαG Pierce	Super Signal
EGFR	Santa Cruz sc-03	1:1000 2.5% Milk	1:5000 5% Milk GαR Biorad	Super
pIGF-1R	Cell Signalling	1:1000 2.5% Milk-BSA/5% BSA	1:5000 5% Milk GαR Biorad	LumiGLO Reserve
IGF-1R	Santa Cruz	1:1000 5% Milk	1:5000 5% Milk GαR Biorad	Super Signal
pAKT (Ser 473)	Cell Signalling 9271	1:1000 5% BSA	1:5000 5% Milk GαR Biorad	LumiGLO Reserve
AKT	Cell Signalling 9272	1:1000 5% BSA	1:5000 5% Milk GαR Biorad	LumiGLO Reserve
pERK 1/2 (Thr 202/Tyr 204)	Cell Signalling 9106	1:1000 1% BSA	1:5000 2.5 % Milk GαM BioRad	Super Signal Dura-extend
ERK 2	Santa Cruz sc-154	1:1000 1% Milk	1:5000 2.5 % Milk GαR Biorad	Super Signal
β-Tubulin	Santa Cruz sc-9104	1:1000 TBS-Tween	1:5000 5% Milk GαR Biorad	Super Signal
Cleaved-PARP	Santa Cruz	1:2000 5% Milk	1:5000 5% Milk GαR Biorad	Super Signal
CXCR2	Santa Cruz	1:1000 TBS-Tween	1:4000 2.5% BSA DαG Pierce	Super Signal
p27	Santa Cruz	1:1000 2.5% Milk	1:5000 5% Milk GαR Biorad	Super Signal Dura-extend
pTyr	Cell Signalling	1:1000 2.5% Milk	1:5000 2.5 % Milk GαM BioRad	LumiGLO Reserve
Cyclin B		1:1000 TBS-Tween	1:5000 2.5 % Milk GαM BioRad	Super Signal
pH2AX	Cell Signalling	1:2000 TBS-Tween	1:5000 5% Milk GαR Biorad	LumiGLO Reserve
p38	Sigma M0800	1:5000 TBST	1:5000 5% Milk GαR Biorad	Super Signal

5.5 RNA Extraction

Cells were washed twice with 2 ml cold PBS and 600 µl per 60 mm dish or 1 ml per 100 mm dish of QIAzol (Qiagen) was added. Cells were incubated at RT for 5 min before being scraped off the dish and transferred to 1.5 ml eppendorf tubes and 0.2 ml of chloroform per 1 ml of QIAzol used was added. Tubes were inverted for 15 sec and incubated on ice for 10 min followed by centrifugation at 8000 rpm for 15 min at 4^{o}C. Following centrifugation the

aqueous phase was transferred to a clean 1.5 ml eppendorf tube and 0.5 ml of isopropanol per 1 ml of QIAzol was added and RNA was precipitated overnight at -20^{o}C. Samples were again centrifuged at 8000 rpm for 30 min at 4^{o}C. The supernatant was removed and the resulting pellet was washed in 1 ml 75% ethanol per 1 ml of QIAzol. Samples were subjected to centrifugation at 8000 rpm for 20 min at 4^{o}C. The supernatant was discarded and the pellet air-dried and then resuspended in 30 µl of DEPC water. RNA concentration was determined with a nano-drop (Thermo Scientific) and the integrity was determined by running 2 µg of RNA on a 1.5% agarose formaldehyde gel at 60 V for 45 min.

5.6 cDNA synthesis

cDNA was synthesized by taking 2 µg of RNA making it up to 8 µl with DEPC H_2O and adding 1 µl of Oligo-dT primer (Promega). This was incubated at 70^{o}C for 10 min followed by a pulse spin and immediately placing the mix on ice. cDNA was synthesized in a reaction containing 1 x first strand buffer, 2 mM $MgCl_2$ (Promega), 1 mM dNTPs (Promega), 40 U RNasin (Promega), 1 µl reverse transcriptase (RT) (Promega) and 1.4 µl DEPC H_2O. 11 µl of the above master mix was added to each tube and placed in a PCR machine set at 42^{o}C for 2 hr followed by 70^{o}C for 10 min. cDNA was aliquotted and stored at -80^{o}C.

5.7 Quantitative real-time RT-PCR (qRT PCR)

Gene-specific primer sequences are shown in Table 4. Primers were synthesised by UCT oligonucleotides synthesis facility, and 20 µM stocks for each primer were prepared. For one realtime PCR reaction 6.5 µl of distilled water, 9.5 µl of SyBrgreen Fast PCR reaction mix (Kapa Biosystems, South Africa), 1 µl (20pmol) each of forward and reverse primer and 2 µl

of cDNA was aliquotted into a PCR fast reaction tube (Applied Biosystems). All reactions for the target gene and housekeeping gene were performed in triplicate. Tubes were placed in a Realt-Time PCR machine (Applied Biosystems) and subjected to 1 cycle of 95^{o}C for 3 min to activate the enzyme, followed by 40 cycles of 95^{o}C for 1 second (denaturation) and 55^{o}C for 20 sec (annealing and extension). Melt curve was performed for analysis of PCR product melt profiles, to ensure the specificity of the reactions

Table 4: Sequences of primers used for real-time RT-PCR

Gene	Sequence	PCR product size (bp)	Ta (°C)
CXCR2 Forward	5' CTCCAATAACAGCAGGTCAC 3'	279	55
CXCR2 Reverse	5' GGCTCAGCAGGAATACCA 3'		
GusB Forward	5' CTCATTTGGAATTTTGCCGATT	81	55
GusB Reverse	5' CCGAGTGAAGATCCCCTTTTTA		

5.8 siRNA Transfection:

Cells were seeded at a density of 1.5 x 10^5 cells per 35 mm dish or 3 x 10^5 cells per 60 mm dish and left overnight in 37^{o}C incubator to settle. The following day the transfection cocktail was prepared as follows:

Transfection cocktail per:	35 mm dish	60 mm dish
Serum and pen/strep free DMEM	50 µl	114 µl
Transfectin (BioRad)	0.625 µl	1.4 µl
Incubate at room temperature for 5 min		
siRNA (control or EGFR) (Santa Cruz) (stock 10 µM)	2 µl	4.57 µl
Incubate at room temperature for 20 min		

Media was removed from cells and replaced with 1 ml of complete DMEM. siRNA transfection cocktail was added dropwise to cells and incubated for 5-6 hr with cells. The transfection mix was then removed from cells and replaced with 2 ml of fresh media for at least 24 hr. Protein was harvested and analysed to determine the extent of knockdown.

5.9 MTT Assay

Cells were seeded in 96 well plates at a density of 1.5 x 10^3 cells per well in triplicate in 90 µl of media and left overnight in, 5% CO_2, 37^oC humidified incubators. The following day 10 µl of drug at 10 x the desired concentration, diluted in complete DMEM was added to each well. Cells were treated with a range of different concentrations of drug. Following a 48 hr incubation with drug 10 µl of sterile 5 mg/ml MTT [3-(4,5-Dimethylthiazol-z-yl)-2,5-diphenyltetrazolium bromide] in PBS was added to each well and incubated with cells for 4 hr followed by the addition of 100 µl of solubilisation solution (10% SDS, 10 mM HCl) which was incubated with cells for 16 hr. The following day of the OD of each well at 595 nm was determined using a microtiter plate reader (Beckman) and results were analyzed using GraphpadPrism3 software (Hearne Scientific Software).

5.10 Fluorescent Activated Cell Sorting (FACS)

Cells were seeded at a density of 3 x 10^5 cells per 60 mm dish and incubated overnight at 37^{o}C. The following day cells were treated as described in specific figures. Cells were then harvested by collecting media in 12 ml tubes, rinsed with 2 ml of trypsin which was also collected. A further 2 ml of trypsin was added to cells and left for 3 min after which cells were trypsinized and collected in the 12 ml tubes corresponding to the appropriate sample. Tubes were centrifuged at 1000 rpm for 5 min and the supernatant was removed. Cells were then resuspended in 2 ml of complete DMEM, counted and finally 8 ml of absolute ethanol was added to fix cells. Samples were stored at -20^{o}C for a period of 24 hr to a maximum of 2 weeks. On the day of acquisition cells were centrifuged at 1000 rpm for 5 min. The supernatant was discarded and the cell pellet was rinsed and resuspended in 1 ml 1 x PBS followed by another round of centrifugation at 1000 rpm for 5 min and resuspension in 1 ml of 1x PBS. A total of 3 x 10^5 cells were aliquoted into 1.5 ml eppendorf tubes, centrifuged at 1000 rpm for 5 min. After the supernatant was discarded, cells were resuspended in 50 µg/ml RNAse A in 1 x PBS to a final volume of 0.2 ml RNAse A per 1x10^6 cells and incubated at 37^{o}C for 15 min. Cells were then stained 20 min before FACS acquisition with 300 µl staining solution per 3 x 10^5 cells (0.1% Triton X-100, 2 mM $MgCl_2$, 100mM NaCl, 10mM PIPES pH6.8 and 10 µg/ml propidium iodide) and cell cycle profiles were analysed using a Flow cytometer (Beckman Coulter).

5.11 Lentiviral production for stable knockdown of IGF-1R and CXCR2

A total of 2 x 10^6 HEK293T cells were cultured in DMEM media containing 10% heat inactivated foetal calf serum, 1% L-Glutamine (Sigma), 1% Non-essential amino acids (Sigma) (penicillin and streptomycin free) in 75 cm^2 tissue culture flasks. Once cells reached ~80% confluency, they were transfected with 3 plasmids encoding parts of the lentivirus and target gene to be silenced. Transfection cocktail mix was prepared as follows: 8250ng pWPI transfer plasmid (Addgene); 3900ng psPAX2 packaging plasmid (Addgene); and 1300ng pMD2.G envelope plasmid (Addgene). Plasmids were equilibrated to a final volume of 105 µl with serum-free OPTI-MEM

To a separate tube, 33.5 µl FuGENE HD was added to 386.5ul of serum-free OPTI-MEM. (do not allow the FuGENE to come into contact with the walls of the tube) The solution was mixed by gently flicking the tube and incubated for 5 min at room temperature.

The plasmid cocktail mix was added to the FuGENE HD serum-free OPTI-MEM mix dropwise. The plasmid and FuGENE cocktail was mixed by swirling or gently flicking the tube and was incubated for 30 min at room temperature.

Finally, the transfection cocktail was added dropwise to the HEK293T cells in the flask which was swirled to ensure even mixing (Do not mix transfection and cells too roughly as cells may be dislodged). Cells were incubated for 12-15 hr with transfection cocktail at 37^oC in an incubator. The following day medium containing the transfection cocktail was removed and 8 ml of fresh medium was added, cells were further incubated for 24 hr. Medium was transferred from HEK293T cells with disposable 10ml pipettes to 50ml polystyrene tubes and centrifuged at 1000 rpm for 5 min to pellet cell debris. A further 8 ml of fresh medium was added to the HEK293T cells, which was harvested 24 hr later. After centrifugation, medium

was aspirated with a syringe through a 0.45 μM filter (MILLEX-HV, PVDF, MILLIPORE) and 4ml aliquots were made in 12ml polystyrene tubes and stored at -80^{o}C for later use. Target cell lines, WHCO1 and WHCO6 cell were seeded at a density of 5 x 10^{5} cells per 60 mm dish and infected with the 4 ml aliquots of lentiviral particles containing Ctrl, CXCR2 or IGF-1R shRNA. Cells were incubated with lentivirus overnight and the next day media was changed and cells further cultured for protein, mRNA and to make cell stocks. IGF-1R shRNA cells were sorted based on GFP positivity while CXCR2 shRNA expressing cells were infected twice with viral particles. WHCO1 and WHCO6 control and IGF-1R shRNA cells were generated by a previous PhD student and CXCR2 shRNA cells were generated with the assistance of a fellow PhD student. A published CXCR2 shRNA sequence, described by Singh *et al.*, (2010), was used to generate stable CXCR2 knockdowns.

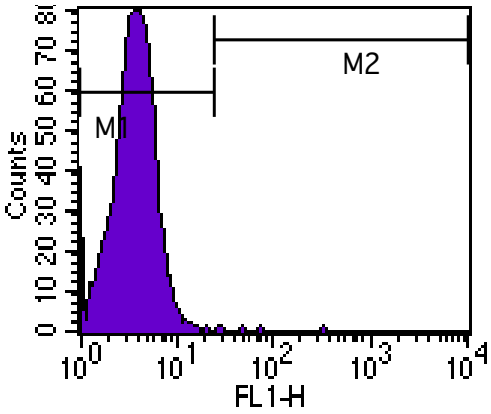

Sample: WHCO1 control GFP negative OSCC cells

Marker	Events	%Gated
All	8185	100.00
M1	8180	99.94
M2	5	0.06

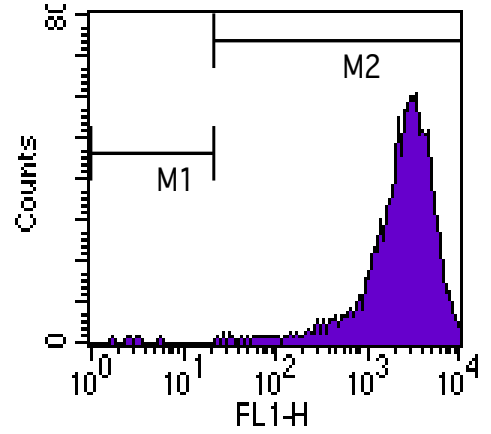

Sample: WHCO1 IGF-1R shRNA GFP positive OSCC cells

Marker	Events	%Gated
All	7487	100.00
M1	8	0.11
M2	7479	99.89

Figure 1: Cell sorting of GFP positive OSCC cells.

WHCO1 and WHCO6 OSCC cells previously infected with lentiviral particles containing Ctrl, IGF-1R or CXCR2 shRNA were cultured to 60-70% confluency. Cells were trypsinized, resuspended in 1 x PBS and transferred to FACS polystyrene tubes for cell sorting. Wild type WHCO1 cells were used as a GFP negative control to set the appropriate gates so that GFP negative cells were excluded. All GFP positive cells were sorted and used for further experiments.

5.12 Solutions:

30% Acrylamide solution

30 g Acrylamide

0.8 g Bisacrylamide

0.1 g SDS (Sodium dodecyle sulphate)

Make up to 100 ml with dH_2O, store at 4^oC

10% Ammonium Persulfate (APS)

Weigh out 100 mg APS and dissolve in 1 ml dH_2O, store at 4^oC ≤1 months

DEPC-treated water

Add diethylpyrocarbonate (DEPC) to a final concentration of 0.01% (v/v), stir, let stand overnight and autoclave.

0.5M EDTA pH 8.0

Dissolve 37.22 g $Na_2EDTA \cdot 2H_2O$ in 140 ml dH_2O, adjust pH to 8 with 10 N NaOH and make up to 200 ml with dH_2O and autoclave.

Freezing Solution for cells

70% DMEM

20% Foetal calf serum

10% Dimethylsulphoxide (DMSO)

1M $MgCl_2$

Dissolve 20.33 g $MgCl_2 \cdot 6H_2O$ in 80 ml dH_2O, make up to 100 ml and autoclave.

5M NaCl

Dissolve 29.17 g NaCl in 80 ml dH2O, make up to 100 ml and autoclave.

10 x PBS

2 g KCl

80 g NaCl

2 g KH_2PO_4

11.5 g Na_2HPO_4

Dissolve in 700 ml dH_2O, adjust pH to 7.4 with 1 N HCL or 1 N NaOH, make up to 1 L with dH_2O and autoclave.

Pepstatin A (1mg/ml)

Dissolve Pepstatin A in absolute ethanol to a final concentration of 1 mg/ml, and store at -20^{o}C.

100mM PMSF

Dissolve PMSF in absolute ethanol to a final concentration of 100 mM, and covered with foil at -20^{o}C.

Resolving Gel Buffer

36.2 g Tris

0.8 g SDS

Dissolve in 150 ml dH_2O, pH to 8.9 with 1 N HCL or 1 N NaOH and make up to 200 ml with dH_2O. Store at 4^oC

Stacking Gel Buffer

5.9 g Tris

0.4 g SDS

Dissolve in 70 ml dH_2O, pH to 6.8 with 1 N HCL or 1 N NaOH and make up to 100 ml with dH_2O. Store at 4^oC

10x Running Buffer

30.2 g Tris

144 g Glycine

10 g SDS

Make up to 1 L with dH_2O

1x Running Buffer

100 ml of 10x running buffer

900 ml of dH_2O

10x Transfer Buffer

144 g Glycine

38 g Tris

Make up to 1 L with dH_2O

1x Transfer

100 ml 10x transfer buffer (in this order)

700 ml dH_2O

200 ml methanol/isopropanol

10x Tris Buffered Saline

60.5 g Tris

87.6 g NaCl

Dissolve in 700 ml dH_2O, pH to 7.5 with 1 N HCL or 1 N NaOH and make up to 1 L with dH_2O.

1x TBST

100 ml 10x TBS

900 ml dH_2O

1 ml Tween20

Stripping Buffer

1.4 ml β-mercaptoethanol

40 ml 10% SDS / 4 g SDS powder

12.5 ml 1M Tris-Cl pH 6.7

Make up to 200 ml with dH_2O

5x Loading Buffer:

1.75 g Tris

30 ml glycerine

Make up to approximately 40 ml with dH_2O pH to 6.8 with 1 N HCl

Add 5 g SDS

Make up to a final volume of 50 ml with dH_2O

5x loading dye

Heat the loading buffer to allow for the SDS precipitate to dissolve.

Mix 100 µl 5 x loading buffer, 50 µl β-Mercaptoethanol and 50 µl 0.025% Bromophenol Blue (ratio of loading buffer to β-Mercaptoethanol to Bromophenol Blue is 2:1:1)

RIPA

150 mM NaCl 1.752 g

1% Triton X 100 2 ml (from 100% stock)

0.1% SDS 0.2 g

10 mM Tris pH 7.5 2 ml (from 1 M stock)

1% Na deoxycholate 2 g

Make up to 200 ml with dH_2O, store at 4^oC.

RIPA + Phosphatase and Protease Inhibitors

	Stock concentration	**Final concentration**	**Volume**
RIPA			817 µl
10x Protease Inhibitors	10x	1x	100 µl
NaF	1 M	50 mM	50 µl
Na_3VO_4	0.1 M	2 mM	20 µl
Pepstatin A	5 mg/ml	40 µg/ml	8 µl
PMSF (light sensitive foil it)	100 mM	0.5 mM	5 µl

Appendix:

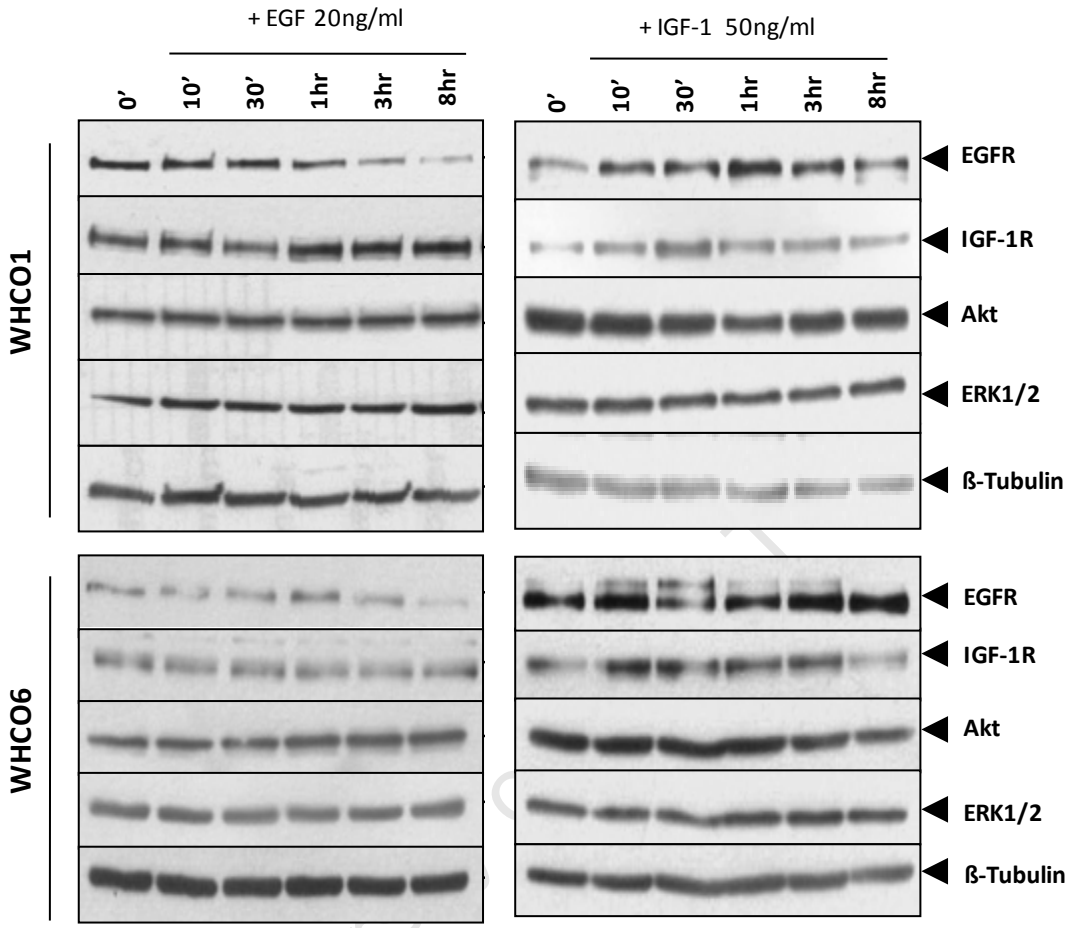

Figure A1: Effect of EGF or IGF-1 ligand on EGFR, IGF-2R, AKT and ERK1/2 levels

WHCO1 and WHCO6 cells were seeded in 60 mm dishes at a density of 3 x 10^5 cells per dish and stimulated with either 20 ng/ml EGF or 50 ng/ml IGF-1 for the indicated time periods. Protein was harvested and subjected to western blot analysis probing for IGF-1R, EGFR, ERK1/2 and AKT.

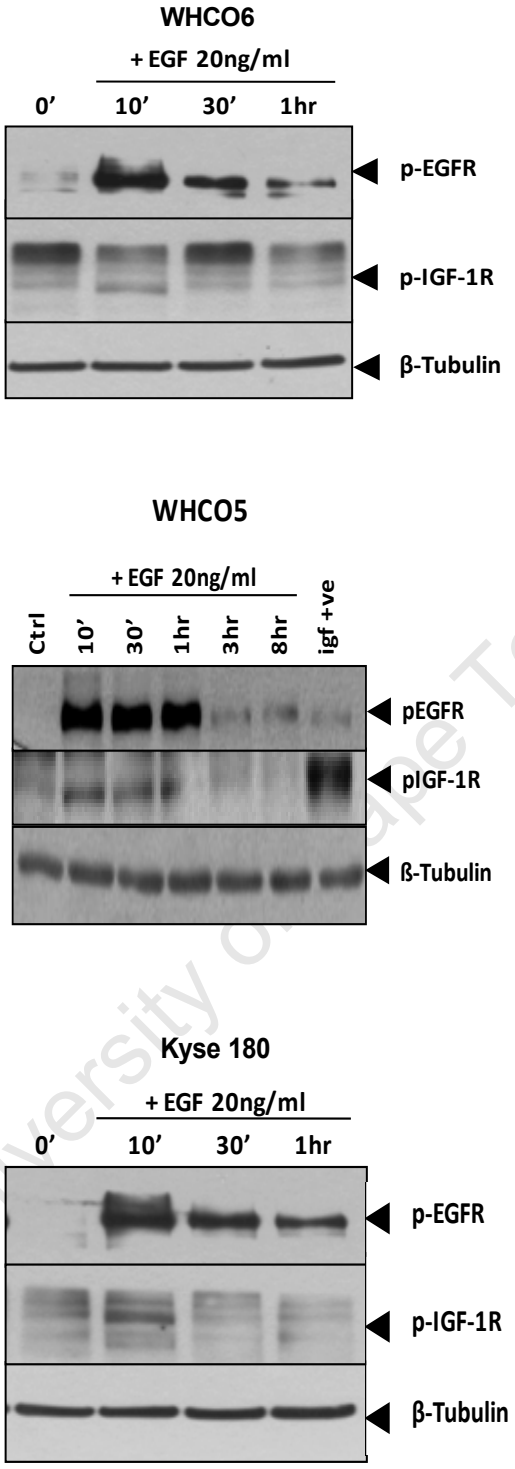

Figure A2: Effect of EGF on pIGF-1R in OSCC cells

WHCO6, WHCO5 and Kyse180 cells were seeded at 3 x 10^5 cells per 60 mm dish and stimulated with 20 ng/ml EGF ligand over the indicated time period. Protein was harvested and subjected to western blot analysis probing for pEGFR and pIGF-1R.

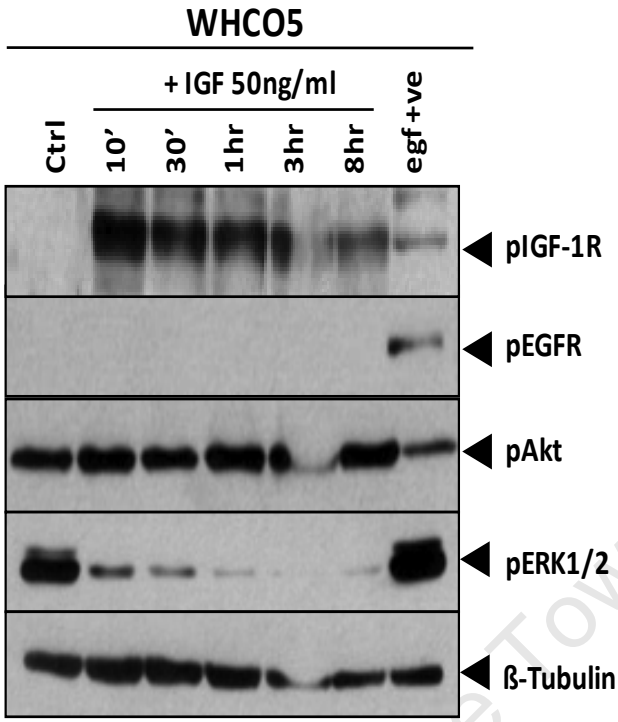

Figure A3: Effect IGF-1 treatment on pEGFR and pERK1/2 in WHCO5 OSCC cells.

3 x 10^5 WHCO5 cells in 60 mm dishes were stimulated with 50 ng/ml of IGF-1 for the indicated time periods. Protein was harvested and 40 µg of protein was subjected to western blot analysis using antibodies specific for pIGF-1R, pEGFR, pERK1/2 and pAKT.

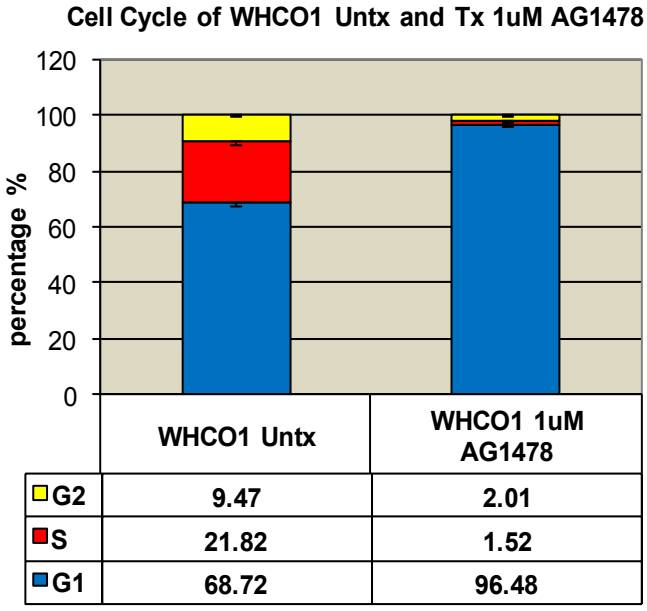

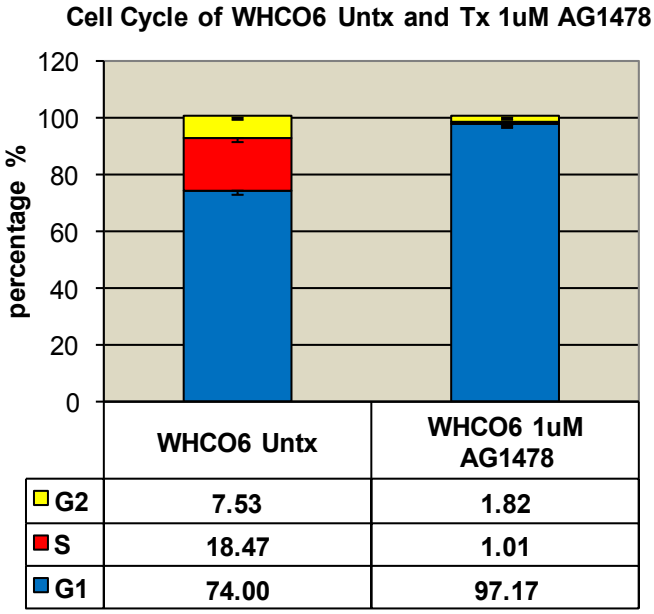

Figure A4: Cell cycle profile of WHCO1 and WHCO6 cells treated with 1 µM AG1478

WHCO1 and WHCO6 cells were plated at 3 x 10^5 cells per 60 mm dish and left overnight to settle. The following day cells were treated with 1 µM AG1478 and cultured for a further 48 hr. Cells were harvested, stained with propidium iodide and the cell cycle was determined using a FACS machine.

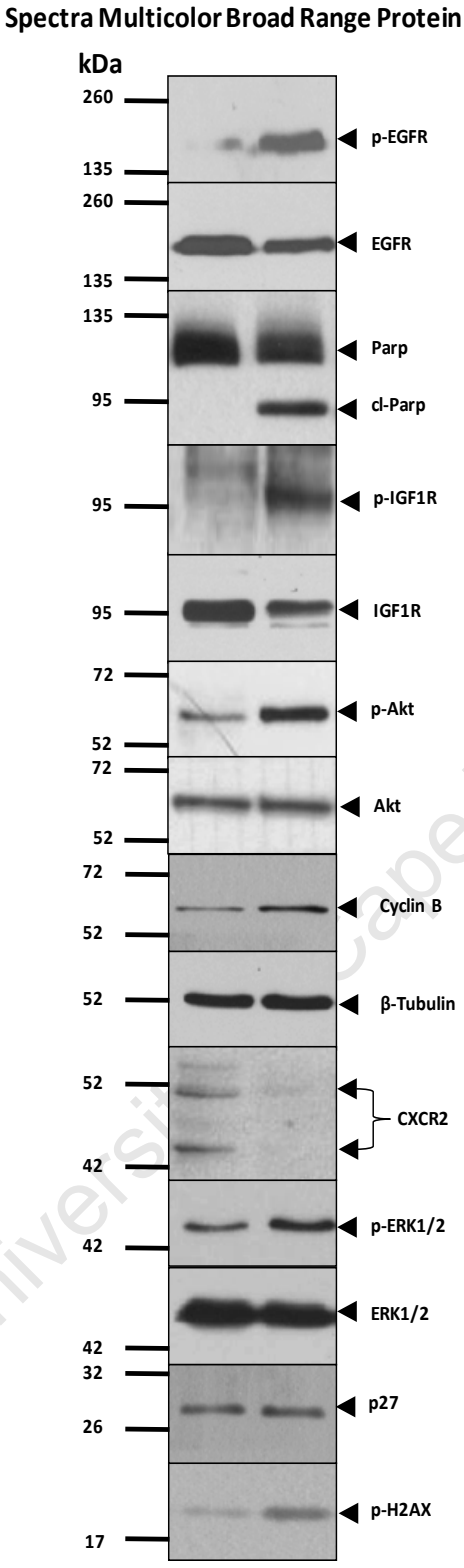

Figure A5: Protein sizes

Protein sizes of all proteins detected relative to Spectra Multicolor Broad Range Protein ladder (kDa - kilodaltons)

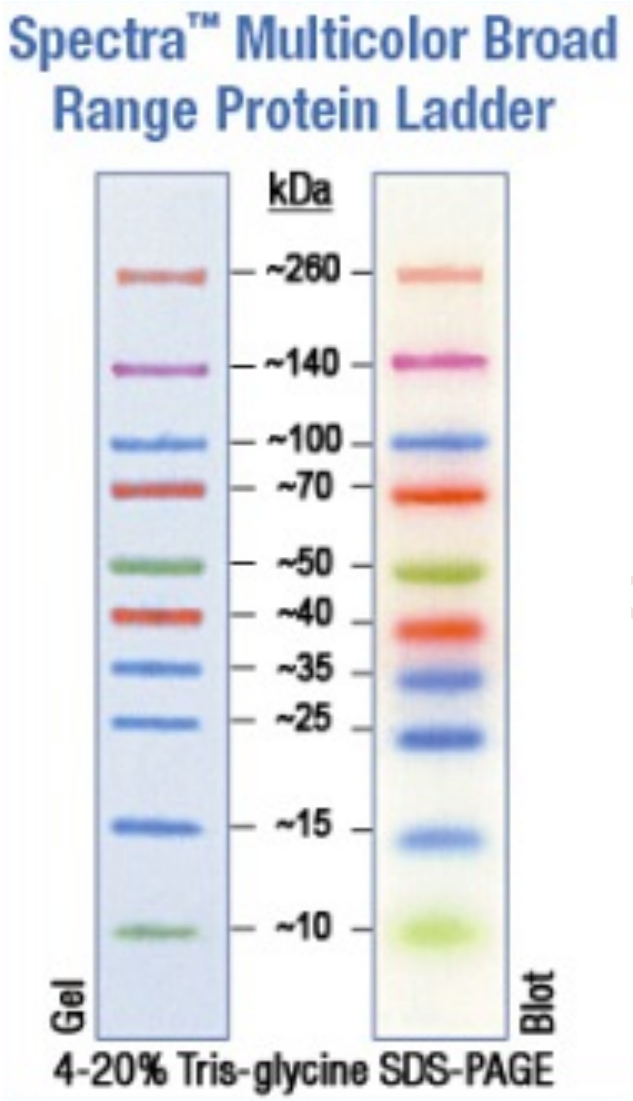

Figure A6: **Spectra Multicolor Broad Range Protein Ladder**

Spectra Multicolor Broad Range Protein ladder band sizes and banding pattern (kDa - kilodaltons)

References

Acosta, J. C., & Gil, J. (2009, March 15). A role for CXCR2 in senescence, but what about in cancer? *Cancer research*.

Acosta, J. C., O'Loghlen, A., Banito, A., Guijarro, M. V., Augert, A., Raguz, S., *et al.* (2008). Chemokine signaling via the CXCR2 receptor reinforces senescence. *Cell*, *133*(6), 1006-18.

Adachi, Y., Yamamoto, H., Ohashi, H., Endo, T., Carbone, D.-P., Imai, K., *et al.* (2010). A candidate targeting molecule of insulin-like growth factor-I receptor for gastrointestinal cancers. *World journal of gastroenterology : WJG*, *16*(46), 5779-89.

Addison, C. L., Daniel, T. O., Burdick, M D, Liu, H., Ehlert, J. E., Xue, Y Y, *et al.* (2000). The CXC chemokine receptor 2, CXCR2, is the putative receptor for ELR+ CXC chemokine-induced angiogenic activity. *Journal of immunology (Baltimore, Md. : 1950)*, *165*(9), 5269-77.

Aggarwal, B. B., Shishodia, S., Sandur, S. K., Pandey, M. K., & Sethi, G. (2006). Inflammation and cancer: how hot is the link? *Biochemical pharmacology*, *72*(11), 1605-21.

Ahmad, T., Farnie, G., Bundred, N. J., & Anderson, N. G. (2004). The mitogenic action of insulin-like growth factor I in normal human mammary epithelial cells requires the epidermal growth factor receptor tyrosine kinase. *The Journal of biological chemistry*, *279*(3), 1713-9.

Amura, C. R., Brodsky, K. S., Gitomer, B., McFann, K., Lazennec, G., Nichols, M. T., *et al.* (2008). CXCR2 agonists in ADPKD liver cyst fluids promote cell proliferation. *American journal of physiology. Cell physiology*, *294*(3), C786-96.

Auten, R. L., Richardson, R. M., White, J. R., Mason, S. N., Vozzelli, M. A., & Whorton, M. H. (2001). Nonpeptide CXCR2 inhibitor prevents neutrophil accumulation in hyperoxia-exposed newborn rats. *The Journal of pharmacology and experimental therapeutics*, *299*(1), 90-5.

Balestrieri, M. L., Balestrieri, A., Mancini, F. P., & Napoli, C. (2008). Understanding the immunoangiostatic CXC chemokine network. *Cardiovascular research*, *78*(2), 250-6.

Basilion, J. P., Schievella, A. R., Burns, E., Rioux, P., Olson, J. C., Monia, B. P., *et al.* (1999). Selective killing of cancer cells based on loss of heterozygosity and normal variation in the human genome: a new paradigm for anticancer drug therapy. *Molecular pharmacology*, *56*(2), 359-69.

Bianco, R., Damiano, V., Gelardi, T., Daniele, G., Ciardiello, F., & Tortora, G. (2007). Rational combination of targeted therapies as a strategy to overcome the mechanisms of resistance to inhibitors of EGFR signaling. *Current pharmaceutical design*, *13*(33), 3358-67.

Bizzarri, C., Beccari, A. R., Bertini, R., Cavicchia, M. R., Giorgini, S., & Allegretti, M. (2006). ELR+ CXC chemokines and their receptors (CXC chemokine receptor 1 and CXC chemokine receptor 2) as new therapeutic targets. *Pharmacology & therapeutics*, *112*(1), 139-49.

Blakesley, V. A., Scrimgeour, A., Esposito, D., & Le Roith, D. (1996). Signaling via the insulin-like growth factor-I receptor: does it differ from insulin receptor signaling? *Cytokine & growth factor reviews*, *7*(2), 153-9.

Bosetti, C., Levi, F., Ferlay, J., Garavello, W., Lucchini, F., Bertuccio, P., *et al.* (2008). Trends in oesophageal cancer incidence and mortality in Europe. *International journal of cancer. Journal international du cancer*, *122*(5), 1118-29.

Boutros, T., Chevet, E., & Metrakos, P. (2008). Mitogen-activated protein (MAP) kinase/MAP kinase phosphatase regulation: roles in cell growth, death, and cancer. *Pharmacological reviews*, *60*(3), 261-310.

Burger, Meike, Hartmann, T., Krome, M., Rawluk, J., Tamamura, H., Fujii, N., *et al.* (2005). Small peptide inhibitors of the CXCR4 chemokine receptor (CD184) antagonize the activation, migration, and antiapoptotic responses of CXCL12 in chronic lymphocytic leukemia B cells. *Blood*, *106*(5), 1824-30.

Burke, P., Schooler, K., & Wiley, H. S. (2001). Regulation of epidermal growth factor receptor signaling by endocytosis and intracellular trafficking. *Molecular biology of the cell*, *12*(6), 1897-910.

Cao, L., Yu, Yunkai, Darko, I., Currier, D., Mayeenuddin, L. H., Wan, X., *et al.* (2008). Addiction to elevated insulin-like growth factor I receptor and initial modulation of the AKT pathway define the responsiveness of rhabdomyosarcoma to the targeting antibody. *Cancer research*, *68*(19), 8039-48.

Cataisson, C., Ohman, R., Patel, G., Pearson, A., Tsien, M., Jay, S., *et al.* (2009). Inducible cutaneous inflammation reveals a protumorigenic role for keratinocyte CXCR2 in skin carcinogenesis. *Cancer research*, *69*(1), 319-28.

Catusse, J., Liotard, A., Loillier, B., Pruneau, D., & Paquet, J.-L. (2003). Characterization of the molecular interactions of interleukin-8 (CXCL8), growth related oncogen alpha (CXCL1) and a non-peptide inhibitor (SB 225002) with the human CXCR2. *Biochemical pharmacology*, *65*(5), 813-21.

Cavallo, F., De Giovanni, C., Nanni, P., Forni, G., & Lollini, P.-L. (2011). 2011: the immune hallmarks of cancer. *Cancer immunology, immunotherapy : CII*, *60*(3), 319-26.

Chakraborty, A. K., Liang, K., & DiGiovanna, M. P. (2008). Co-targeting insulin-like growth factor I receptor and HER2: dramatic effects of HER2 inhibitors on nonoverexpressing breast cancer. *Cancer research*, *68*(5), 1538-45.

Chandarlapaty, S., Sawai, A., Scaltriti, M., Rodrik-Outmezguine, V., Grbovic-Huezo, O., Serra, V., *et al.* (2011). AKT inhibition relieves feedback suppression of receptor tyrosine kinase expression and activity. *Cancer cell*, *19*(1), 58-71.

Chapman, R. W., Phillips, J. E., Hipkin, R. W., Curran, A. K., Lundell, D., & Fine, J. S. (2009). CXCR2 inhibitors for the treatment of pulmonary disease. *Pharmacology & therapeutics*, *121*(1), 55-68.

Chen, Y. L., Law, P.-Y., & Loh, H. H. (2005). Inhibition of PI3K/Akt signaling: an emerging paradigm for targeted cancer therapy. *Current medicinal chemistry. Anti-cancer agents*, *5*(6), 575-89.

Cohen, E. E. W., Lingen, M. W., Martin, L. E., Harris, P. L., Brannigan, B. W., Haserlat, S. M., *et al.* (2005). Response of some head and neck cancers to epidermal growth factor receptor tyrosine kinase inhibitors may be linked to mutation of ERBB2 rather than EGFR. *Clinical cancer research : an official journal of the American Association for Cancer Research*, *11*(22), 8105-8.

Dallas, N. A., Xia, L., Fan, F., Gray, M. J., Gaur, P., Buren, G. van, *et al.* (2009). Chemoresistant colorectal cancer cells, the cancer stem cell phenotype, and increased sensitivity to insulin-like growth factor-I receptor inhibition. *Cancer research*, *69*(5), 1951-7.

Devalaraja, R. M., Nanney, L. B., Du, J., Qian, Q., Yu, Y, Devalaraja, M. N., *et al.* (2000). Delayed wound healing in CXCR2 knockout mice. *The Journal of investigative dermatology*, *115*(2), 234-44.

Dragovich, T., & Campen, C. (2009). Anti-EGFR-Targeted Therapy for Esophageal and Gastric Cancers: An Evolving Concept. *Journal of oncology*, *2009*, 804108.

Dupont, J., Dunn, S. E., Barrett, J. C., & LeRoith, D. (2003). Microarray analysis and identification of novel molecules involved in insulin-like growth factor-1 receptor signaling and gene expression. *Recent progress in hormone research*, *58*, 325-42.

Ekman, S., Bergqvist, M., Heldin, C.-H., & Lennartsson, J. (2007). Activation of growth factor receptors in esophageal cancer--implications for therapy. *The oncologist*, *12*(10), 1165-77.

Enzinger, P. C., & Mayer, R. J. (2003). Esophageal cancer. *The New England journal of medicine*, *349*(23), 2241-52.

Fan, G.-H., Lapierre, L. A., Goldenring, J. R., & Richmond, Ann. (2003). Differential regulation of CXCR2 trafficking by Rab GTPases. *Blood*, *101*(6), 2115-24.

Ferry, D. R., Anderson, M., Beddard, K., Tomlinson, S., Atherfold, P., Obszynska, J., *et al.* (2007). A phase II study of gefitinib monotherapy in advanced esophageal adenocarcinoma: evidence of gene expression, cellular, and clinical response. *Clinical cancer research : an official journal of the American Association for Cancer Research*, *13*(19), 5869-75.

García-Echeverría, C., Pearson, M. A., Marti, A., Meyer, T., Mestan, J., Zimmermann, J., *et al.* (2004). In vivo antitumor activity of NVP-AEW541-A novel, potent, and selective inhibitor of the IGF-IR kinase. *Cancer cell*, *5*(3), 231-9.

Godsland, I. F. (2010). Insulin resistance and hyperinsulinaemia in the development and progression of cancer. *Clinical science (London, England : 1979)*, *118*(5), 315-32.

Guo, Y.-M., Wang, Q., Liu, Y.-Z., Chen, H.-M., Qi, Z., & Guo, Q.-H. (2008). Genetic polymorphisms in cytochrome P4502E1, alcohol and aldehyde dehydrogenases and the risk of esophageal squamous cell carcinoma in Gansu Chinese males. *World journal of gastroenterology : WJG*, *14*(9), 1444-9.

Hajdu, S. I. (2011). A note from history: landmarks in history of cancer, part 2. *Cancer*, *117*(12), 2811-20.

Hamilton, W. (2010). Cancer diagnosis in primary care. *The British journal of general practice : the journal of the Royal College of General Practitioners*, *60*(571), 121-8.

Hansen, B. F., Danielsen, G. M., Drejer, K., Sørensen, A. R., Wiberg, F. C., Klein, H. H., *et al.* (1996). Sustained signalling from the insulin receptor after stimulation with insulin analogues exhibiting increased mitogenic potency. *The Biochemical journal*, *315 (Pt 1*, 271-9.

Hartog, H., Wesseling, J., Boezen, H. M., & Graaf, W. T. A. van der. (2007). The insulin-like growth factor 1 receptor in cancer: old focus, new future. *European journal of cancer (Oxford, England : 1990)*, *43*(13), 1895-904.

Ho, K.-K., Auld, D. S., Bohnstedt, A. C., Conti, P., Dokter, W., Erickson, S., *et al.* (2006). Imidazolylpyrimidine based CXCR2 chemokine receptor inhibitors. *Bioorganic & medicinal chemistry letters*, *16*(10), 2724-8.

Hopfner, M., Sutter, A. P., Huether, A., Baradari, V., & Scherubl, H. (2006). Tyrosine kinase of insulin-like growth factor receptor as target for novel treatment and prevention strategies of colorectal cancer. *World journal of gastroenterology : WJG*, *12*(35), 5635-43.

Hu, Y. P., Patil, S. B., Panasiewicz, M., Li, W., Hauser, J., Humphrey, L. E., *et al.* (2008a). Heterogeneity of receptor function in colon carcinoma cells determined by cross-talk between type I insulin-like growth factor receptor and epidermal growth factor receptor. *Cancer research*, *68*(19), 8004-13.

Hu, Y. P., Patil, S. B., Panasiewicz, M., Li, W., Hauser, J., Humphrey, L. E., *et al.* (2008b). Heterogeneity of receptor function in colon carcinoma cells determined by cross-talk between type I insulin-like growth factor receptor and epidermal growth factor receptor. *Cancer research*, *68*(19), 8004-13.

Huang, F., Greer, A., Hurlburt, W., Han, X., Hafezi, R., Wittenberg, G. M., *et al.* (2009). The mechanisms of differential sensitivity to an insulin-like growth factor-1 receptor

inhibitor (BMS-536924) and rationale for combining with EGFR/HER2 inhibitors. *Cancer research*, *69*(1), 161-70.

Hynes, N. E., & Schlange, T. (2006). Targeting ADAMS and ERBBs in lung cancer. *Cancer cell*, *10*(1), 7-11.

Höpfner, M., Huether, A., Sutter, A. P., Baradari, V., Schuppan, D., & Scherübl, H. (2006). Blockade of IGF-1 receptor tyrosine kinase has antineoplastic effects in hepatocellular carcinoma cells. *Biochemical pharmacology*, *71*(10), 1435-48.

Imsumran, A., Adachi, Y., Yamamoto, H., Li, R., Wang, Y., Min, Y., *et al.* (2007). Insulin-like growth factor-I receptor as a marker for prognosis and a therapeutic target in human esophageal squamous cell carcinoma. *Carcinogenesis*, *28*(5), 947-56.

Janmaat, M. L., Gallegos-Ruiz, M. I., Rodriguez, J. A., Meijer, G. A., Vervenne, W. L., Richel, D. J., *et al.* (2006). Predictive factors for outcome in a phase II study of gefitinib in second-line treatment of advanced esophageal cancer patients. *Journal of clinical oncology : official journal of the American Society of Clinical Oncology*, *24*(10), 1612-9.

Jin, Q., & Esteva, F. J. (2008). Cross-talk between the ErbB/HER family and the type I insulin-like growth factor receptor signaling pathway in breast cancer. *Journal of mammary gland biology and neoplasia*, *13*(4), 485-98.

Kakinuma, T., & Hwang, S. T. (2006). Chemokines, chemokine receptors, and cancer metastasis. *Journal of leukocyte biology*, *79*(4), 639-51.

Karl, E., Warner, K., Zeitlin, B., Kaneko, T., Wurtzel, L., Jin, T., *et al.* (2005). Bcl-2 acts in a proangiogenic signaling pathway through nuclear factor-kappaB and CXC chemokines. *Cancer research*, *65*(12), 5063-9.

Katz, M., Amit, I., & Yarden, Y. (2007). Regulation of MAPKs by growth factors and receptor tyrosine kinases. *Biochimica et biophysica acta*, *1773*(8), 1161-76.

Keane, M. P., Belperio, J. A., Xue, Ying Y, Burdick, Marie D, & Strieter, Robert M. (2004). Depletion of CXCR2 inhibits tumor growth and angiogenesis in a murine model of lung cancer. *Journal of immunology (Baltimore, Md. : 1950)*, *172*(5), 2853-60.

Kern, F., Niault, T., & Baccarini, M. (2011). Ras and Raf pathways in epidermis development and carcinogenesis. *British journal of cancer*, *104*(2), 229-34.

Khavari, T. A., & Rinn, J. (2007). Ras/Erk MAPK signaling in epidermal homeostasis and neoplasia. *Cell cycle (Georgetown, Tex.)*, *6*(23), 2928-31.

Kim, S.-H., Nakagawa, H., Navaraj, A., Naomoto, Y., Klein-Szanto, A. J. P., Rustgi, A. K., *et al.* (2006). Tumorigenic conversion of primary human esophageal epithelial cells using oncogene combinations in the absence of exogenous Ras. *Cancer research*, *66*(21), 10415-24.

Knowlden, J. M., Hutcheson, I. R., Barrow, D., Gee, J. M. W., & Nicholson, R. I. (2005). Insulin-like growth factor-I receptor signaling in tamoxifen-resistant breast cancer: a supporting role to the epidermal growth factor receptor. *Endocrinology*, *146*(11), 4609-18.

Kuribayashi, A., Kataoka, K., Kurabayashi, T., & Miura, M. (2004). Evidence that basal activity, but not transactivation, of the epidermal growth factor receptor tyrosine kinase is required for insulin-like growth factor I-induced activation of extracellular signal-regulated kinase in oral carcinoma cells. *Endocrinology*, *145*(11), 4976-84.

Kurmasheva, R. T., & Houghton, P. J. (2006). IGF-I mediated survival pathways in normal and malignant cells. *Biochimica et biophysica acta*, *1766*(1), 1-22.

Kwon, J., Stephan, S., Mukhopadhyay, A., Muders, M. H., Dutta, S. K., Lau, J. S., *et al.* (2009). Insulin receptor substrate-2 mediated insulin-like growth factor-I receptor overexpression in pancreatic adenocarcinoma through protein kinase Cdelta. *Cancer research*, *69*(4), 1350-7.

Lagerström, M. C., & Schiöth, H. B. (2008). Structural diversity of G protein-coupled receptors and significance for drug discovery. *Nature reviews. Drug discovery*, *7*(4), 339-57.

Layke, J. C., & Lopez, P. P. (2006). Esophageal cancer: a review and update. *American family physician*, *73*(12), 2187-94.

Lazennec, G., & Richmond, Ann. (2010). Chemokines and chemokine receptors: new insights into cancer-related inflammation. *Trends in molecular medicine*, *16*(3), 133-44.

Lee, K. H., Zhang, J., & Underwood, L. E. (2002). Hepatic reduction of insulin-like growth factor (IGF)-I and IGF binding protein-3 that results from fasting is not attenuated in genetically obese rats. *The Journal of nutritional biochemistry*, *13*(11), 664-670.

LoPiccolo, J., Blumenthal, G. M., Bernstein, W. B., & Dennis, P. A. (n.d.). Targeting the PI3K/Akt/mTOR pathway: effective combinations and clinical considerations. *Drug resistance updates : reviews and commentaries in antimicrobial and anticancer chemotherapy*, *11*(1-2), 32-50.

Loukinova, E., Dong, G., Enamorado-Ayalya, I., Thomas, G. R., Chen, Z., Schreiber, H., *et al.* (2000). Growth regulated oncogene-alpha expression by murine squamous cell carcinoma promotes tumor growth, metastasis, leukocyte infiltration and angiogenesis by a host CXC receptor-2 dependent mechanism. *Oncogene*, *19*(31), 3477-86.

Luppi, F., Longo, A. M., Boer, W. I. de, Rabe, K. F., & Hiemstra, P. S. (2007). Interleukin-8 stimulates cell proliferation in non-small cell lung cancer through epidermal growth factor receptor transactivation. *Lung cancer (Amsterdam, Netherlands)*, *56*(1), 25-33.

Mandic, R., Rodgarkia-Dara, C. J., Zhu, L., Folz, B. J., Bette, M., Weihe, E., *et al.* (2006). Treatment of HNSCC cell lines with the EGFR-specific inhibitor cetuximab (Erbitux)

results in paradox phosphorylation of tyrosine 1173 in the receptor. *FEBS letters*, *580*(20), 4793-800.

Massoner, P., Ladurner-Rennau, M., Eder, I. E., & Klocker, H. (2010). Insulin-like growth factors and insulin control a multifunctional signalling network of significant importance in cancer. *British journal of cancer*, *103*(10), 1479-84.

Matsuo, Y., Raimondo, M., Woodward, T. A., Wallace, M. B., Gill, K. R., Tong, Z., *et al.* (2009). CXC-chemokine/CXCR2 biological axis promotes angiogenesis in vitro and in vivo in pancreatic cancer. *International journal of cancer. Journal international du cancer*, *125*(5), 1027-37.

McCubrey, J. A., Steelman, L. S., Chappell, W. H., Abrams, S. L., Wong, E. W. T., Chang, F., *et al.* (2007). Roles of the Raf/MEK/ERK pathway in cell growth, malignant transformation and drug resistance. *Biochimica et biophysica acta*, *1773*(8), 1263-84.

Meng, D., Shi, X., Jiang, B.-H., & Fang, J. (2007). Insulin-like growth factor-I (IGF-I) induces epidermal growth factor receptor transactivation and cell proliferation through reactive oxygen species. *Free radical biology & medicine*, *42*(11), 1651-60.

Mestas, J., Burdick, Marie D, Reckamp, K., Pantuck, A., Figlin, R. A., & Strieter, Robert M. (2005). The role of CXCR2/CXCR2 ligand biological axis in renal cell carcinoma. *Journal of immunology (Baltimore, Md. : 1950)*, *175*(8), 5351-7.

Mitry, E., Rachet, B., Quinn, M. J., Cooper, N., & Coleman, M. P. (2008). Survival from cancer of the oesophagus in England and Wales up to 2001. *British journal of cancer*, *99 Suppl 1*, S11-3.

Mitsiades, C. S., Mitsiades, N. S., McMullan, C. J., Poulaki, V., Shringarpure, R., Akiyama, M., *et al.* (2004). Inhibition of the insulin-like growth factor receptor-1 tyrosine kinase activity as a therapeutic strategy for multiple myeloma, other hematologic malignancies, and solid tumors. *Cancer cell*, *5*(3), 221-30.

Moelling, K., Schad, K., Bosse, M., Zimmermann, S., & Schweneker, M. (2002). Regulation of Raf-Akt Cross-talk. *The Journal of biological chemistry*, *277*(34), 31099-106.

Morgillo, F., Bareschino, M. A., Bianco, R., Tortora, G., & Ciardiello, F. (2007). Primary and acquired resistance to anti-EGFR targeted drugs in cancer therapy. *Differentiation; research in biological diversity*, *75*(9), 788-99.

Morgillo, F., Kim, W.-Y., Kim, E. S., Ciardiello, F., Hong, W. K., & Lee, H.-Y. (2007). Implication of the insulin-like growth factor-IR pathway in the resistance of non-small cell lung cancer cells to treatment with gefitinib. *Clinical cancer research : an official journal of the American Association for Cancer Research*, *13*(9), 2795-803.

Moser, C., Schachtschneider, P., Lang, S. A., Gaumann, A., Mori, A., Zimmermann, J., *et al.* (2008). Inhibition of insulin-like growth factor-I receptor (IGF-IR) using NVP-AEW541, a small molecule kinase inhibitor, reduces orthotopic pancreatic cancer

growth and angiogenesis. *European journal of cancer (Oxford, England : 1990)*, *44*(11), 1577-86.

Mueller, S. G., White, J. R., Schraw, W. P., Lam, V., & Richmond, A. (1997). Ligand-induced desensitization of the human CXC chemokine receptor-2 is modulated by multiple serine residues in the carboxyl-terminal domain of the receptor. *The Journal of biological chemistry*, *272*(13), 8207-14.

Mukherjee, A., Dutta, S., Shanmugavel, M., Mondhe, D. M., Sharma, P. R., Singh, S. K., *et al.* (2010). 6-Nitro-2-(3-hydroxypropyl)-1H-benz[de]isoquinoline-1,3-dione, a potent antitumor agent, induces cell cycle arrest and apoptosis. *Journal of experimental & clinical cancer research : CR*, *29*, 175.

Neel, N. F., Schutyser, E., Sai, J., Fan, G.-H., & Richmond, Ann. (2005). Chemokine receptor internalization and intracellular trafficking. *Cytokine & growth factor reviews*, *16*(6), 637-58.

Normanno, N., De Luca, A., Bianco, C., Strizzi, L., Mancino, M., Maiello, M. R., *et al.* (2006). Epidermal growth factor receptor (EGFR) signaling in cancer. *Gene*, *366*(1), 2-16.

Okawa, T., Michaylira, C. Z., Kalabis, J., Stairs, D. B., Nakagawa, H., Andl, C. D., *et al.* (2007). The functional interplay between EGFR overexpression, hTERT activation, and p53 mutation in esophageal epithelial cells with activation of stromal fibroblasts induces tumor development, invasion, and differentiation. *Genes & development*, *21*(21), 2788-803.

Ono, M., & Kuwano, M. (2006). Molecular mechanisms of epidermal growth factor receptor (EGFR) activation and response to gefitinib and other EGFR-targeting drugs. *Clinical cancer research : an official journal of the American Association for Cancer Research*, *12*(24), 7242-51.

Pandini, G., Wurch, T., Akla, B., Corvaia, N., Belfiore, A., & Goetsch, L. (2007). Functional responses and in vivo anti-tumour activity of h7C10: a humanised monoclonal antibody with neutralising activity against the insulin-like growth factor-1 (IGF-1) receptor and insulin/IGF-1 hybrid receptors. *European journal of cancer (Oxford, England : 1990)*, *43*(8), 1318-27.

Pickens, A., & Orringer, M. B. (2003). Geographical distribution and racial disparity in esophageal cancer. *The Annals of thoracic surgery*, *76*(4), S1367-9.

Raman, D., Baugher, P. J., Thu, Y. M., & Richmond, Ann. (2007). Role of chemokines in tumor growth. *Cancer letters*, *256*(2), 137-65.

Revankar, C. M., Vines, C. M., Cimino, D. F., & Prossnitz, E. R. (2004). Arrestins block G protein-coupled receptor-mediated apoptosis. *The Journal of biological chemistry*, *279*(23), 24578-84.

Riedemann, J., Sohail, M., & Macaulay, V. M. (2007). Dual silencing of the EGF and type 1 IGF receptors suggests dominance of IGF signaling in human breast cancer cells. *Biochemical and biophysical research communications*, *355*(3), 700-6.

Riedemann, J., Takiguchi, M., Sohail, M., & Macaulay, V. M. (2007). The EGF receptor interacts with the type 1 IGF receptor and regulates its stability. *Biochemical and biophysical research communications*, *355*(3), 707-14.

Rigamonti, E., Fontaine, C., Lefebvre, B., Duhem, C., Lefebvre, P., Marx, N., *et al.* (2008). Induction of CXCR2 receptor by peroxisome proliferator-activated receptor gamma in human macrophages. *Arteriosclerosis, thrombosis, and vascular biology*, *28*(5), 932-9.

Romanini, J., Mielcke, T. R., Leal, P. C., Figueiredo, C. P., Calixto, J. B., Morrone, F. B., *et al.* (2011). The role of CXCR2 chemokine receptors in the oral squamous cell carcinoma. *Investigational new drugs*.

Roudabush, F. L., Pierce, K. L., Maudsley, S., Khan, K. D., & Luttrell, L. M. (2000). Transactivation of the EGF receptor mediates IGF-1-stimulated shc phosphorylation and ERK1/2 activation in COS-7 cells. *The Journal of biological chemistry*, *275*(29), 22583-9.

Rowinsky, E. K. (2004). The erbB family: targets for therapeutic development against cancer and therapeutic strategies using monoclonal antibodies and tyrosine kinase inhibitors. *Annual review of medicine*, *55*, 433-57.

Sai, J., Walker, G., Wikswo, J., & Richmond, Ann. (2006). The IL sequence in the LLKIL motif in CXCR2 is required for full ligand-induced activation of Erk, Akt, and chemotaxis in HL60 cells. *The Journal of biological chemistry*, *281*(47), 35931-41.

Schneider, M. R., Sibilia, M., & Erben, R. G. (2009). The EGFR network in bone biology and pathology. *Trends in endocrinology and metabolism: TEM*, *20*(10), 517-24.

Schraufstätter, I. U., Burger, M, Hoch, R. C., Oades, Z. G., & Takamori, H. (1998). Importance of the carboxy-terminus of the CXCR2 for signal transduction. *Biochemical and biophysical research communications*, *244*(1), 243-8.

Sharma, S. V., Bell, D. W., Settleman, J., & Haber, D. A. (2007). Epidermal growth factor receptor mutations in lung cancer. *Nature reviews. Cancer*, *7*(3), 169-81.

Shaw, R. J., & Cantley, L. C. (2006). Ras, PI(3)K and mTOR signalling controls tumour cell growth. *Nature*, *441*(7092), 424-30.

Shukla, V., Coumoul, X., Vassilopoulos, A., & Deng, C.-X. (2008). IGF signaling pathway as a selective target of familial breast cancer therapy. *Current molecular medicine*, *8*(8), 727-40.

Singh, S., Sadanandam, A., Nannuru, K. C., Varney, M. L., Mayer-Ezell, R., Bond, R., *et al.* (2009). Small-molecule inhibitors for CXCR2 and CXCR1 inhibit human melanoma growth by decreasing tumor cell proliferation, survival, and angiogenesis. *Clinical*

cancer research : an official journal of the American Association for Cancer Research, *15*(7), 2380-6.

Slomiany, M. G., Black, L. A., Kibbey, M. M., Day, T. A., & Rosenzweig, S. A. (2006). IGF-1 induced vascular endothelial growth factor secretion in head and neck squamous cell carcinoma. *Biochemical and biophysical research communications*, *342*(3), 851-8.

Stark, G. R., & Taylor, W. R. (2006). Control of the G2/M transition. *Molecular biotechnology*, *32*(3), 227-48.

Steelman, L. S., Chappell, W. H., Abrams, S. L., Kempf, R. C., Long, J., Laidler, P., *et al.* (2011). Roles of the Raf/MEK/ERK and PI3K/PTEN/Akt/mTOR pathways in controlling growth and sensitivity to therapy-implications for cancer and aging. *Aging*, *3*(3), 192-222.

Stoner, G. D., Wang, L.-S., & Chen, T. (2007). Chemoprevention of esophageal squamous cell carcinoma. *Toxicology and applied pharmacology*, *224*(3), 337-49.

Strieter, Robert M, Burdick, Marie D, Mestas, J., Gomperts, B., Keane, M. P., & Belperio, J. A. (2006). Cancer CXC chemokine networks and tumour angiogenesis. *European journal of cancer (Oxford, England : 1990)*, *42*(6), 768-78.

Sudo, T., Mimori, K., Nagahara, H., Utsunomiya, T., Fujita, H., Tanaka, Y., *et al.* (2007). Identification of EGFR mutations in esophageal cancer. *European journal of surgical oncology : the journal of the European Society of Surgical Oncology and the British Association of Surgical Oncology*, *33*(1), 44-8.

Sutter, A. P., Höpfner, M., Huether, A., Maaser, K., & Scherübl, H. (2006). Targeting the epidermal growth factor receptor by erlotinib (Tarceva) for the treatment of esophageal cancer. *International journal of cancer. Journal international du cancer*, *118*(7), 1814-22.

Svensson, M., Irjala, H., Svanborg, C., & Godaly, G. (2008). Effects of epithelial and neutrophil CXCR2 on innate immunity and resistance to kidney infection. *Kidney international*, *74*(1), 81-90.

Tew, W. P., Kelsen, D. P., & Ilson, D. H. (2005). Targeted therapies for esophageal cancer. *The oncologist*, *10*(8), 590-601.

Thomas, S. M., Bhola, N. E., Zhang, Q., Contrucci, S. C., Wentzel, A. L., Freilino, M. L., *et al.* (2006). Cross-talk between G protein-coupled receptor and epidermal growth factor receptor signaling pathways contributes to growth and invasion of head and neck squamous cell carcinoma. *Cancer research*, *66*(24), 11831-9.

Varney, M. L., Li, Aihua, Dave, B. J., Bucana, C. D., Johansson, S. L., & Singh, R. K. (2003). Expression of CXCR1 and CXCR2 receptors in malignant melanoma with different metastatic potential and their role in interleukin-8 (CXCL-8)-mediated modulation of metastatic phenotype. *Clinical & experimental metastasis*, *20*(8), 723-31.

Varney, M. L., Singh, S., Li, Aihua, Mayer-Ezell, R., Bond, R., & Singh, R. K. (2011). Small molecule inhibitors for CXCR2 and CXCR1 inhibit human colon cancer liver metastases. *Cancer letters*, *300*(2), 180-8.

Villanueva, J., Vultur, A., Lee, J. T., Somasundaram, R., Fukunaga-Kalabis, M., Cipolla, A. K., *et al.* (2010). Acquired resistance to BRAF inhibitors mediated by a RAF kinase switch in melanoma can be overcome by cotargeting MEK and IGF-1R/PI3K. *Cancer cell*, *18*(6), 683-95.

Wagener, B. M., Marjon, N. A., Revankar, C. M., & Prossnitz, E. R. (2009). Adaptor protein-2 interaction with arrestin regulates GPCR recycling and apoptosis. *Traffic (Copenhagen, Denmark)*, *10*(9), 1286-300.

Wang, B., Hendricks, D. T., Wamunyokoli, F., & Parker, M. I. (2006). A growth-related oncogene/CXC chemokine receptor 2 autocrine loop contributes to cellular proliferation in esophageal cancer. *Cancer research*, *66*(6), 3071-7.

Wang, B., Khachigian, L. M., Esau, L., Birrer, M. J., Zhao, X., Parker, M. I., *et al.* (2009). A key role for early growth response-1 and nuclear factor-kappaB in mediating and maintaining GRO/CXCR2 proliferative signaling in esophageal cancer. *Molecular cancer research : MCR*, *7*(5), 755-64.

Wang, S. E., Narasanna, A., Perez-Torres, M., Xiang, B., Wu, F. Y., Yang, S., *et al.* (2006). HER2 kinase domain mutation results in constitutive phosphorylation and activation of HER2 and EGFR and resistance to EGFR tyrosine kinase inhibitors. *Cancer cell*, *10*(1), 25-38.

Watanabe, H., Iwase, M., Ohashi, M., & Nagumo, M. (2002). Role of interleukin-8 secreted from human oral squamous cell carcinoma cell lines. *Oral oncology*, *38*(7), 670-9.

Waugh, D. J. J., & Wilson, C. (2008). The interleukin-8 pathway in cancer. *Clinical cancer research : an official journal of the American Association for Cancer Research*, *14*(21), 6735-41.

Wei, Q., Chen, L., Sheng, L., Nordgren, H., Wester, K., & Carlsson, J. (2007). EGFR, HER2 and HER3 expression in esophageal primary tumours and corresponding metastases. *International journal of oncology*, *31*(3), 493-9.

Weihua, Z., Tsan, R., Huang, W.-C., Wu, Q., Chiu, C.-H., Fidler, I. J., *et al.* (2008). Survival of cancer cells is maintained by EGFR independent of its kinase activity. *Cancer cell*, *13*(5), 385-93.

Wente, M. N., Keane, M. P., Burdick, Marie D, Friess, H., Büchler, M. W., Ceyhan, G. O., *et al.* (2006). Blockade of the chemokine receptor CXCR2 inhibits pancreatic cancer cell-induced angiogenesis. *Cancer letters*, *241*(2), 221-7.

Whibley, C. E., Keyzers, R. A., Soper, A. G., Davies-Coleman, M. T., Samaai, T., & Hendricks, D. T. (2005). Antiesophageal cancer activity from Southern African marine organisms. *Annals of the New York Academy of Sciences*, *1056*, 405-12.

Whibley, C. E., McPhail, K. L., Keyzers, R. A., Maritz, M. F., Leaner, V. D., Birrer, M. J., *et al.* (2007). Reactive oxygen species mediated apoptosis of esophageal cancer cells induced by marine triprenyl toluquinones and toluhydroquinones. *Molecular cancer therapeutics*, *6*(9), 2535-43.

Wickenden, J. A., & Watson, C. J. (2010). Key signalling nodes in mammary gland development and cancer. Signalling downstream of PI3 kinase in mammary epithelium: a play in 3 Akts. *Breast cancer research : BCR*, *12*(2), 202.

Wislez, M., Fujimoto, N., Izzo, J. G., Hanna, A. E., Cody, D. D., Langley, R. R., *et al.* (2006). High expression of ligands for chemokine receptor CXCR2 in alveolar epithelial neoplasia induced by oncogenic kras. *Cancer research*, *66*(8), 4198-207.

Yan, L., Anderson, G. M., DeWitte, M., & Nakada, M. T. (2006). Therapeutic potential of cytokine and chemokine inhibitors in cancer therapy. *European journal of cancer (Oxford, England : 1990)*, *42*(6), 793-802.

Yang, G., Rosen, D. G., Liu, G., Yang, F., Guo, X., Xiao, X., *et al.* (2010). CXCR2 promotes ovarian cancer growth through dysregulated cell cycle, diminished apoptosis, and enhanced angiogenesis. *Clinical cancer research : an official journal of the American Association for Cancer Research*, *16*(15), 3875-86.

Yang, W., Wang, D., & Richmond, A. (1999). Role of clathrin-mediated endocytosis in CXCR2 sequestration, resensitization, and signal transduction. *The Journal of biological chemistry*, *274*(16), 11328-33.

Yi, H.-K., Kim, S.-Y., Hwang, P.-H., Kim, C.-Y., Yang, D.-H., Oh, Y., *et al.* (2005). Impact of PTEN on the expression of insulin-like growth factors (IGFs) and IGF-binding proteins in human gastric adenocarcinoma cells. *Biochemical and biophysical research communications*, *330*(3), 760-7.

Yun, C.-H., Boggon, T. J., Li, Yiqun, Woo, M. S., Greulich, H., Meyerson, M., *et al.* (2007). Structures of lung cancer-derived EGFR mutants and inhibitor complexes: mechanism of activation and insights into differential inhibitor sensitivity. *Cancer cell*, *11*(3), 217-27.

Zha, J., & Lackner, M. R. (2010). Targeting the insulin-like growth factor receptor-1R pathway for cancer therapy. *Clinical cancer research : an official journal of the American Association for Cancer Research*, *16*(9), 2512-7.

Zhao, M., Wimmer, A., Trieu, K., Discipio, R. G., & Schraufstatter, I. U. (2004). Arrestin regulates MAPK activation and prevents NADPH oxidase-dependent death of cells expressing CXCR2. *The Journal of biological chemistry*, *279*(47), 49259-67.

Zheng, Y.-L., Hu, N., Sun, Q., Wang, C., & Taylor, P. R. (2009). Telomere attrition in cancer cells and telomere length in tumor stroma cells predict chromosome instability in esophageal squamous cell carcinoma: a genome-wide analysis. *Cancer research*, *69*(4), 1604-14.

Zhou, R.-M., Li, Yan, Wang, N., Zhang, X.-J., Dong, X.-J., & Guo, W. (2006). [Correlation of XPC Ala499Val and Lys939Gln polymorphisms to risks of esophageal squamous cell carcinoma and gastric cardiac adenocarcinoma]. *Ai zheng = Aizheng = Chinese journal of cancer*, *25*(9), 1113-9.